Available online at www.sciencedirect.com
SCIENCE DIRECT®
Biochimica et Biophysica Acta 1612 (2003) 1–40
BIOCHIMICA ET BIOPHYSICA ACTA
BBA
www.bba-direct.com

Review

Lipid–protein interactions in biological membranes: a structural perspective

A.G. Lee*

Division of Biochemistry and Molecular Biology, School of Biological Sciences, University of Southampton, Bassett Crescent East, Southampton SO16 7PX, UK

Received 19 November 2002; received in revised form 6 February 2003; accepted 14 February 2003

Abstract

Lipid molecules bound to membrane proteins are resolved in some high-resolution structures of membrane proteins. An analysis of these structures provides a framework within which to analyse the nature of lipid–protein interactions within membranes. Membrane proteins are surrounded by a shell or annulus of lipid molecules, equivalent to the solvent layer surrounding a water-soluble protein. The lipid bilayer extends right up to the membrane protein, with a uniform thickness around the protein. The surface of a membrane protein contains many shallow grooves and protrusions to which the fatty acyl chains of the surrounding lipids conform to provide tight packing into the membrane. An individual lipid molecule will remain in the annular shell around a protein for only a short period of time. Binding to the annular shell shows relatively little structural specificity. As well as the annular lipid, there is evidence for other lipid molecules bound between the transmembrane α-helices of the protein; these lipids are referred to as non-annular lipids. The average thickness of the hydrophobic domain of a membrane protein is about 29 Å, with a few proteins having significantly smaller or greater thicknesses than the average. Hydrophobic mismatch between a membrane protein and the surrounding lipid bilayer generally leads to only small changes in membrane thickness. Possible adaptations in the protein to minimise mismatch include tilting of the helices and rotation of side chains at the ends of the helices. Packing of transmembrane α-helices is dependent on the chain length of the surrounding phospholipids. The function of membrane proteins is dependent on the thickness of the surrounding lipid bilayer, sometimes on the presence of specific, usually anionic, phospholipids, and sometimes on the phase of the phospholipid.

Keywords: Annular lipid; Non-annular site; Hydrophobic mismatch; Membrane protein structure; Lipid bilayer; Lipid–protein interaction; Membrane structure

1. Introduction

There has long been an interest in how integral membrane proteins interact with the lipid molecules that surround them in a biological membrane. Clearly, the lipid and protein components of a biological membrane must have co-evolved to allow membrane proteins to function in the environment provided by the lipid bilayer and to allow membrane proteins to be inserted into the bilayer without destroying it. Over the last few years, useful information about lipid–protein interactions has started to emerge from high-resolution structural studies of membrane proteins, which sometimes include lipid molecules. The aim of this review is to describe this new structural information and to relate it to what is known about the specificity of lipid–protein interactions and to studies of the effects of lipid structure on the function of membrane proteins.

A number of questions can be asked about how intrinsic membrane proteins interact with the lipids that surround them in a membrane. Do lipid molecules form a distinct shell around a membrane protein or is the hydrophobic, transmembrane region of a membrane protein covered by methylene groups coming from large numbers of fatty acyl chains, some of the chains being parts of lipid molecules with headgroups a long way from the protein? Does the presence of an intrinsic membrane protein affect the proper-

Abbreviations: DGK, diacylglycerol kinase; ESR, electron spin resonance; LPS, lipopolysaccharide; STGA, sulfated triglycosylarchaeol; di(C14:0)PC, dimyristoylphosphatidylcholine; di(C14:1)PC, dimyristoleoylphosphatidylcholine; di(C16:0)PC, dipalmitoylphosphatidylcholine; di(C18:0)PC, distearoylphosphatidylcholine; di(C18:1)PC, dioleoylphosphatidylcholine; di(C20:1)PC, dieicosenoylphosphatidylcholine; di(C22:1)PC, dierucoylphosphatidylcholine; di(C24:1)PC, dinervonylphosphatidylcholine; di(C18:1)PS, dioleoylphosphatidylserine

* Tel.: +44-23-8059-4331; fax: +44-23-8059-4459.
E-mail address: agl@soton.ac.uk (A.G. Lee).

0005-2736/03/$ - see front matter © 2003 Elsevier Science B.V. All rights reserved.
doi:10.1016/S0005-2736(03)00056-7

ties of all the lipids in the membrane or just those in the immediate vicinity of the protein? If there is a distinct shell of lipid molecules around a membrane protein, what are the properties of the lipid molecules in the shell? If there is a distinct shell of lipid molecules around a membrane protein, how does the composition of the annular shell compare with the bulk composition of the membrane? Do all lipid molecules interact with a protein in the same way, or are some lipid molecules more tightly bound than others, acting more like cofactors for a protein than as a simple 'solvent'? Are there particular features of the transmembrane α-helices that help ensure a tight packing into the lipid bilayer? How is the hydrophobic, transmembrane domain of a membrane protein matched to the hydrophobic core of the surrounding lipid bilayer? Does any hydrophobic mismatch between lipid and protein lead to distortion of the lipid bilayer, to distortion of the protein, or to distortion of both? How important are the surrounding lipid molecules in determining the packing of transmembrane α-helices in a membrane protein? What range of lipid structures is compatible with proper function of a membrane protein? Does the phase of the lipid (liquid crystalline, gel or hexagonal H_{II}) affect the function of a membrane protein?

The first information about how lipid molecules might interact with an intrinsic membrane protein came from electron spin resonance (ESR) studies using phospholipid molecules with nitroxide spin labels attached to selected positions in the fatty acyl chains. Spin-labelled lipids incorporated into membranes provide information about the rates and amplitudes of motion of the lipid fatty acyl chains and ESR spectra of spin-labelled lipids in native membranes or reconstituted lipid–protein systems show the presence of a subpopulation of highly immobilised spin labels, not present in protein-free membranes [1–3]. This subpopulation corresponds to lipid molecules whose rotational mobility is impeded by interaction with the protein. The term *immobilised* is used to indicate that the ESR spectrum is that which would be seen in a powder; that is, it corresponds to a random array of spin labels moving only slowly. The lipid is not as well oriented as is the bulk lipid, and it can occupy a broader distribution of orientations; it is disordered. These are the properties that would be expected for lipid molecules in contact with the transmembrane domain of a membrane protein. The rough surface presented by a membrane protein to the surrounding lipid bilayer will result in poor packing unless the lipid fatty acyl chains distort to match the surface of the protein, and poor packing must be avoided to maintain the membrane as an effective permeability barrier. The presence of a rigid protein surface will reduce the extent of the motional fluctuations of the chains and the chains will have to tilt and become conformationally disordered to maximise contact with the surface of the protein. The hydrophobic surface of a membrane protein will therefore be covered by a shell of disordered lipids, referred to as boundary or annular lipids, the latter term referring to the fact that the lipid molecules form a ring or annulus around the protein [4].

The ESR approach can be used to estimate the number of lipid molecules binding to the surface of a membrane protein [1–3]. In a series of studies, Marsh et al. [1] have shown that the number of bound lipid molecules fits reasonably well to the expected circumference of the transmembrane region of the protein. For example, the circumference of the hydrophobic surface of the Ca^{2+}-ATPase of sarcoplasmic reticulum can be estimated from the crystal structure [5] to be about 140 Å. Assuming that a lipid in the liquid crystalline bilayer occupies a surface area of 70 $Å^2$, the effective diameter of a lipid molecule will be 9.4 Å, so that about 30 lipid molecules will be required to form a bilayer shell around the ATPase. The number of lipid molecules forming an annular shell around the Ca^{2+}-ATPase has been estimated from ESR measurements to be 32 at 0 °C [6], in excellent agreement with the dimensions of the Ca^{2+}-ATPase. The close relationship between the numbers of lipid molecules estimated to surround a membrane protein and the circumference of the protein is strong evidence for the presence of a distinct annular shell of lipid molecules around the protein.

ESR studies also report on the length of time that a lipid molecule remains in the annular shell. To observe two distinct environments for lipids on the ESR time scale requires that the time for a lipid molecule to exchange between the annular shell and the bulk phase be long on the ESR time scale, which is about 10^{-8} s. This requirement is met at low temperatures, but, at temperatures closer to physiological temperatures, rates of exchange become appreciable and have characteristic effects on the ESR spectra, which can be used to obtain the on and off rate constants; the on rate constant is diffusion controlled and the off rate constant reflects any specificity in binding [1,7]. Off rates for phosphatidylcholines are typically about $1–2 \times 10^7$ s^{-1} at 30 °C [1]. This is significantly slower than the rate of exchange of two lipid molecules in the bulk phase resulting from translational diffusion in the membrane (ca. 8×10^7 s^{-1} at 30 °C). Thus, it appears that the off rate is lowered by a slightly more favourable lipid–protein interaction than lipid–lipid interaction. The differences are, however, relatively small, suggesting that the lipid–protein interaction is a nonsticky one, consistent with the observation that lipid–protein binding constants depend rather weakly on lipid structure, as described in Section 5.

Molecular dynamics simulations of lipid–protein systems also show that the effects of insertion of a membrane protein into a lipid bilayer are generally restricted to the layer of lipid immediately around the protein, consistent with the idea of a lipid annulus. For example, in molecular dynamics simulations of the gramicidin channel in liquid crystalline dimyristoylphosphatidylcholine [di(C14:0)PC], it was possible to distinguish between phosphatidylcholine molecules next to the channel (phospholipids that were either hydrogen bonded directly to the channel or via one

intervening water molecule) and the 'bulk' phospholipid, not hydrogen bonded to the channel [8,9]. The presence of the channel was found to have no effect on the properties of the bulk phospholipid but increased the order parameters for the fatty acyl chains of the phospholipids bound to the channel. An important result emerging from these simulations was that the range of interaction energies between the bound phospholipids and the channel was very broad; the energies of individual phospholipid–protein interactions fluctuated over a very wide range on a time scale of 50–500 ps [8]. For example, the choline headgroup of the most strongly interacting lipid was involved in electrostatic interactions with gramicidin, and a hydrogen bond had formed between one of the ester groups of the phospholipid and the -NH of Trp-15 of gramicidin. The total interaction energy between the phospholipid and gramicidin molecules represents the sum of many weak van der Waals and electrostatic interactions and so fluctuates widely; there is no single deep energy well into which the phospholipid falls to give a single favoured conformation. Lipid molecules are not frozen in a single long-lived conformation on the protein surface.

As well as the annular shell of lipid molecules around a membrane protein, evidence has been presented from fluorescence-quenching experiments for the presence of other sites on a membrane protein to which hydrophobic molecules can bind; these sites have been called non-annular sites and have been suggested to be located between transmembrane α-helices or at protein–protein interfaces in multimeric membrane proteins [10–12]. The presence of non-annular sites was first suggested to explain effects of cholesterol on the Ca^{2+}-ATPase of sarcoplasmic reticulum that were incompatible with competitive binding of cholesterol and phospholipids to the annular sites around the ATPase [10,13]. Subsequent experiments suggested the presence of non-annular binding sites on the Ca^{2+}-ATPase for a variety of other hydrophobic molecules [12,14], for fatty acids on bacteriorhodopsin [15], and for cholesterol on the acetylcholine receptor [16].

1.1. High-resolution structures

Only a small number of lipid molecules have been resolved in high-resolution X-ray and EM structures of membrane proteins. Since only highly ordered lipid molecules are resolved in these structures, the resolved lipid molecules may not be typical of the bulk of the lipid molecules surrounding a protein in a membrane. Membrane proteins are generally crystallised from detergent solution; crystals of membrane proteins will therefore probably contain less lipid molecules per protein molecule than the native membrane, and the lipid molecules remaining in the crystal could well correspond to a few tightly bound 'special' lipid molecules. It is also possible that packing constraints in the crystal could force the remaining lipid molecules to adopt conformations unlike those in the native membrane. Nevertheless, as described in Section 2, the locations observed for lipid molecules in membrane protein crystal structures are generally compatible with the idea of an annular shell of lipid molecules around a membrane protein and so provide useful information about how lipid molecules interact with membrane proteins in biological membranes.

No high-resolution structure yet available shows a complete annular shell of lipid molecules around a membrane protein. Rather, a micelle-like girdle of disordered detergent molecules, not resolved in the high-resolution structure, covers the hydrophobic, transmembrane region of a protein in a crystal. It is then difficult to identify exactly where the lipid-embedded parts of the transmembrane α-helices start and end. The problem is made more complex by the fact that the lipid bilayer itself is a complex structure. Although it is often represented as a 'slab' of hydrocarbon surrounded by the polar headgroups of the lipids and by water, this is far from the truth. The structure of a bilayer of dioleoylphosphatidylcholine [di(C18:1)PC] in the liquid crystalline phase at relatively low hydration has been determined by a combination of X-ray and neutron diffraction methods (Fig. 1) [17]. The structure is represented by a number of fragments, each described by a Gaussian distribution; the position of the Gaussian describes the most probable location of the fragment and the width of the Gaussian provides an estimate of the range of thermal motion for the fragment, in the direction of the bilayer normal. The narrowest of the regions is that corresponding to the glycerol backbone of the lipid molecule, indicating that this is the most rigid part of the structure (Fig. 1). Extents of motion increase with increasing distance from the backbone, both out to the choline of the headgroup and down the fatty acyl chains to the terminal methyl groups [18]. The hydrocarbon core of the bilayer, shown by the vertical lines in Fig. 1, is made up of the fatty acyl chains, beginning with the C2 carbons, and corresponds closely with the positions of the carbonyl groups [17]. The thickness of the hydrocarbon core (the hydrophobic thickness) defined in this way is 32 Å, but this corresponds to the hydrophobic thickness of a bilayer at low hydration; as discussed in Section 5.3, the thickness of a fully hydrated bilayer will be somewhat less than this. The hydrophobic, transmembrane part of an α-helix is defined here as the part required to span the hydrocarbon core of a lipid bilayer. Given a helix translation of 1.5 Å/residue in a perfect α-helix, about 21 residues are required to span a hydrocarbon core of thickness 32 Å if the helix is untilted with respect to the bilayer normal; a tilt of about 20°, typical of that found in many membrane proteins, would increase this by about 10%. The full length of a transmembrane α-helix may, however, be greater than that of the hydrophobic part because of the need to span the glycerol backbone and lipid headgroup regions of the bilayer and the need to provide hydrogen bonding partners for the initial four -NH and final four -C=O groups of an α-helix. One way is to extend the helix by three or four residues at each end with polar residues containing suitable hydrogen bonding part-

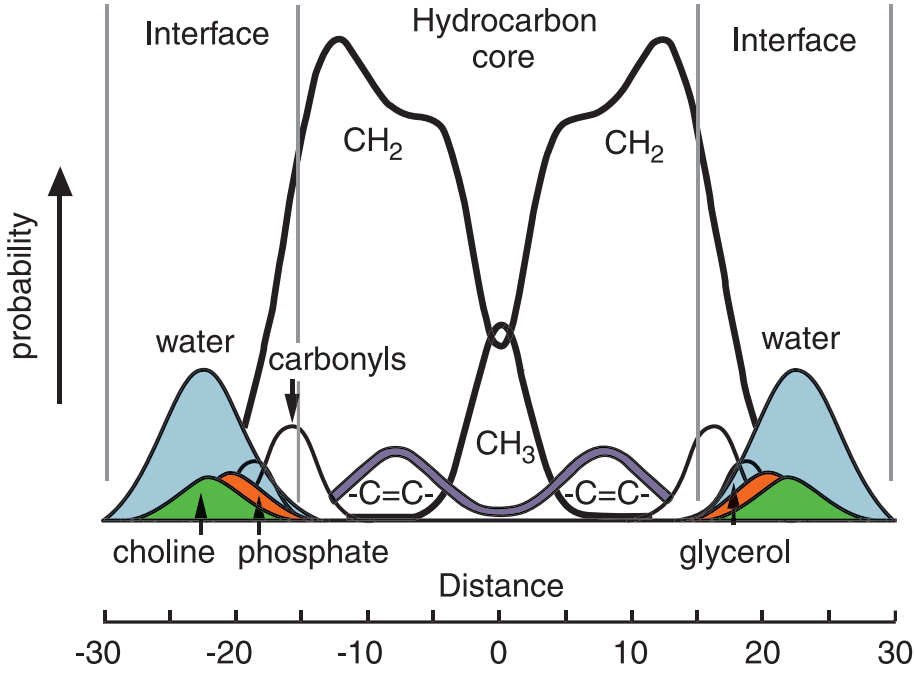

Fig. 1. The structure of a bilayer of di(C18:1)PC at 23 °C and low hydration. The figure shows projections onto the bilayer normal of the time-averaged transbilayer distributions of the principal structural groups. The hydrocarbon core of the bilayer contains the acyl chains beginning with the C2 carbons, and corresponds closely to the position of the carbonyl groups. Modified from Ref. [222].

ners such as Pro and Asn. Alternatively, hydrogen bonds could form with suitable groups in the glycerol backbone and headgroup regions of the lipid bilayer. The result is that there is a degree of uncertainty in where the ends of transmembrane α-helices should be drawn.

Identification of the ends of transmembrane α-helices in crystal structures of membrane proteins is made easier by the fact that Trp and Tyr residues are often found at the ends of the hydrophobic regions of transmembrane α-helices where they have been suggested to act as 'floats' at the interface, serving to fix the helix within the lipid bilayer [19,20]. A preference of Trp residues for the lipid–water interface region of a lipid bilayer reflects the amphipathic nature of the Trp residue; Trp has the largest nonpolar surface of all the amino acids, but its NH group is capable of forming hydrogen bonds. The preference of Trp residues for the interface region has been demonstrated experimentally in studies of the effects of Trp residues on the location of poly-Leu helices in the endoplasmic reticulum membrane [21]. The exact location of the Trp residues at the interface is, however, unclear; some experiments suggest that Trp residues have a preference for the lipid headgroup side of the interface but others suggest that the preference is for the fatty acyl chain side [22–25].

Also helpful in identifying the ends of transmembrane α-helices in membrane protein crystal structures are any unpaired charged residues close to the hydrophobic core of the α-helix. The cost of burying a charged residue within the hydrocarbon core of a lipid bilayer is so high (about 37 kJ mol^{-1} for a Lys residue [26]) that unpaired charged residues at the ends of transmembrane α-helices are much more likely to be located in the headgroup region of the bilayer than in the hydrophobic core of the bilayer. Particularly interesting are Arg and Lys residues; these contain long, flexible side chains consisting of a hydrophobic segment linked to a terminal charged group. These residues can therefore be located within the hydrophobic core of a lipid bilayer 'snorkelling' up to the membrane surface to expose the charged group in the headgroup region of the bilayer, whilst still burying an appreciable fraction of their nonpolar surface area in the core of the bilayer [27]. This effect is well illustrated in a molecular dynamics simulation of the transmembrane α-helix shown in Fig. 2 [28]. The N-terminal end of the helix consisted of the sequence PheTrpGlyLys followed by a stretch of hydrophobic residues. The simulation locates the polar end of the helix in the lipid headgroup region with the Lys residue snorkelling up from the hydrocarbon core of the bilayer to hydrogen bond to both a phosphate and an ester oxygen. The Trp side chain is located close to the glycerol backbone region of the bilayer, hydrogen bonded to the ester oxygen of a lipid molecule. Interactions of this type have been suggested to be important in locking a transmembrane α-helix into the lipid bilayer. Simulations of other transmembrane α-helices also show considerable hydrogen bonding between polar residues at the ends of the helices and lipid polar groups and water [29,30]. Also clear in Fig. 2 is the disruption in packing of the lipid bilayer in the glycerol backbone region caused by the large Trp residue; the Trp side chain has the largest volume of all the amino acid side chains, with a volume of

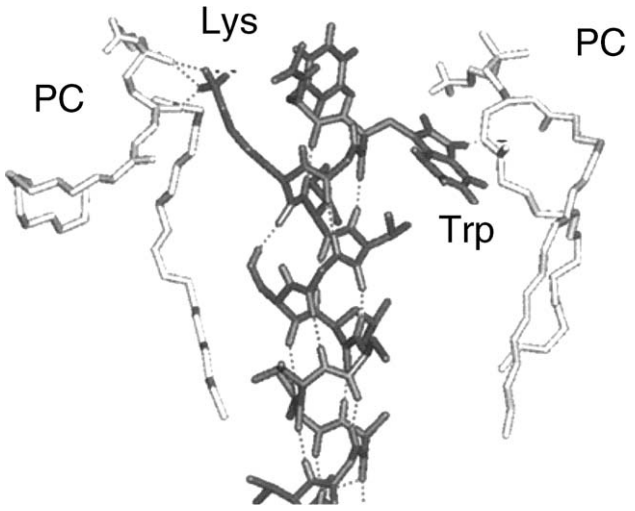

Fig. 2. A snapshot of a molecular dynamics simulation of a transmembrane α-helix in a lipid bilayer. The helix is the sixth transmembrane α-helix of the potassium channel Kv, with an N-terminal sequence PheTrpGlyLys. The Lys side chain can be seen hydrogen bonding to phosphate and ester oxygens of a phosphatidylcholine (PC) molecule, and the Trp side chain forms a hydrogen bond to an ester oxygen. Modified from Ref. [28].

228 Å^3 [31], comparable, for example, to the volume of a phosphatidylcholine headgroup (319 Å^3; [32]).

2. High-resolution structures that include lipid molecules

Membrane proteins are generally purified and crystallised using detergents; in both processes, lipid molecules will be lost from the protein. Nevertheless, some lipid molecules remain and some are sufficiently ordered in the crystal to be resolved at high resolution. An analysis of these lipid molecules can provide much useful information about how a membrane protein is likely to interact with lipid molecules in a biological membrane. The following section describes those membrane proteins whose high-resolution structures show resolved lipid molecules.

2.1. Bacteriorhodopsin

Bacteriorhodopsin forms trimers that pack in the purple membrane of *Halobacterium salinarum* (previously *Halobacterium halobium*) in a hexagonal lattice. Lipid molecules are located between the trimers and within the central space enclosed by each trimer. The purple membrane is about 75% protein by weight, with about 30 lipid molecules per bacteriorhodopsin trimer in the membrane [33,34]; six are positioned in the centre of the trimer with the other 24 surrounding the trimer [35]. The lipids contain mostly phytanyl chains rather than fatty acyl chains and the linkages to the glycerol backbone are by ether rather than ester bonds [36]. The five major classes of lipid present (Fig. 3) are phosphatidylglycerophosphate *O*-methyl ester (24%), sulfated triglycosylarchaeol (STGA; 30%), squalene (20%), phosphatidylglycerol (12%) and phosphatidylglycerosulfate (4%) [34]. Small amounts of two novel lipids have also been detected, each containing two diphytanoylglycerol moieties and, as four-chain lipids, related in structure to cardiolipin [37]. One of the novel lipids, archaeal glycocardiolipin, is based on sulfated triglycosylarchaeol and the other, archaeal cardiolipin, is based on phosphatidylglycerophosphate methyl ester. Archaeal glycocardiolipin makes

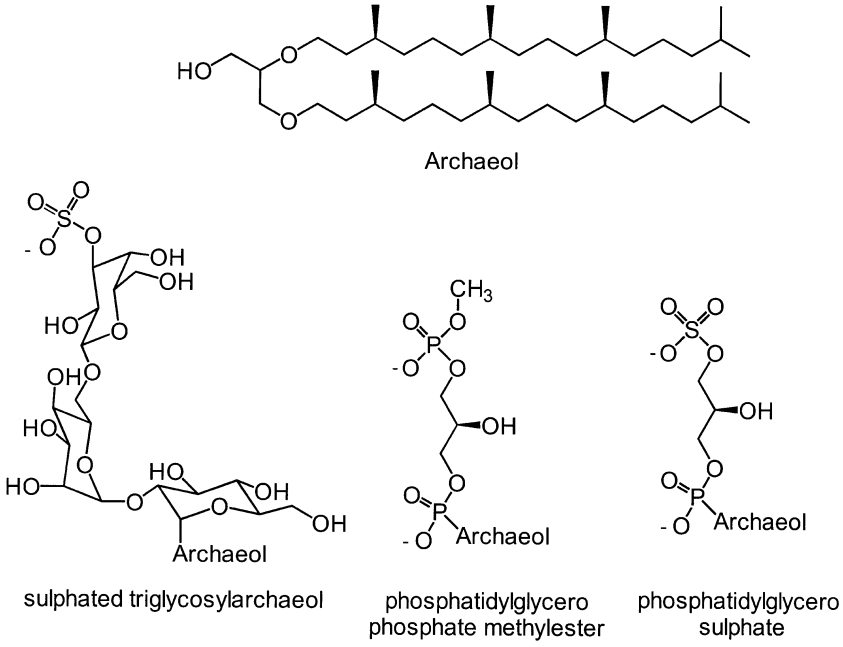

Fig. 3. Structures of the three major polar lipids found in the purple membrane of *H. salinarium*. The lipids are derivatives of 2,3-di-*O*-phytanyl-*sn*-glycerol (archaeol).

up about 10% of the lipid in the purple membrane, with just small traces of archaeal cardiolipin [34]. The membrane has an unusually high negative charge because of the presence of sulfate and phosphate headgroups on many of the lipids.

The locations of the various classes of lipid within the purple membrane are not known, except for STGA. Studies of the binding of ferritin-labelled avidin to purple membranes biotinylated with a reagent specific for sugar residues has shown STGA to be located only in the extracellular leaflet of the purple membrane [38]. Neutron diffraction studies of plasma membranes labelled with deuterated glycolipids showed STGA molecules in the space in the middle of the trimers and in the spaces between the trimers [39].

Several lipid molecules have been localised in electron crystallographic structures of bacteriorhodopsin, in the space in the middle of the trimer and in the regions between trimers [40,41]. Lipids are also seen in X-ray crystal structures of bacteriorhodopsin in a hexagonal lattice identical to that in the purple membrane [35,42]. In these structures, the lipid headgroups are disordered, suggesting considerable mobility for the headgroups, but with a number of well-defined density features that corresponded to phytanyl chains. Belrhali et al. [35] modelled the lipids as 2,3-di-*O*-phytanyl-*sn*-propane. Luecke et al. [42] identified 18 lipid chains, eight of which were modelled as four diether lipids. Fig. 4 shows some of the lipids located at the trimer surface [35]. Clear is the considerable static disorder of the chains on the surface of the protein, the rotational disorder of the chains presumably being necessary to obtain good van der Waals contacts with the molecularly rough surface of the bacteriorhodopsin trimer. Despite this disorder, it is noticeable that all of the lipid molecules adopt extended structures; none of the lipid molecules bend back on themselves. It is also clear that the glycerol backbones of the lipid molecules are aligned in planes on the two faces of the membrane, defining a fairly uniform hydrophobic thickness for the lipid annulus around the protein. This is a nontrivial result and suggests that the lipid bilayer can be pictured as extending right up to the membrane protein. The average distance between the glycerol backbone oxygens for lipids on the two sides of the membrane is about 35 Å (Fig. 4; Table 1).

Charged residues often mark ends of transmembrane α-helices. This is illustrated in Fig. 4 for helix A of bacteriorhodopsin where the charged groups of Arg-7 and Glu-9 are located just above the glycerol backbone region of the bilayer on the extracellular side and Lys-30 is located with its charged NH_3^+ group just in the glycerol backbone region of the bilayer, on the cytoplasmic side. Trp-10 is located with its ring system within the hydrocarbon core of the bilayer but with its -NH group in the glycerol backbone region. The other Trp residues on the extracellular side are also located just below the plane defined by the glycerol backbones, forming a girdle on the extracellular side of the membrane. There is no corresponding girdle of Trp residues on the cytoplasmic side.

The disorder of the chains seen in Fig. 4 is consistent with the results of molecular dynamics simulations of the

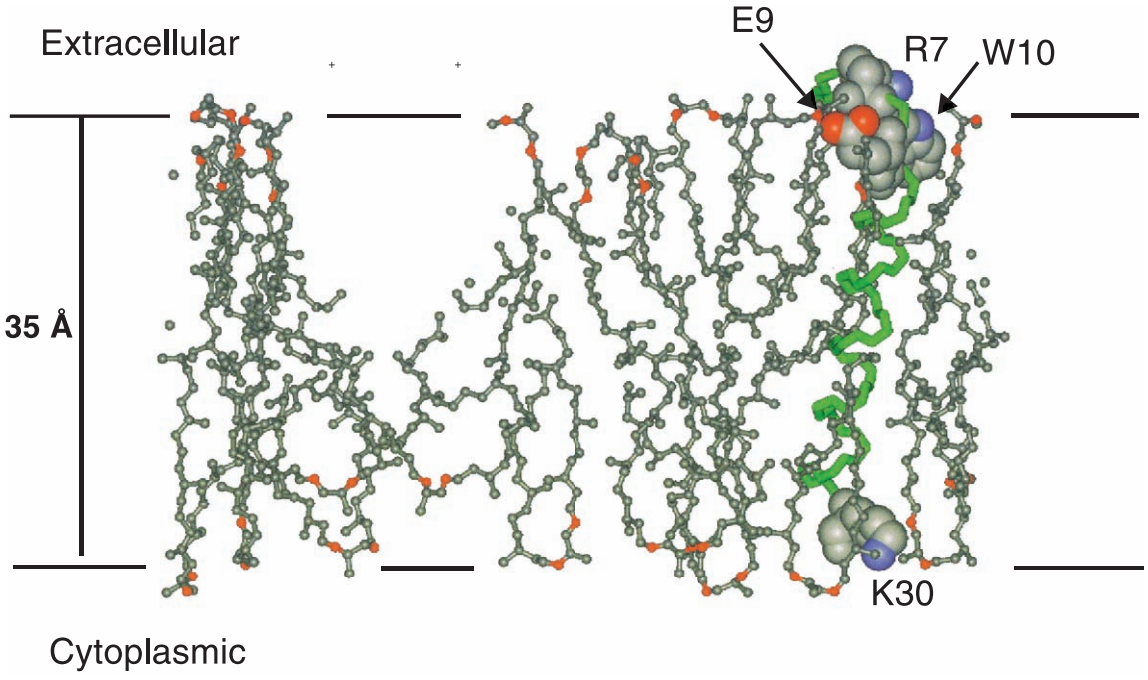

Fig. 4. Structures of lipid molecules identified in an X-ray crystallographic study of bacteriorhodopsin [35]. The lipids are those associated with the outer surface of the bacteriorhodopsin trimer and have been modelled as 2,3-di-*O*-phytanyl-*sn*-propane. The oxygens are shown in red. Also shown is helix A (green) of one of the monomers with Arg-7, Glu-9 and Trp-10 at the extracellular end of the helix and Lys-30 at the cytoplasmic end of the helix in space-fill representation. These residues lie at the extracellular and cytoplasmic surfaces of the membrane, shown by the horizontal lines 35 Å apart. (PDB file 1QHJ).

Table 1
Hydrophobic thicknesses for intrinsic membrane proteins estimated from high-resolution structures

Protein	PDB code	Hydrophobic thickness (Å)
Seven helix proteins		
Bacteriorhodopsin	1QHJ	35[a]
Halorhodopsin	1E12	29[b]
Sensory rhodopsin II	1JGJ	27[b]
Rhodopsin	1F88	35[b]
Bacterial photosynthetic reaction centres		
Rhodobacter sphaeroides	1QOV	28[c]
Rhodopseudomonas viridis	1DXR	31[b]
Thermochromatium tepidum	1EYS	28[c]
Bacterial light-harvesting complexes		
Rhodopseudomonas acidophila	1KZU	31[b]
Rhodospirillum molischianum	1LGH	31[b]
Photosystem I		
Synechococcus elongates	1JBO	32[c]
Cytochrome *c* oxidase		
Paracoccus denitrificans	1QLE	33[a]
Thermus thermophilus	1EHK	31[b]
Bovine heart mitochondria	2OCC	29[b]
Ubiquinol oxidase		
Escherichia coli	1FFT	29[b]
Cytochrome bc_1 complexes		
Bovine heart mitochondria	1BE3	32[b]
Saccharomyces cerevisiae	1KB9	21 or 28[a]
Fumerate reductase		
Escherichia coli	1KF6	25[b]
Wolinella succinogenes	1QLA	25[b]
Channels		
KcsA potassium channel of *Streptomyces lividans*	1K4C	37[c]
MscL mechanosensitive channel of *Mycobacterium tuberculosis*	1MSL	18 or 34[b]
ClC chloride channel from *Escherichia coli*	1KPK	23[b]
GlpF glycerol facilitator of *Escherichia coli*	1FX8	26[b]
AQP1 aquaporin of bovine red blood cells	1J4N	26[b]
P-type ATPase		
Ca^{2+}-ATPase of skeletal muscle sarcoplasmic reticulum	1EUL	21[b]
β-barrel membrane proteins		
OmpF of *Escherichia coli*	2OMF	24[b]
Maltoporin of *Salmonella typhimurium*	2MPR	22[b]
OmpA of *Escherichia coli*	1QJP	24[b]
OmpX of *Escherichia coli*	1QJ8	24[b]
FhuA of *Escherichia coli*	1FCP	24[c]

[a] Measured as the separation between lipid glycerol backbone oxygens on the two sides of the membrane.
[b] Measured as the minimum separation between charged residues and Trp residues on the two sides of the membrane.
[c] Measured as the minimum separation between lipid glycerol backbone oxygens on one side of the membrane and Trp residues on the other.

bacteriorhodopsin trimer in a bilayer of diphytanyl phosphatidylglycerophosphate, where the lipid molecules were seen to tilt and become conformationally disordered to allow them to nestle against the surface of the protein [43]. The calculated order parameters for the chains were low, as in a lipid bilayer in the liquid crystalline phase, but the reasons for the low-order parameters were different. In the liquid crystalline phase, extensive movement of the chains gives a low-order parameter; in the purple membrane, the low-order parameters are caused mainly by a static tilt of the chains; the chains in the purple membrane behave more like parts of the proteins than parts of a fluid lipid phase, consistent with the idea of an annular lipid shell [43]. Good van der Waals contact between the phytanyl chains and the surface of the protein is ensured by binding of some at least of the lipid molecules in distinct grooves on the hydrophobic surface of the protein, formed by specific arrangements of the side chains. Lipid molecules are associated with these grooves along their length. The nature of these grooves is more apparent in Fig. 5, which shows part of the lipid-exposed surface of the bacteriorhodopsin molecule with identified bound lipid molecules.

Although lipid headgroups are generally not visible in crystal structures of bacteriorhodopsin, an X-ray diffraction study of the bacteriorhodopsin trimer crystallised in an arrangement different to that in the native membrane did reveal STGA headgroups in the middle of the trimer [44]. Although only two STGA molecules were observed in the structure, the symmetry of the system suggests that three STGA molecules will be located at the centre of the trimer [44]. The binding site for STGA is illustrated in Fig. 6. The STGA headgroup interacts with the faces of two bacteriorhodopsin monomers, on the extracellular side of the membrane. The structure shows Tyr-64 forming a hydrogen bond with a glycerol oxygen of the lipid, and the hydroxyl group of Thr-67 forming a hydrogen bond with the hydroxyl groups of the glucose and mannose moieties of the lipid headgroup. Hydrogen bonds are also formed between a hydroxyl group of mannose and the

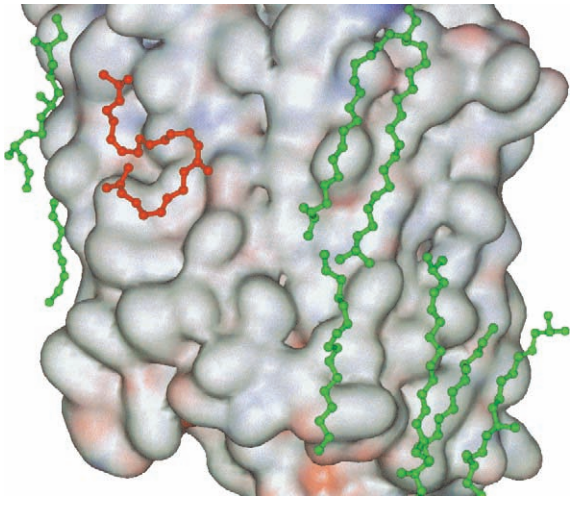

Fig. 5. The surface of the bacteriorhodopsin molecule showing bound lipid molecules (green). A squalene molecule is shown in red. (PDB file 1C3W).

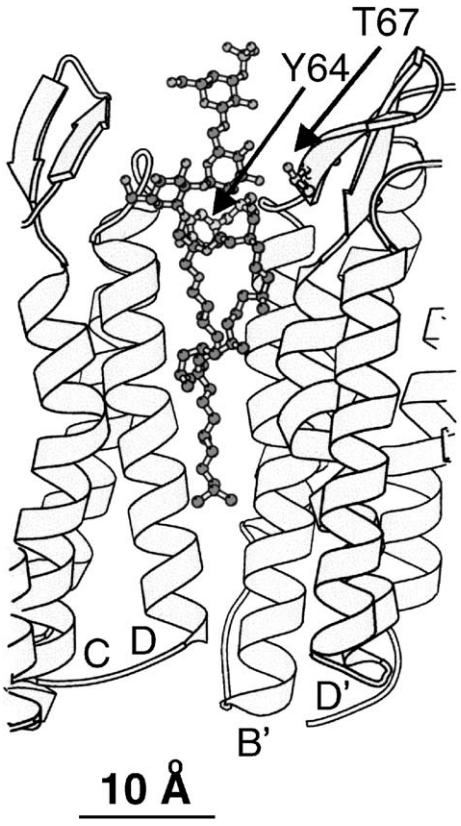

Fig. 6. The structure of an STGA molecule bound at the interior of the bacteriorhodopsin trimer. The view is from the trimer interior with the extracellular face at the top. Helices from two neighbouring bacteriorhodopsin monomers are marked. Tyr-64 and Thr-67 with which STGA forms hydrogen bonds are shown in ball-and-stick representation. This and other figures were produced using Bobscript [228]. (PDB file 1BRR).

backbone carbonyl oxygens of Tyr-64 and Leu-66. An electrostatic interaction between Lys-129 and the lipid sulfate group is also possible [44]. Since the locations of the STGA headgroups correspond to the positions of the most ordered phytanyl chains, it is likely that these STGA molecules are tightly bound to bacteriorhodopsin [39]. Strong binding will be partly the result of favourable interactions between the lipid headgroup and the protein, but favourable hydrophobic interactions will also be important with one of the phytanyl chains of the lipid binding in a cleft formed by Gly residues on helix D (Fig. 6).

Fig. 5 shows a probable binding site for squalene on bacteriorhodopsin, located in a groove on the protein surface within the hydrophobic core of the bilayer [42]. Unlike the lipid molecules, all of which adopt an essentially extended conformation, the squalene molecule adopts an S shape. The squalene molecule is located near to a distorted region of helix G, thought to be an important feature of the bacteriorhodopsin molecule, consistent with the fact that the presence of squalene affects the photochemical cycle of bacteriorhodopsin [45].

2.2. The potassium channel KcsA

The potassium channel KcsA of *Streptomyces lividans* is a homotetramer [46,47]. The Trp residues in KcsA form clear girdles at the two faces of the lipid bilayer, the rings of the Trp residues being almost parallel to the surface of the membrane (Fig. 7). Tyr residues also form a clear girdle 'above' the band formed by the Trp residues on the extracellular side of the membrane. Above and below the girdles of aromatic residues on the two sides of the membrane are girdles of charged residues, Arg-52, Arg-64, Arg-89 and Glu-51 on the extracellular side and Arg-27, Arg-117, Arg-121, Glu-118 and Glu-120 on the intracellular side. These residues presumably provide charged residues required for good interaction with the lipid headgroup region of the bilayer. Of the five Trp residues in KcsA, Trp-26 and Trp-113, at the intracellular ends of transmembrane α-helices M1 and M2, respectively, are exposed to the lipid bilayer. At the extracellular end of M2, Trp-87 is also exposed to the lipid bilayer, but Trp-67 and Trp-68 are located away from the lipid–protein interface as part of the short pore helix that points into the intracellular cavity.

Two partial lipid molecules are seen in the X-ray structure (Fig. 8), one modelled as nonan-1-ol and the other as a diacylglycerol with one C14 and one C9 chain [47]. Purified KcsA contains ca 0.7 phosphatidylglycerol molecules per KcsA monomer so that the molecule modelled as a diacylglycerol is probably a phosphatidylglycerol whose headgroup is too disordered to be resolved [48]. The diacylglycerol moiety of the lipid binds into a groove on the surface close to Trp-87, between two monomers in the tetrameric structure. The first nine carbons of the *sn*-1 chain are located in a groove between the pore helix of one monomer and the transmembrane α-helix M2 of the

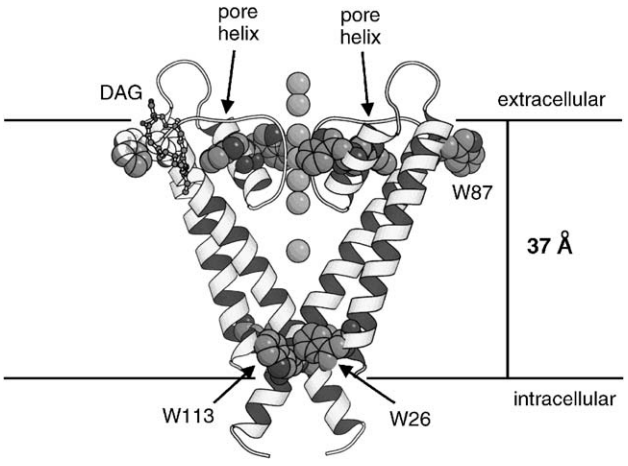

Fig. 7. Location of Trp residues in the potassium channel KcsA. For clarity, only two monomers from the tetrameric structure are shown. The Trp residues are shown in space-fill representation. The lipid molecule modelled as a diacylglycerol (DAG) is shown in ball-and-stick representation. Also shown are the positions of the K^+ ions moving through the selectivity filter. (PDP file 1K4C).

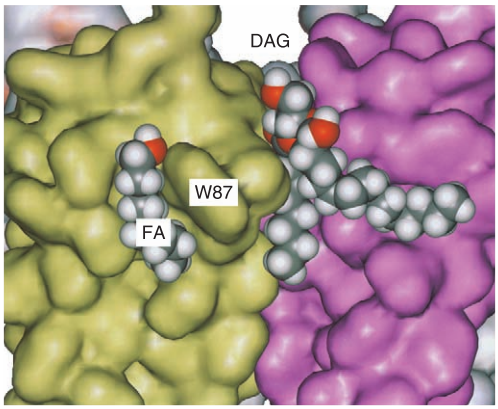

Fig. 8. The surface of the KcsA channel on the extracellular side of the membrane, showing two partial lipid molecules, modelled as a DAG molecule and a fatty alcohol (FA) binding to grooves on the protein surface close to Trp-87. The DAG molecule binds at the interface between two monomers, shown in yellow and purple. (PDP file 1K4C).

adjacent monomer. The first 14 carbons of the *sn*-2 chain are located more peripherally on the surface of the pore helix and the transmembrane α-helix M1 of the same monomer. The single chain modelled as nonan-1-ol is located in a groove between transmembrane α-helices M1 and M2 of a single monomer (Fig. 8). The anionic headgroup of the phosphatidylglycerol molecule probably interacts with Arg-64 and Arg-89 located in the girdle of charged residues above Trp-87. The interaction appears to be relatively nonspecific since there is little difference between the affinity of KcsA for phosphatidylserine, phosphatidic acid and phosphatidylglycerol (Alvis, Williamson, East and Lee, unpublished observations).

As shown in Figs. 7 and 8, the diacylglycerol molecule is located with the Trp ring system of Trp-87 just below the glycerol backbone of the diacylglycerol. This is consistent with ESR studies of KcsA in lipid bilayers that suggest that Trp-87 is located close to the glycerol backbone region of the lipid bilayer [49]. Trp-113 on the intracellular side of the membrane has also been suggested, on the basis of ESR results, to be located within the hydrocarbon region of the bilayer [50]. If, like Trp-87, Trp-113 is located just below the glycerol backbone region, the thickness of the hydrocarbon core of the lipid bilayer would be about 37 Å, similar to the thickness of a bilayer of di(C22:1)PC.

2.3. Photosynthetic reaction centre

The X-ray crystal structure of an Ala to Trp mutant of the photosynthetic reaction centre from the purple bacterium *Rhodobacter sphaeroides* contains a cardiolipin molecule bound to the hydrophobic surface of the protein [51]. Cardiolipin is a minor component of the cytoplasmic membrane of many purple bacteria; its function in the membrane is not yet known [51]. The photosynthetic reaction centre contains three subunits, L, M and H, and the transmembrane region of the reaction centre consists of a bundle of 11 transmembrane α-helices, five each from the L and M subunits and one from the H subunit (Fig. 9). Within the bundle are a number of chlorophyll, ubiquinone and carotenoid cofactors. The cardiolipin molecule occupies a depression in the transmembrane surface of the reaction centre, located between the single transmembrane α-helix of the H subunit and transmembrane α-helices 3 and 5 of the M subunit, on the cytoplasmic face of the membrane (Fig. 10). It is involved in a number of hydrogen bonding interactions, including interactions between phosphate oxygens of the lipid headgroup and the side chains of His-145 and Arg-267 of the M subunit, and the backbone amide of Lys-144 in subunit M (Fig. 10). Indirect interactions mediated by water molecules are also made with Lys-144, Trp-148, Arg-267 and Trp-271 of the M subunit, and Tyr-30 of the H subunit. The fatty acyl chains are located in grooves in the hydrophobic surface of the protein. The result is that the lipid headgroup and the upper parts of the chains are immobile, and so are well resolved in the electron density maps, whereas the ends of the chains are mobile and disordered and do not appear in the X-ray structure [51].

The specificity of the binding site for cardiolipin presumably follows from the unusual, four-chain structure of cardiolipin and from its small headgroup; the region of the protein overlying the binding site could limit the size of the headgroup that can bind. Nevertheless, other hydrophobic molecules can bind to this site since crystal structures of other bacterial photosynthetic reaction centres show detergent molecules in the groove between transmembrane α-helices M3 and M5, in a location corresponding to the most deeply buried fourth chain of cardiolipin [52].

The photosynthetic reaction centre contains a relatively large number of Trp residues, most of which are located in

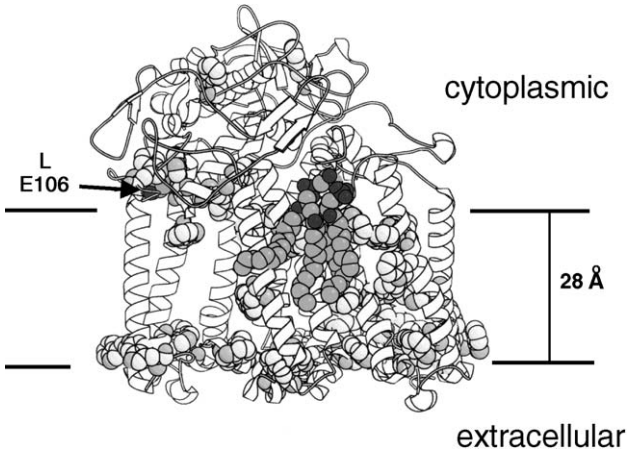

Fig. 9. The photosynthetic reaction centre of *R. sphaeroides* showing the bound cardiolipin molecule. Trp residues are shown in space-fill representation. The glycerol backbone region of the cardiolipin molecule, also shown in space-fill representation, defines the cytoplasmic surface of the bilayer. The position of Glu-106 in subunit L also helps define the cytoplasmic surface. The extracellular surface is well defined by the girdle of Trp residues, giving a hydrophobic thickness of about 28 Å for the bilayer. (PDB file 1QOV).

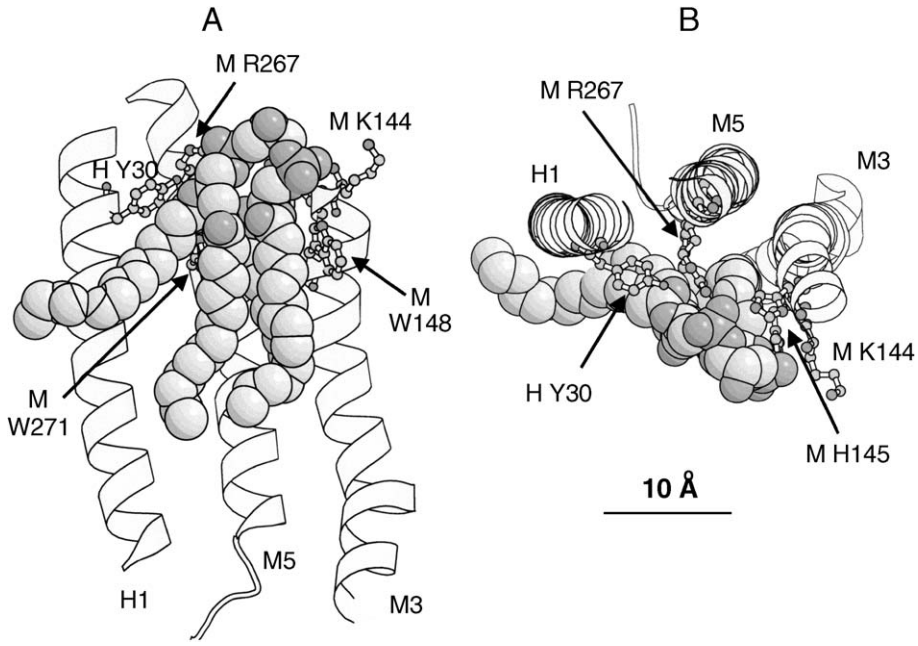

Fig. 10. The location of the binding site for cardiolipin on the photosynthetic reaction centre. (A) shows a side view and (B) a view from the cytoplasm. The binding site is located in a depression between the single transmembrane α-helix of subunit H and transmembrane α-helices 3 and 5 of the M subunit. Residues involved in interaction with the cardiolipin molecule (shown in space-fill representation) are shown in ball-and-stick representation. (PDB file 1QOV).

the transmembrane region of the protein (Fig. 9). Two girdles of Trp residues exposed to the lipids can be identified; that on the cytoplasmic side of the membrane contains four Trp residues, and that on the external surface contains 16 Trp residues, many of which serve to anchor interhelical loops into the membrane surface (Fig. 9). If it is assumed that the glycerol backbone region of the bound cardiolipin molecule defines the cytoplasmic boundary of the hydrocarbon core of the bilayer, then the lipid-exposed Trp residues on the cytoplasmic side of the membrane are located just within the hydrocarbon core of the bilayer. Helping to define the cytoplasmic surface is the charged Glu-106 residue in subunit L (Fig. 9). Assuming that the Trp residues on the extracellular surface of the membrane are also located just within the hydrocarbon core of the bilayer gives a hydrophobic thickness of about 28 Å for the protein.

Camara-Artigas et al. [53] have identified two other lipid molecules in a crystal structure of the photosynthetic reaction centre from *R. sphaeroides*, a phosphatidylcholine and a glucosylgalactosyl diacylglycerol. These lipids are suggested to adopt very unusual orientations in the membrane, the phosphatidylcholine lying almost parallel to the membrane surface and the glucosylgalactosyl diacylglycerol being buried with its headgroup close to the centre of the membrane (Fig. 11). The disaccharide group of the glycolipid is proposed to be located near to a molecule of bacteriochlorophyll with its fatty acyl chains close to an isoprenoid chain of a quinone [53]. The phosphatidylcholine molecule is bound at the interface between the L and M subunits with its phosphate group close to a molecule of bacteriopheophytin. The suggested locations for the phosphatidylcholine and glucosylgalactosyl diacylglycerol molecules in *R. sphaeroides* are very different to those reported for lipid molecules identified in other protein crystal structures.

The crystal structure of the photosynthetic reaction centre from the purple bacterium *Thermochromatium tepidum* shows a detergent molecule occupying the site occupied by cardiolipin in the photosynthetic reaction centre of *R. sphaeroides* but shows a phosphatidylethanolamine molecule bound at a further site, as shown in Fig. 12 [54]. In this case, the fatty acyl chains of the lipid are not located within grooves on the protein surface but, rather, interact with the exposed chains of two bacteriochlorophyll and one quinone molecule [54]. The headgroup of the phosphatidylethanolamine interacts electrostatically with Arg-31 and Lys-35 of the H subunit, with hydrogen bonds between the phosphate group and Tyr-39 of the H subunit and between the $-NH_3^+$ group and Gly-256 of the M subunit (Fig. 12). The phosphatidylethanolamine molecule binds in a sideways-on fashion, as does the cardiolipin molecule in *R. sphaeroides*.

The pattern of interactions around the phosphatidylethanolamine headgroup makes it likely that this site will show a preference for phosphatidylethanolamine over other lipids. For example, a phosphatidylcholine molecule would be expected to bind weakly at the site because of steric clashes with the bulky choline group and because of the loss of the hydrogen bonding interaction with the $-NH_3^+$ group in phosphatidylethanolamine. This is important because, in some cases, effects of phosphatidylethanolamines on membrane protein function have been interpreted in terms of the effects of phosphatidylethanolamines on bulk properties of

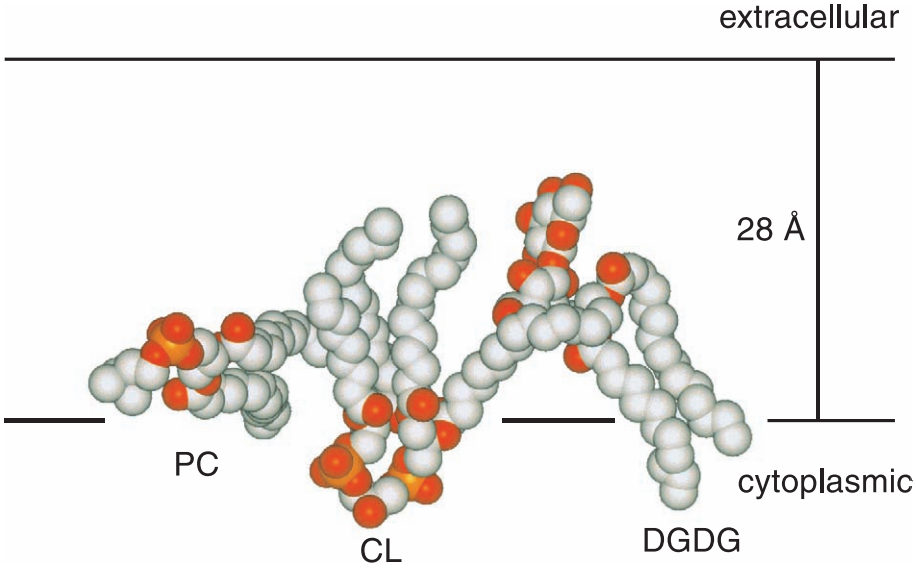

Fig. 11. Bound lipid molecules in the photosynthetic reaction centre of *R. sphaeroides*. Shown are the lipid molecules identified by Camara-Artigas et al. [53]: PC, phosphatidylcholine; CL, cardiolipin; DGDG, glucosylgalactosyl diacylglycerol. The probable locations of the membrane surfaces are shown, as defined in Fig. 9 (PDB file 1M3X).

the bilayer such as internal pressure, as described in Section 8.2. Clearly, effects due directly to the specific headgroup structure of phosphatidylethanolamine need to be considered as well as any effects that might arise indirectly from effects on the bulk properties of the bilayer.

The two girdles of Trp residues are clearer in *T. tepidum* than in *R. sphaeroides* because there are less Trp residues in the middle of the hydrocarbon core of the bilayer in *T. tepidum* than in *R. sphaeroides* (compare Figs. 9 and 12). Again assuming that the glycerol backbone region of the lipid defines the cytoplasmic edge of the hydrocarbon core of the bilayer and that the girdles of Trp residues are located just within the hydrocarbon core, the hydrophobic thickness for the protein will be about 28 Å (Fig. 12; Table 1).

Four lipid molecules have been identified in the crystal structure of Photosystem I of the cyanobacterium *Synechococcus elongates*, three molecules of phosphatidylglycerol and one molecule of monogalactosyldiglyceride [55]. These are all located on the stromal side of the membrane with their glycerol backbones lying in a plane also defined, for example, by Trp-21 of subunit PsaB (Fig. 13). Charge groups and Trp residues define the location of the lumenal surface, with a hydrophobic thickness for the bilayer of about 32 Å (Fig. 13).

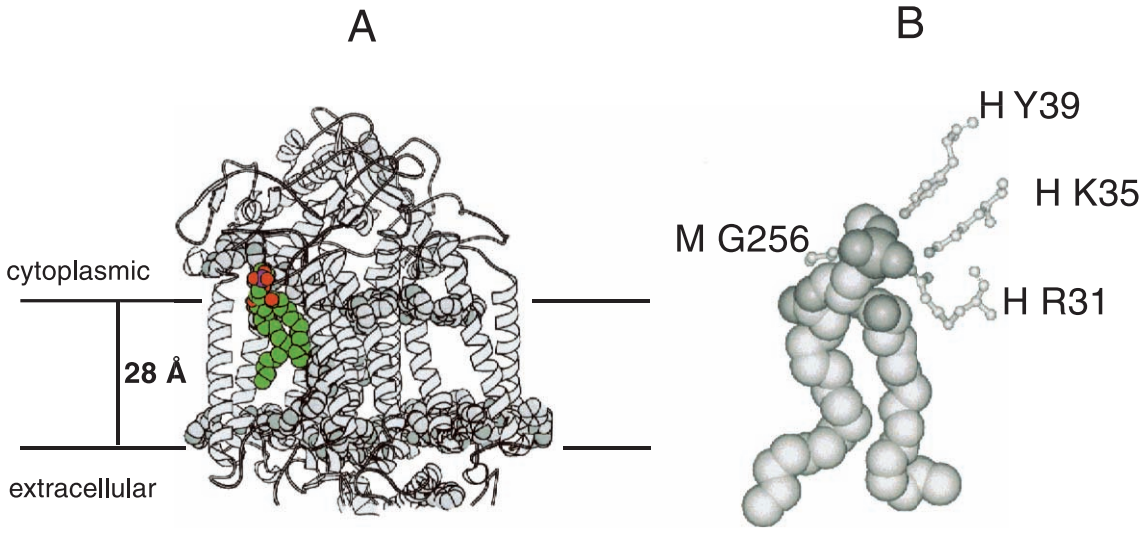

Fig. 12. The photosynthetic reaction centre from *T. tepidum* showing the bound phosphatidylethanolamine molecule. (A) The structure with the Trp residues and the bound phosphatidylethanolamine shown in space-fill representation. The location of the Trp residues and of the glycerol backbone of the bound phosphatidylethanolamine molecule define a hydrophobic thickness of about 28 Å for the bilayer. (B) The phosphatidylethanolamine molecule (in space-fill representation) and the residues with which the lipid headgroup interact. (PDB file 1EYS).

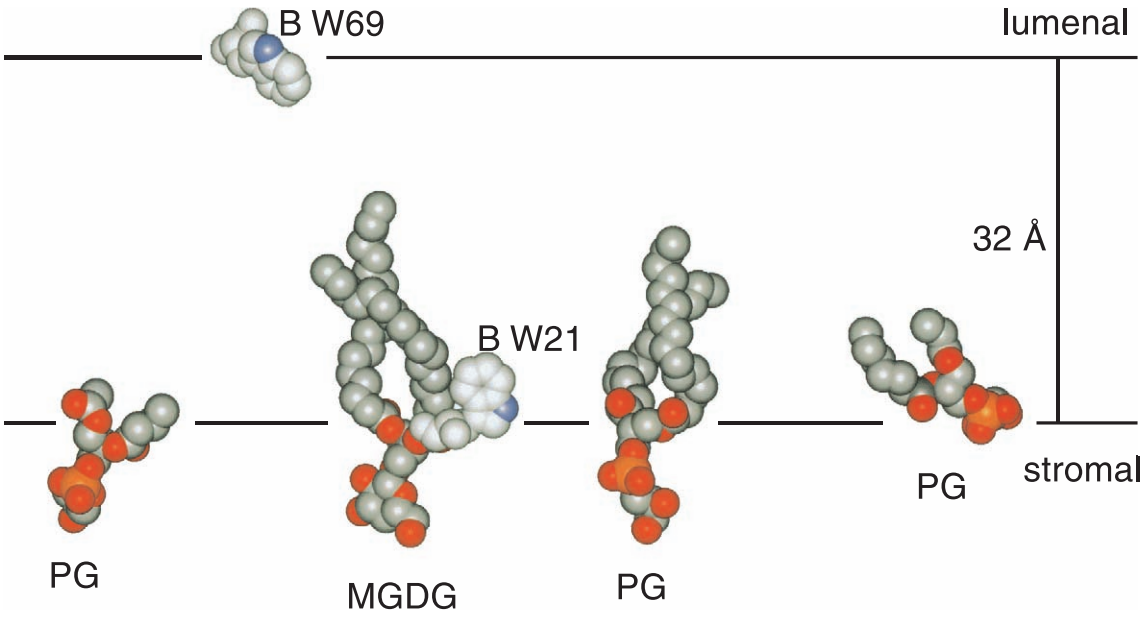

Fig. 13. Bound lipid molecules in Photosystem I of the cyanobacterium *S. elongates*. The three phosphatidylglycerol (PG) molecules and the molecule of monogalactosyl diglyceride (MGDG) define the stromal surface of the membrane, consistent with the location of Trp residues such as Trp-21 of subunit PsaB (B), as shown. A possible location for the lumenal side of the membrane is also shown, defined, for example, by the location of Trp-69 of subunit PsaB. (PDB file 1JBO).

2.4. Cytochrome c oxidase and cytochrome bc_1

Cytochrome *c* oxidase is a large complex of four-membrane-embedded subunits with 22 transmembrane α-helices. The crystal structure of cytochrome *c* oxidase from *Paracoccus denitrificans* includes two molecules of phosphatidylcholine, one on each side of the membrane [56,57]. Both lipid molecules bind edge-ways on in deep grooves in the protein surface, as shown in Fig. 14. The phosphate and quaternary ammonium groups of the lipid headgroups form ion pairs with Arg and Asp or Glu residues (Arg-233 and Glu-74 of subunit III for the lipid on the periplasmic side and Arg-198 of subunit II and Asp-124 of subunit III for the lipid on the cytoplasmic side). The separation between the glycerol backbones of the lipids on the two sides of the membrane is about 33 Å and girdles of Trp residues are again located just within the hydrocarbon core of the lipid bilayer, as defined by the positions of the two glycerol backbones, although some Trp residues are also located in the lipid headgroup regions.

The crystal structure of bovine heart cytochrome *c* oxidase contains eight lipid molecules modelled as phosphatidylethanolamines and phosphatidylglycerols [58] but these have not been included in the structure deposited in the Protein Data Bank. The headgroups are reported to be bound by salt bridges and hydrogen bonds and the phospholipid fatty acyl chains are involved in hydrophobic interactions [58].

Cytochrome bc_1 (ubiquinol:cytochrome *c* oxidoreductase) is a homodimer mediating electron transfer between quinones in the inner mitochondrial membrane and cytochrome *c* in the intermembrane space. Cytochrome bc_1 contains a tightly bound cardiolipin molecule, believed to be essential for activity; other mitochondrial proteins such as the ADP–ATP carrier and cytochrome *c* oxidase also require cardiolipin for activity [59]. The crystal structure of yeast cytochrome bc_1 shows five resolved lipid molecules per monomer: one cardiolipin, two phosphatidylethanolamines, one phosphatidylcholine and one phosphatidylinositol [60]. One phosphatidylethanolamine molecule and the phosphatidylcholine and phosphatidylinositol molecules are bound in large clefts at the dimer interface, the other two lipid molecules being bound to the transmembrane surface of the protein (Fig. 15). The phosphatidylcholine molecule is stabilised by a hydrogen bond between His-22 of the cytochrome *b* subunit and the phosphate moiety of the lipid headgroup [60]. Binding of the phosphatidylethanolamine molecule at the dimer interface is also stabilised by hydrogen bonding, this time to backbone oxygens. The lipid interacts with both monomers at the interface and so could be important for dimer formation [60]. The phosphatidylinositol molecule is in an unusual arrangement, wrapped around the transmembrane α-helix of the Rieske protein with the ends of the fatty acyl chains pointing towards the interface [60]. The highly distorted structure for the phosphatidylinositol chains is apparent in Fig. 16. The phosphate forms an ion pair with Lys-272 in cytochrome c_1 and the hydroxyl groups of the inositol ring form several hydrogen bonds with neighbouring amino acid residues; the phosphatidylinositol molecule could serve to anchor the Rieske protein to the rest of the complex [60]. It has also been suggested that the presence

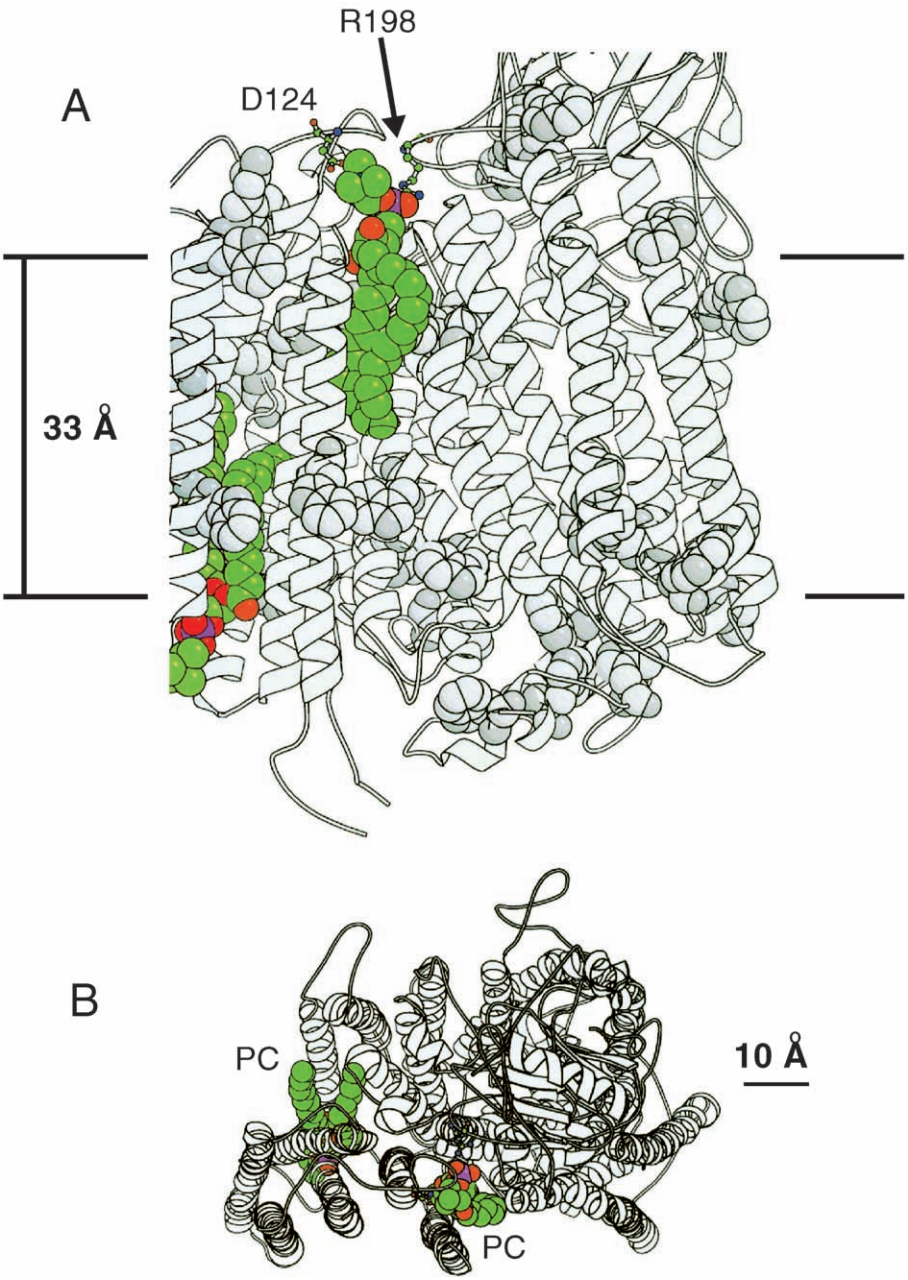

Fig. 14. The binding sites for phosphatidylcholine on cytochrome *c* oxidase of *P. denitrificans*. The top shows part of the transmembrane region of the protein, showing the two bound phosphatidylcholine molecules. On the periplasmic side, salt bridges are formed between the phosphate and quaternary ammonium in the lipid headgroup and, respectively, Arg-198 in subunit II and Asp-124 in subunit III, shown in ball-and-stick representation. The bottom shows a view of the complex from the periplasm, showing how the phosphatidylcholine molecules (PC) bind in deep grooves in the side of the protein. (PDB files 1QLE).

of phospholipid molecules at the dimer interface could provide a hydrophobic surface aiding the diffusion of ubiquinol and uniquinone in and out of their protein binding sites [60].

The phosphatidylethanolamine and cardiolipin molecules located on the surface of the protein bind in grooves on the surface (Fig. 15). The amine group of the phosphatidylethanolamine molecule interacts with Glu-82 of subunit VII and the phosphate group hydrogen bonds to two Tyr residues (Fig. 15). A Trp residue is located with its indole N atom very close to the glycerol backbone of the lipid. One of the acyl chains is highly kinked, inserting into a narrow channel between the transmembrane α-helices of cytochrome *b*. The cardiolipin molecule makes many hydrogen bonds with neighbouring residues, and, via a water molecule, with the headgroup of the neighbouring phosphatidylethanolamine molecule. Interactions in the cardiolipin headgroup region are similar to those at the cardiolipin binding site in the reaction centre from *R. sphaeroides* (Section 2.3). It has been suggested that cardiolipin has a

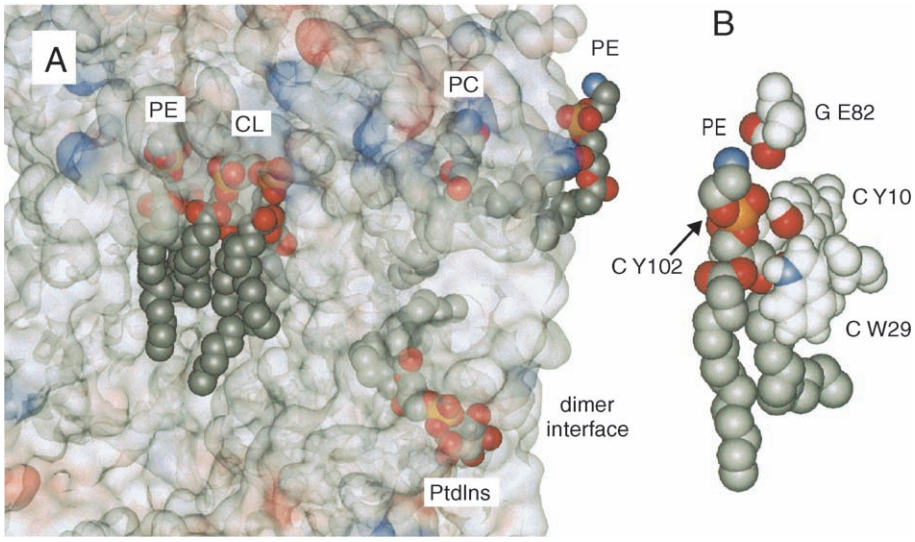

Fig. 15. The transmembrane surface of cytochrome bc_1 with bound lipid molecules. (A) The surface of a monomer from the heterodimeric cytochrome bc_1 is shown, coloured by electrostatic potential (red, negative; blue, positive; grey, neutral). Five lipid molecules are resolved, shown in space-fill representation. The location of the dimer interface is marked. (B) The phosphatidylethanolamine molecule bound to the surface of the protein (on the left) is shown in the same orientation as in (A) together with residues interacting with it. PE, phosphatidylethanolamine; PC, phosphatidylcholine; CL, cardiolipin, PtdIns, phosphatidylinositol; C, cytochrome *b*; G; subunit VII. (PDB file 1KB9).

structural role in cytochrome bc_1, in either the assembly or stability of the enzyme; it could also have a functional role since the bound cardiolipin molecule is located close to the site of quinone reduction where it could be part of a proton 'wire' conducting protons from the aqueous phase to the quinone headgroup [60].

Four of the resolved lipid molecules are on the mitochondrial matrix side of the membrane and one is on the

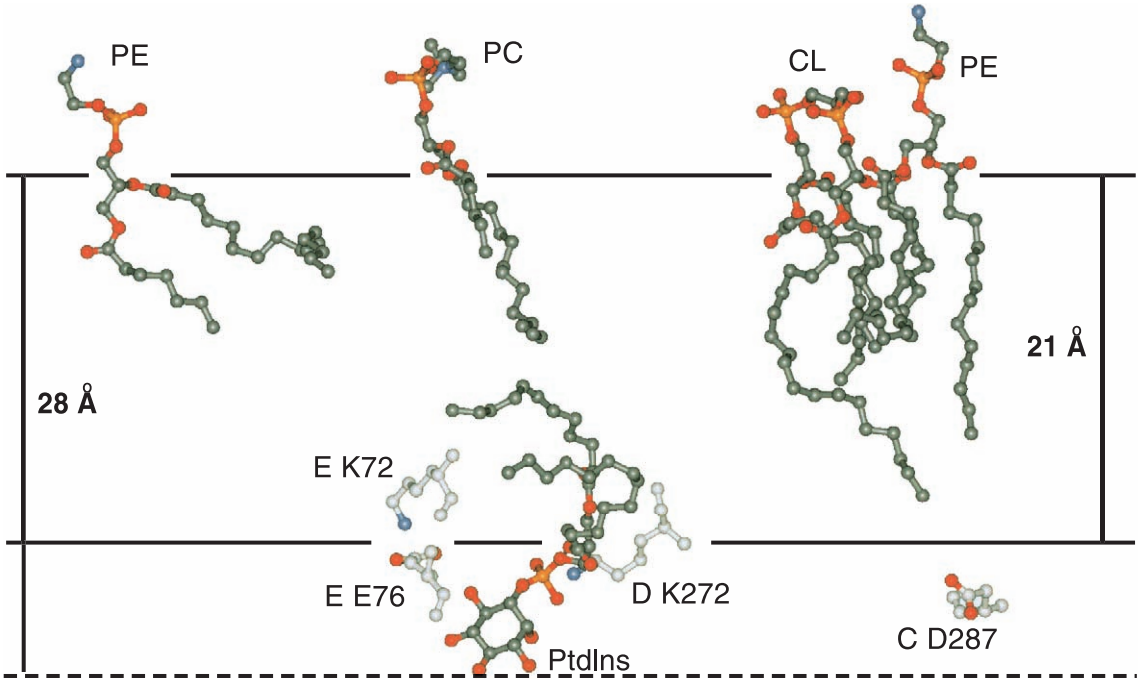

Fig. 16. The lipid molecules resolved in the structure of cytochrome bc_1. The five lipid molecules resolved in the structure of cytochrome bc_1 are shown, together with lipid-exposed residues on the intermembrane side of the membrane. The matrix side of the membrane is at the top and the intermembrane side is at the bottom. The glycerol backbones of the lipid molecules define a hydrophobic thickness for the protein of about 21 Å. However, an analysis of water distribution in the crystal suggests a hydrophobic thickness of about 28 Å [60]. If the hydrophobic surface on the matrix side is defined by the glycerol backbone regions of the lipid molecules, then the hydrophobic surface on the intermembrane side would then be given by the dotted line with the headgroup of the phosphatidylinositol molecule located below the membrane surface. Protein subunits are as follows: C, cytochrome *b*; D, cytochrome c_1; E, Rieske protein. (PDB file 1KB9).

intermembrane side (Fig. 16). The fatty acyl chains are highly distorted, the long axes of some of the chains being tilted far away from the bilayer normal. The hydrophobic thickness of the membrane, defined by the positions of the glycerol backbones of the lipid molecules is about 21 Å, as shown in Fig. 16. This is unusually thin and it might be that the phosphatidylinositol molecule on the intermembrane side of the membrane does not give a good indication of the position of the lipid bilayer surface on this side of the membrane, even though a number of lipid-exposed, charged residues are located close to the plane defined by the glycerol backbone (Fig. 16). Indeed, the phosphatidylinositol headgroup appears from plots of electrostatic potential to be located within the hydrophobic, transmembrane region of the protein (Figs. 15 and 16) and it has been estimated from the distribution of water molecules in the crystal that the hydrophobic thickness of cytochrome bc_1 is closer to 28 Å [60]; this would locate the intermembrane surface of the lipid bilayer just beyond the inositol headgroup (Fig. 16). Unfortunately, the distribution of Trp residues in cytochrome bc_1 does not help in defining the hydrophobic thickness; whereas there are a number of Trp residues on the matrix side of the membrane helping to define the interface on this side of the membrane, the distribution of Trp residues on the intermembrane side is sparse and does not provide any useful information.

It is noticeable that the plane occupied by the glycerol backbones of the phosphatidylethanolamine and phosphatidylcholine molecules at the dimer interface is very similar to that occupied by the glycerol backbones of the two lipid molecules bound on the matrix side of the membrane, as shown in Fig. 16, despite the unusual environment of the lipid molecules at the dimer interface. This suggests both that the lipid bilayer extends right up to the surface of the protein and that even lipid molecules bound to regions on the protein where they make little contact with the bulk of the lipid molecules in the membrane are located in a plane similar to that of the bulk lipid molecules. Whether or not the position of the phosphatidylinositol molecule represents an exception to this general observation remains to be determined.

2.5. Formate dehydrogenase

Formate dehydrogenase-N is a major component of nitrate respiration in *Escherichia coli*. It is a symmetrical trimer and the crystal structure shows three cardiolipin molecules at the trimer interface [223] The cardiolipin molecules interact primarily with the single transmembrane α-helix of the β subunit and with the fourth transmembrane α-helix of the γ subunit of the same monomer, and with the first transmembrane α-helix of the γ subunit of the neighbouring subunit. The location of the cardiolipin molecules suggests that they are essential for trimer formation [223]. The cardiolipin molecules are located with their backbones in the plane defined by Trp residues on the periplasmic side of the membrane.

2.6. FhuA, a β-barrel protein

The porins are β-barrel proteins located in the outer membranes of bacteria. The lipid component of the outer (extracellular) leaflet of the outer membrane of *E. coli* is composed exclusively of lipopolysaccharides (LPS) whereas the inner (periplasmic) leaflet contains phosphatidylethanolamines and phosphatidylglycerols. LPS adopts a bilayer structure in the presence of divalent metal ions such as Mg^{2+} to reduce electrostatic repulsions between LPS molecules [61–63]. Deuterium NMR studies of *E. coli* grown on deuterated palmitic acid suggest that, at the growth temperature, the outer membrane is in a normal liquid crystalline state, although the order parameters for the fatty acyl chains are somewhat higher than for fatty acyl chains in the inner membrane [64].

The crystal structure of the monomeric β-barrel protein FhuA, the receptor for the siderophore ferrichrome, contains a single LPS molecule [65], as shown in Fig. 17. Five of the six fatty acyl chains of the LPS molecule (all except for the 3-hydroxymyristate chain) make contact with hydrophobic side chains of FhuA, fixing the chains roughly parallel to the β-barrel axis. The LPS molecule is positioned so that the glucosamine moieties are located slightly above an upper aromatic girdle of Trp and Tyr residues [65]. The upper girdle of aromatic residues is located about 24 Å from a lower aromatic girdle (Fig. 17). Eleven charged or polar residues in FhuA interact with the phosphates of the inner core and the diglucosamine backbone of lipid A, and are responsible for the tight binding of LPS to FluA [66]. The fatty acyl chain lengths of the phospholipid component of the bacterial outer membrane are predominantly C16 or C18, but for the LPS component, the fatty acyl chains are mostly saturated with a length of C14, with some C12 [67], suggesting that the thickness of the bacterial outer membrane will be similar to that of a bilayer of di(C14:0)PC, which is about 23 Å, matching well the hydrophobic thickness of the protein.

2.7. The nature of the lipid binding site

A few general conclusions can be drawn from these studies about the nature of the lipid binding sites on membrane proteins. Not surprisingly, the residues surrounding the lipid fatty acyl chains are hydrophobic, Trp residues being common near the tops of the chains, with Ile, Leu, Phe, and Val commonly surrounding the rest of the chain. The environment around the chains of the resolved phosphatidylethanolamine molecule in the photosynthetic reaction centre of *T. tepidum* is unusual in containing major contributions from the chains of two bacteriochlorophyll and one quinone molecule [54]. Good van der Waals contact between the chains and the protein is often ensured by

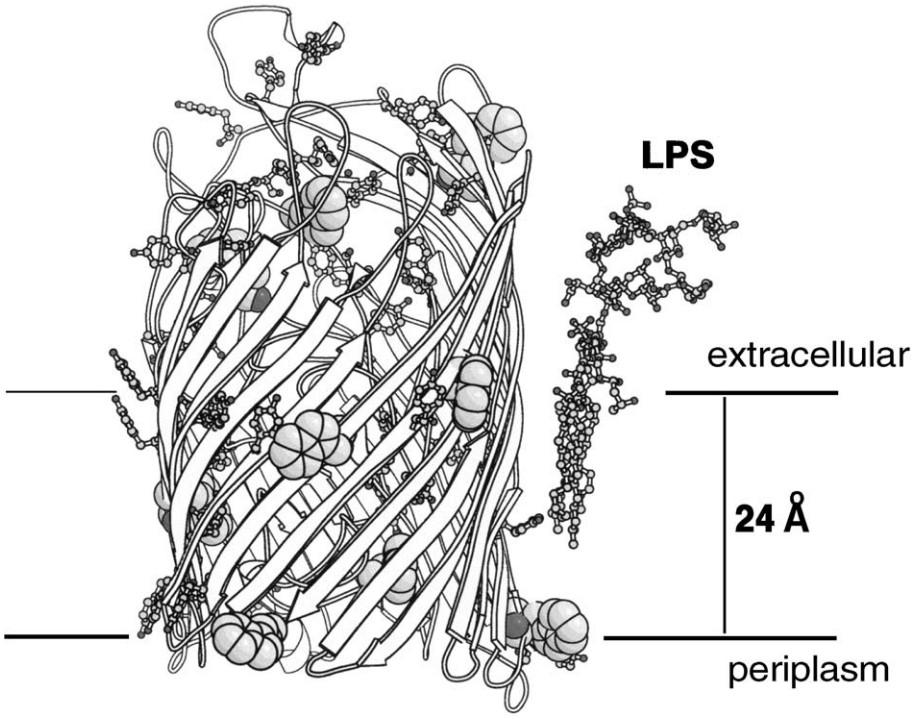

Fig. 17. The structure of FhuA with bound ferrichrome. The bound LPS molecule is shown in ball-and-stick representation. Trp residues are shown in space-fill format and Tyr residues are shown in ball-and-stick representation. The two girdles of aromatic residues are separated by about 24 Å. (PDB file 1FCP).

binding of at least the top parts of the chains in distinct groves on the surface of the protein, but this may not be true for all of the bound lipid molecules; it may be that only those lipid molecules whose chains are bound in grooves are sufficiently immobilised to be resolved in the X-ray structures.

In many of the structures, lipid headgroups are disordered, suggesting that the headgroups interact less tightly with the protein than the lipid fatty acyl chains; examples include bacteriorhodopsin and the potassium channel KcsA. Where headgroups are resolved, they are involved in charge and hydrogen bonding interactions with the protein, as illustrated by the binding site for phosphatidylethanolamine on the photosynthetic reaction centre of *T. tepidum* (Fig. 12). Differences in the patterns of hydrogen bonding for the headgroups of phosphatidylethanolamine and phosphatidylcholine could be important in explaining effects of phosphatidylethanolamines on membrane protein function and need to be considered as well as any effects that might follow from the preference of phosphatidylethanolamine for the hexagonal H_{II} phase (Section 8.2).

3. Hydrophobic thicknesses for membrane proteins whose high-resolution structures lack lipid molecules

Hydrophobic thicknesses for membrane proteins whose crystal structures do not include any resolved lipid molecules can be estimated from the locations of aromatic and charged residues, as described above (Table 1). The crystal structure of the light harvesting complex from *Rhodopseudomonas acidophila* [68] shows the importance of charged residues in locating the membrane surface (Fig. 18). The $-NH_3^+$ group on the unpaired Lys-13 residue in this homotrimeric structure must be located in a polar environment because of the high cost of burying a charged residue in the hydrophobic core of a bilayer.

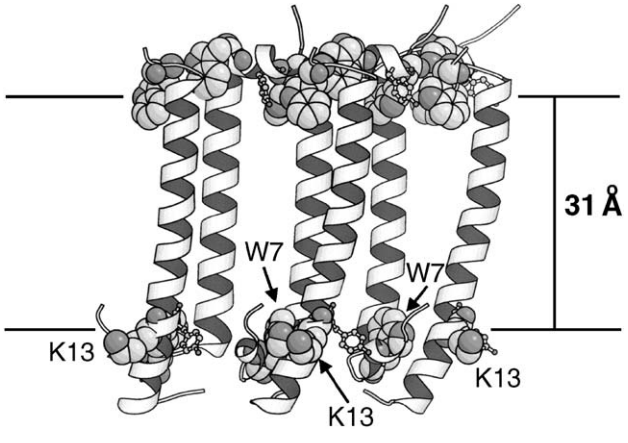

Fig. 18. Structure of the light-harvesting complex from *R. acidophila*. Trp and Tyr residues are shown in space-fill and ball-and-stick representations, respectively. The lower surface is defined by Lys-13 and passes through the indole N of Trp-7. If the upper surface passes through the indole N atoms of Trp-39 and Trp-45, then the hydrophobic thickness of the bilayer is 31 Å. (PDB file 1KZU).

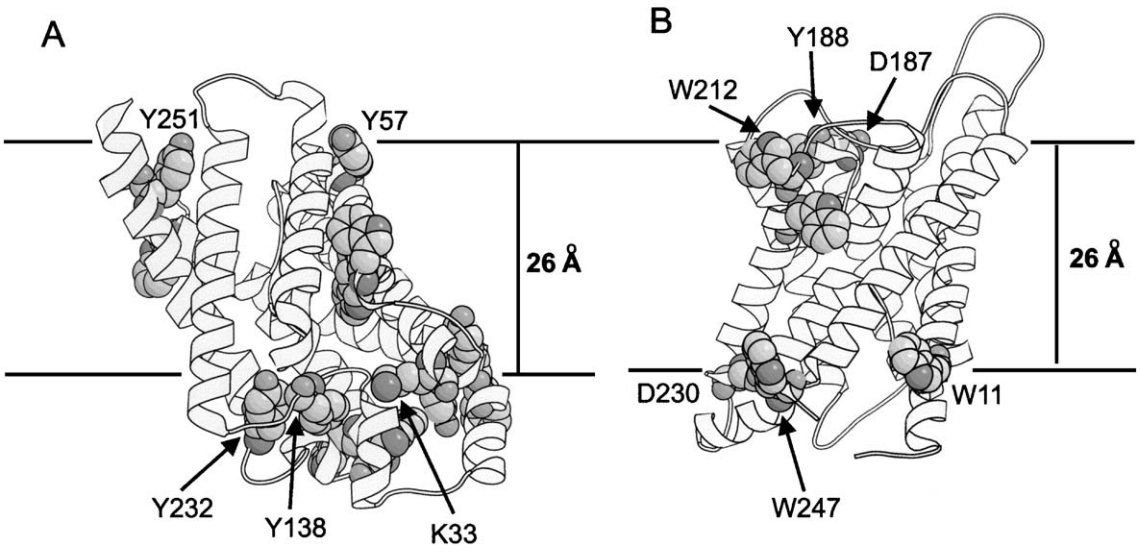

Fig. 19. Structures of *E. coli* glycerol facilitator (A) and red blood cell aquaporin (B). Residues defining the membrane surface are shown in space-fill representation. (PDB files 1FX8 and 1J4N).

The plane defined by the charged group on the Lys-13 residues coincides with the planes defined by the indole N atoms of Trp-7 and by the -OH group of Tyr-14 and thus is likely to correspond to the glycerol backbone region of the bilayer (Fig. 18). If the plane containing the indole N atoms of Trp-39 and Trp-45 defines the other glycerol backbone region, then the hydrophobic thickness of the protein is 31 Å (Fig. 18).

Red blood cell aquaporin and the bacterial glycerol facilitator have very similar structures [69,70] and identical hydrophobic thickness of 26 Å, defined by the positions of exposed Trp, Tyr and charged residues (Fig. 19; Table 1). A molecular dynamics simulation of aquaporin in a lipid bilayer shows several charged residues at the lipid–water interface forming salt bridges with lipid phosphate groups and other residues, including Trp, Ser and Asn, forming hydrogen bonds with the lipids [71]. Similar thicknesses for corresponding eukaryotic and prokaryotic membrane proteins seems to be common (Table 1). For example, the hydrophobic thicknesses of bacterial and bovine heart mitochondrial cytochrome *c* oxidase are very similar, as are the hydrophobic thicknesses of rhodopsin (Fig. 20A) and bacteriorhodopsin (Fig. 4). However, rhodopsin is considerably thicker than sensory rhodopsin II from *N. pharaonis* [72], as shown in Fig. 20B, with hydrophobic thicknesses of 35 and 27 Å, respectively.

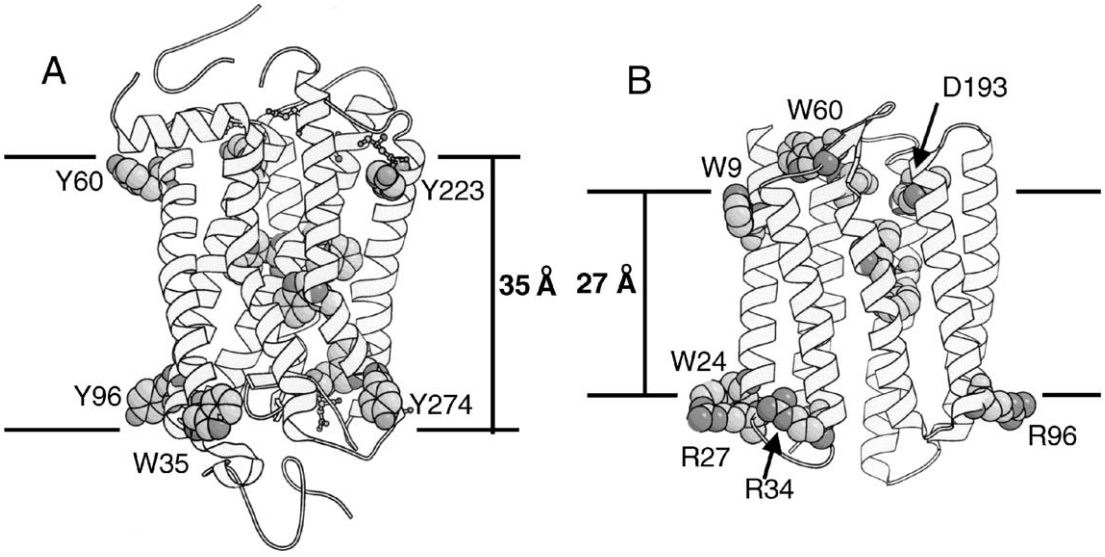

Fig. 20. Structures of rhodopsin (A) and sensory rhodopsin II (B). The hydrophobic thickness of rhodopsin is defined largely by the Tyr and Trp residues shown in space-fill representation and by Asp-190 and Glu-201 on one surface, and Glu-134, Glu-150, Glu-232 and Glu-249 on the other, shown in ball-and-stick representation. The hydrophobic thickness of sensory rhodopsin II is defined largely by Trp residues on the two surfaces, together with Asp-193 on one surface and Arg-27, Arg-34 and Arg-96 on the other. (PDB files 1F88 and 1JGJ).

Some membrane proteins appear to have unusually thin transmembrane regions (Table 1). For example, the thickness of the ClC chloride channel of *E. coli* [73] is only about 23 Å (Fig. 21). In this case, the thickness of the dimeric channel is defined by the position of Lys-271 on one surface and Lys-55 and Trp-59 on the other, with a Trp residue (Trp-272) totally buried within the hydrophobic core of the bilayer. The ClC channel of *Salmonella* lacks a Lys residue at the position equivalent to Lys-271 in the *E. coli* protein, but Arg-275 occupies a position in the 3D structure very similar to that of Lys-271 in the *E. coli* protein [73], suggesting very similar hydrophobic thicknesses for the two proteins. The hydrophobic thickness of the mechanosensitive channel MscL from *Mycobacterium tuberculosis* [74] is unclear (Fig. 21). The hydrophobic thickness of the pentameric channel, defined by a girdle of Asp-68 residues on one side of the membrane and a girdle of Tyr-87 residues on the other, is just 18 Å. However, if it is assumed that Tyr-87 is buried in the hydrophobic core of the bilayer, then the hydrophobic thickness could be defined by a girdle of Tyr-94 residues, giving a thickness of 34 Å. The mechanosensitive channel undergoes extensive changes in conformation during channel opening, and this may be related to the unusual structure of this channel [75,76].

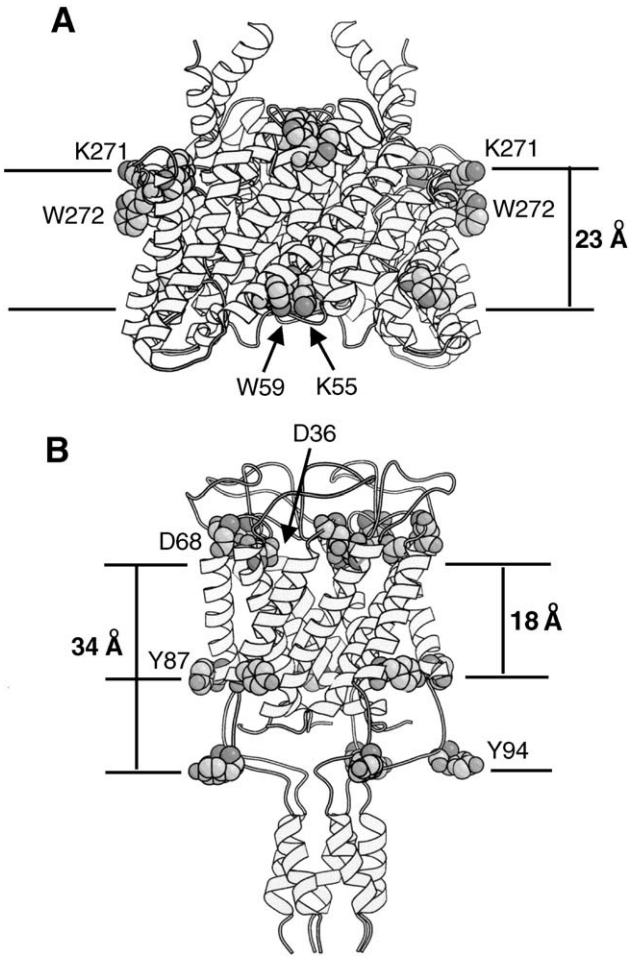

Fig. 21. Structures of the chloride channel ClC of *E. coli* (A) and the mechanosensitive channel MscL (B). Residues defining the hydrophobic thicknesses of the proteins are shown in space-fill representation (PDB files 1KPL and 1MSL).

The Ca^{2+}-ATPase of skeletal muscle sarcoplasmic reticulum [5] also appears to have an unusually thin transmembrane region (Table 1). The structure of the Ca^{2+}-bound form of the Ca^{2+}-ATPase ($E1Ca_2$) is shown in Fig. 22. Identifying the hydrophobic core of the bilayer surrounding the Ca^{2+}-ATPase is difficult because many of the transmembrane α-helices extend above the membrane surface to form a central stalk linking the transmembrane region to the cytoplasmic head of the protein. As a consequence, some of the helices are very long; helix M5 for example contains 41 residues. A girdle of Trp residues on the cytoplasmic side of the membrane helps to define the location of the membrane surface on the cytoplasmic side (Fig. 22). A Lys residue (Lys-262) in transmembrane α-helix M3 snorkels up from the hydrophobic core of the bilayer to the surface [77]. Since this group cannot be buried within the hydrophobic core of the bilayer, it is likely that the amino group on Lys-262 will be located at the interface; the Trp residues in the Ca^{2+}-ATPase will then be located in the headgroup region of the bilayer [77]. The structure of the Ca^{2+}-bound form of the Ca^{2+}-ATPase is unusual in that the first transmembrane α-helix contains two polar residues Asp-59 and Arg-63 pointing out into the hydrocarbon core; presumably, stacking of Asp-59 against Arg-63 allows formation of an ion pair within the core of the bilayer (Fig. 22).

The distribution of Trp residues on the lumenal face of the Ca^{2+}-ATPase is much more diffuse than that on the cytoplasmic side (Fig. 22). The hydrophobic thickness of the Ca^{2+}-ATPase would be expected to be about 30 Å since that is the hydrophobic thickness of a bilayer of di(C18:1)PC, the phospholipid that supports highest activity for the ATPase [78]. However, as shown in Fig. 22, this definition would locate a Lys residue (Lys-972) totally within the hydrocarbon core, which seems unlikely. The hydrophobic thickness of the bilayer would have to be about 21 Å to locate Lys-972 at the lumenal surface (Fig. 22); this is unusually thin for a membrane protein.

The structure of the Ca^{2+}-free ATPase with a bound molecule of the inhibitor thapsigargin has also been determined [79]. Thapsigargin binds to the Ca^{2+}-ATPase to give a form that has been described as a modified E2 state, $E2^{A}Tg$ [80]. Changes in positions of the cytoplasmic domains are directly related to tilting of the TM α-helices [79,81]. These changes are complex, movement of any one element of the structure requiring movement of several others, for steric reasons. Changes in helices M7–M10 are relatively small, but there are major changes for the other helices (Fig. 22). The changes in M1 are particularly complex. In the Ca^{2+}-bound form, charged residues Glu-51 and Glu-55 are located at the top of M1, Glu-58 facing in towards one of the Ca^{2+}-binding sites, with Asp-59 and

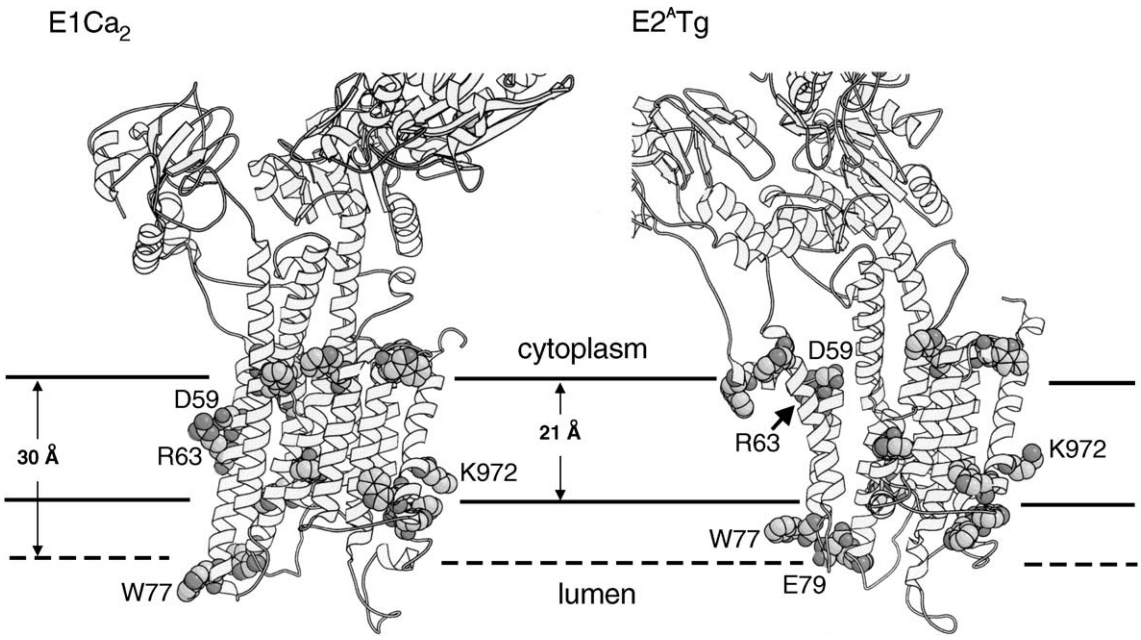

Fig. 22. The transmembrane region of the Ca^{2+}-ATPase of skeletal muscle sarcoplasmic reticulum. Structures of the Ca^{2+}-bound ($E1Ca_2$) and Ca^{2+}-free, thapsigargin (Tg)-bound ($E2^ATg$) forms are shown. Trp residues are shown in space-fill representation. In the $E1Ca_2$ structure, the positions of Asp-59 and Arg-63 in transmembrane α-helix M1 are shown in space-fill representation; in the $E2^ATg$ structure, all the charged residues in helix M1 are shown in space-fill representation. The location of Lys-972 in both structures helps to define the likely position of the lumenal surface, giving a hydrophobic thickness of about 21 Å for the protein. A possible location for the lumenal surface giving a hydrophobic thickness of 30 Å for the protein is given by the dotted line. (PDB files 1EUL and 1IWO).

Arg-63 forming an ion pair exposed to the lipid bilayer (Fig. 22). In the modified E2 state, these residues have moved upwards with a bend at Asp-59 to form an amphipathic helix with hydrophobic residues on one side and Glu-58 and Asp-59 on the other, and Arg-63 now snorkels up to the lipid–water interface (Fig. 22). The bottom of helix M1 is defined in the modified E2 state by Trp-77 and by Glu-79. As shown in Fig. 22, Trp-77 moves upwards in the modified E2 state compared to $E1Ca_2$ as a result of the upward movement of the whole helix M1. Despite these complex changes, the hydrophobic thickness of the Ca^{2+}-ATPase (21 Å) appears to be unchanged. The cytoplasmic surface is again well defined by the positions of the Trp residues and by the position of Asp-59. Lys-972 is in a similar position in the two structures although it appears to be rather disordered in the $E2^ATg$ structure.

The small β-barrel proteins OmpA and OmpX contain girdles of aromatic residues, as shown in Fig. 23 [82,83]. In OmpX, if it is assumed that the Trp residues are located just within the hydrophobic core of the bilayer, then the thickness of the hydrocarbon core would be 24 Å (Table 1). In OmpA, the situation is more complex, with the Trp residues occupying a broader band, so that some are presumably located just within the hydrophobic core of the bilayer whereas others will be located in the headgroup region, but the hydrophobic thickness appears to be the same as in OmpX (Fig. 23). A number of molecules of the detergent *n*-octyltetraoxyethylene (C_8E_4) were identified in the crystal, with the octyl moieties located on the hydrophobic surface, making weak van der Waals interactions with neighbouring protein atoms (Fig. 23).

The general porin OmpF of *E. coli* is a homotrimer. The membrane-facing surface of a single monomer in the trimer shows a clear pattern of residue distribution, illustrated in Fig. 24 [84]. The central region is a belt of nonpolar residues bordered at each edge by girdles of aromatic amino acids. The girdles are defined predominantly by Tyr residues with their hydroxyl groups pointing towards the aqueous phase. If it is assumed that the hydroxy groups of the Tyr residues are located in the glycerol backbone region of the bilayer, then the thickness of the hydrophobic core of the bilayer would be about 24 Å, as shown in Fig. 24. OmpF contains just two Trp residues per monomer, one at the trimer interface and one exposed to the lipid; the lipid exposed Trp residue is located just below the plane defined by the Tyr residues (Fig. 24). Neutron diffraction studies have shown that, in crystals grown from β-octyl glucoside or lauryl dimethyl-*N*-amineoxide (LDAO), the hydrophobic region of OmpF is covered by detergent, with the two girdles of aromatic residues coinciding with the boundary between the polar and nonpolar regions of the detergents [85], a location for the aromatic residues also seen in molecular dynamics simulations of OmpF in bilayers of di(C14:0)PC [86]. Beyond the external girdle of aromatic residues, the external barrel surface contains a number of acidic residues, which could interact with LPS molecules through divalent metal ion bridges.

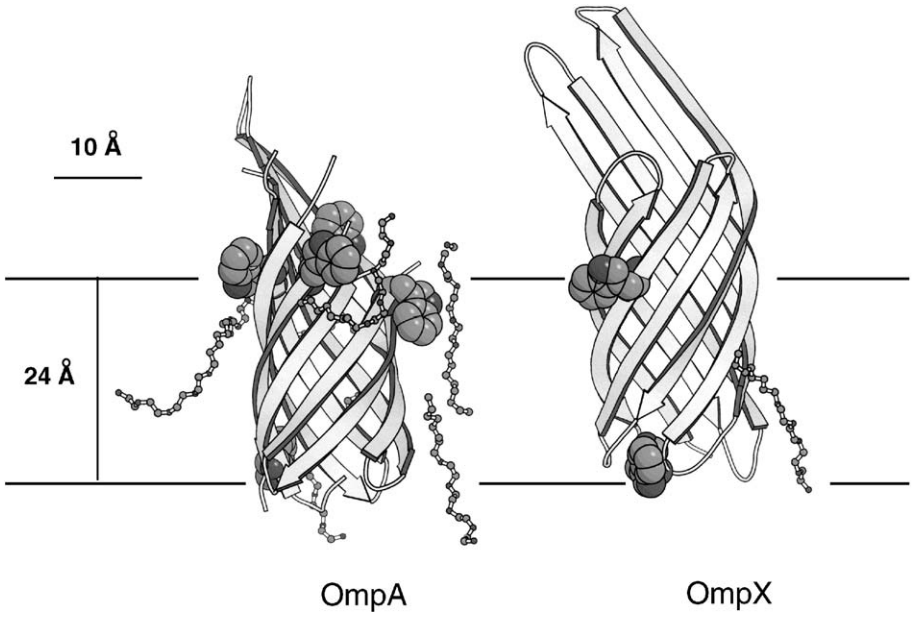

Fig. 23. The structures of OmpX and of the transmembrane domain of OmpA. Trp residues are shown in space-fill representation. Detergent molecules are shown in ball-and-stick representation. (PDB files 1QJP and 1QJ8).

A number of general conclusions can be drawn from the data collected in Table 1. The average thickness of the transmembrane, hydrophobic region of an α-helical membrane protein is 29 Å (Table 1), very similar to the hydrophobic thickness of a bilayer of di(C18:1)PC, suggesting that lipids and proteins will generally be well matched in the membrane. The average hydrophobic thickness of a β-barrel protein in the bacterial outer membrane is 24 Å, significantly less than the thickness of an α-helical membrane protein, but likely to match the hydrophobic thickness of the bacterial outer membrane. However, the hydrophobic thicknesses of some membrane proteins do not seem to match so well the thickness of the surrounding lipid bilayer. For example, the hydrophobic thicknesses of bacteriorhodopsin, rhodopsin, and the potassium channel KcsA, appear to be greater than the hydrophobic thickness of a typical lipid bilayer and the ClC chloride channel, and the Ca^{2+}-ATPase have hydrophobic thicknesses significantly less than that of a typical lipid bilayer (Table 1). Either the structures of these proteins are slightly different in the native membrane to that in the detergent-solubilised protein, or these proteins exist in a state of stress in the native membrane, surrounded by phospholipids with stretched or compressed fatty acyl chains; this is discussed further in Section 5.3.

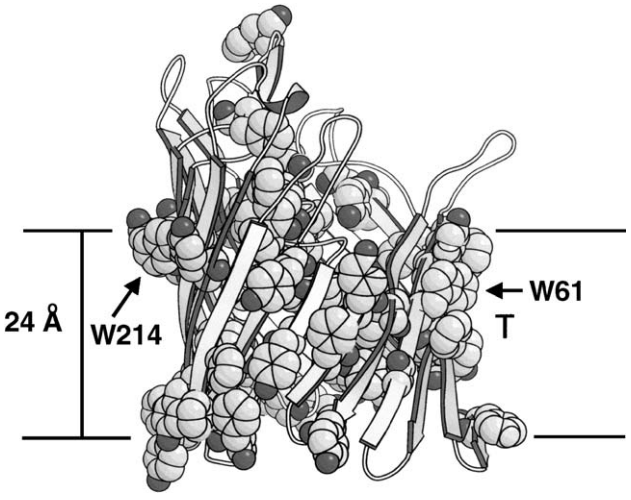

Fig. 24. Structure of OmpF showing aromatic residues. The aromatic residues are shown in space-fill representation. Possible locations for the hydrophobic core of a lipid bilayer of thickness 24 Å are shown, defined by the positions of the Tyr hydroxyl groups. The positions of the two Trp residues are shown. The position of the trimer interface (T) is indicated. (PDB file 2OMF).

4. Non-annular sites

Evidence has been presented for the presence of binding sites for hydrophobic molecules on membrane proteins, distinct from the sites to which the 'solvent' or annular lipids bind; these additional sites have been referred to as non-annular sites [10]. The first evidence for the presence of non-annular sites came from experiments studying the effects of cholesterol on the Ca^{2+}-ATPase of sarcoplasmic reticulum [10], but non-annular sites were later suggested on the Ca^{2+}-ATPase for a variety of long-chain hydrophobic molecules [12,13]. These non-annular sites were suggested to be located between transmembrane α-helices or at protein–protein interfaces [10,12]. The nature of such a site is illustrated by the recently published structure for the Ca^{2+}-free form of the Ca^{2+}-ATPase with a bound molecule of the hydrophobic inhibitor thapsigargin (Fig. 25). Thapsigargin

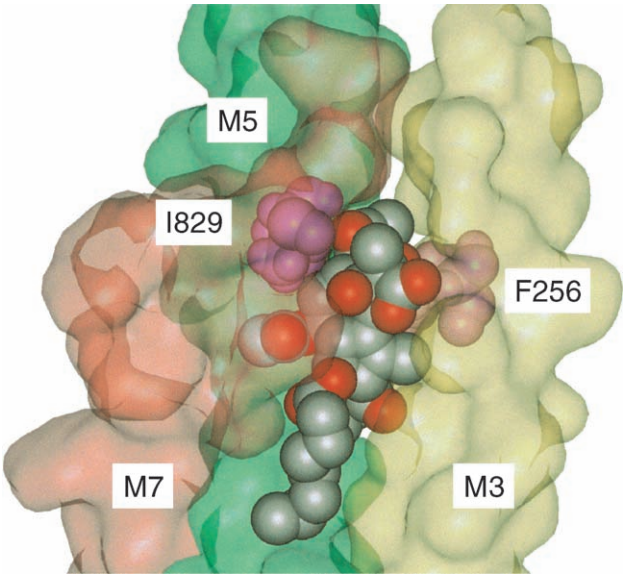

Fig. 25. The binding site for thapsigargin on the Ca^{2+}-ATPase. For simplicity, just helices M3, M5 and M7 are shown in surface format. The bound thapsigargin molecule is shown in space-fill representation as are residues Phe-256 and Ile-829, important in binding the inhibitor. (PDB file 1IW0).

binds to the Ca^{2+}-ATPase in a cleft between helices M3, M5 and M7, on the lipid-exposed surface of the Ca^{2+}-ATPase [79]. The polar end of the thapsigargin molecule is located between Phe-256 and Ile-829, close to the expected position of the glycerol backbone region of the surrounding lipid bilayer. The alkyl chain of the thapsigargin molecule lies along the hydrophobic surface of helix M5. In the structure of the Ca^{2+}-bound ATPase, the space between Phe-256 and Ile-829 is much narrower than in the Ca^{2+}-free form [79,81]. By keeping transmembrane α-helices M3 and M7 apart, thapsigargin prevents the ATPase from adopting a conformation in which it can bind Ca^{2+} ions and be active. Thus, inhibition by thapsigargin is indirect and based on steric factors. A variety of other clefts exist on the surface of the ATPase between transmembrane α-helices, including a cleft between helices M2 and M9 to which the inhibitor phospholamban binds [87]. These clefts could also be the non-annular sites to which cholesterol and long-chain hydrophobic molecules bind [10,13].

The effects of binding to non-annular sites on Ca^{2+}-ATPase activity depend on the nature of the phospholipids surrounding the Ca^{2+}-ATPase [10,11,14,88–90]. The activity of Ca^{2+}-ATPase is low in bilayers of short-chain or long-chain phospholipids (Section 8.4). The presence of cholesterol and other hydrophobic molecules increases ATPase activity in bilayers of short-chain phospholipids, but not in long-chain phospholipids. Evidence that effects of cholesterol on the activity of the Ca^{2+}-ATPase are not due to effects on bilayer thickness are presented in Ref. [13]. It is possible that occupancy of the non-annular sites on the Ca^{2+}-ATPase by cholesterol prevents the reorganisation of transmembrane α-helices responsible for the low activity in short-chain phospholipids but not that responsible for the low activity in long-chain phospholipids.

The presence of non-annular binding sites for cholesterol has also been suggested on the nicotinic acetylcholine receptor (AChR), which requires the presence of cholesterol for function [91,92]; in the presence of phosphatidylcholines alone, the receptor exists in a nonconducting, desensitised-like conformation [93]. On the basis of competition studies, Jones and McNamee [16] suggested the presence of two classes of lipid site on the AChR; annular sites occupied by phospholipids and non-annular sites to which cholesterol can bind, but from which phospholipids are excluded. Just a few mole percent cholesterol allows activation of the channel, and many other neutral hydrophobic species can substitute for cholesterol, including α-tocopherol, coenzyme Q_{10} and vitamins D_3 and K_1. The -OH group of the cholesterol molecule is not essential for activity, and cholesterol hemisuccinate and cholesterol sulfate are as effective as cholesterol [94]. Further, the AChR is active in bilayers of a cholesterol-containing phospholipid in the absence of any free cholesterol, suggesting that the binding site for cholesterol and its analogues on the receptor cannot be deeply buried in the structure, a long way from the lipid–protein interface [94]. The most likely site of action is at the lipid–protein interface, but with the cholesterol ring penetrating into crevices (possibly at subunit interfaces) from which the phospholipid fatty acyl chains are excluded. An essential role for cholesterol has been suggested for a number of other proteins from mammalian plasma membranes. Thus function of the GABA [95] and serotonin transporters [96] both require the presence of small amounts of cholesterol, suggesting the presence of specific binding site(s) for cholesterol on the transporters. The Na^+,K^+-ATPase also requires the presence of cholesterol for full activity, stimulation of activity being observed up to about 30 mol% cholesterol in the membrane, the activity decreasing at higher cholesterol contents [97,224,225]. It has been suggested that stimulation follows from binding of cholesterol to specific sites on the Na^+,K^+-ATPase, with inhibition being due to effects of cholesterol on the bulk properties of the lipid bilayer [225]. Strong interactions have also been detected between cholesterol and two proteins of the red blood cell membrane, band 3 and glycophorin [226,227].

Several of the crystal structures described in Section 2 (KcsA, bacterial photosynthetic reaction centre, cytochrome *c* oxidase, cytochrome bc_1) show phospholipid molecules bound to crevices in the transmembrane surface of the protein, much like the site to which thapsigargin binds on the Ca^{2+}-ATPase (Fig. 25). These observations suggest that the definition of non-annular sites should be extended from sites to which hydrophobic molecules other than phospholipids can bind to include sites between transmembrane α-helices to which specific phospholipids can bind. The fact that lipid molecules occupy these sites even in crystals grown from detergent solution suggests that the lipid molecules in these sites are tightly bound to the protein, because

otherwise they would have been lost on treatment with detergent. It is possible that these 'special' lipids will be in slow exchange with the lipids in the bulk lipid bilayer, although there appears, as yet, to be no direct evidence for this.

5. Lipid–protein interactions and lipid binding constants

As already described, the hydrophobic surface of a membrane protein is heterogeneous and rough and covered by a shell of annular lipids, acting as a 'solvent' for the protein. A full description of binding to such a heterogeneous surface is an impossibly difficult task but, as long as the surface is not too heterogeneous, binding can reasonably be described in terms of a uniform surface. A number of equations have been presented to describe binding to a uniform surface [98], but the only one that is readily applicable is the Langmuir binding isotherm, which is equivalent to the conventional equation describing equilibrium binding to a number of distinct binding sites. Fig. 26 represents the hydrophobic surface of a membrane protein covered by annular lipids. With total coverage of the surface by lipids, one lipid molecule must leave the surface before another can enter. Although some rearrangement of lipids on the surface is possible during this process, a simple concerted exchange of two lipid molecules on the surface seems more likely. In this sense, therefore, the process can be described as competitive binding of lipids at a number of 'sites' on the protein surface. For a membrane protein P in a lipid bilayer containing a mixture of two lipid species A and B, the equilibrium at each site is described by the equation:

$$PA + B \leftrightarrows PB + A$$

where PA and PB are complexes of the protein with lipids A and B, respectively. This exchange equilibrium can be described by a relative association constant K given by:

$$K = [PB][A]/[PA][B] \quad (1)$$

where the square brackets denote concentrations [99,100]. The value for K obtained from such an analysis represents an average over all N lipid binding sites on the protein, and so will be dominated by the interaction of the bulk lipid molecules with the protein. Values for K have been estimated from ESR studies [2,3] and from studies of the quenching of protein fluorescence by spin-labelled [99] or brominated phospholipids [78,100]. The assumption of 1:1 exchange of lipid molecules at the annular sites raises interesting problems when considering exchange of lipid molecules containing different numbers of fatty acyl chains. For example, a molecule such as a cardiolipin with four chains would be expected to exchange with two two-chain phospholipid molecules. The necessary equations have been presented elsewhere [101].

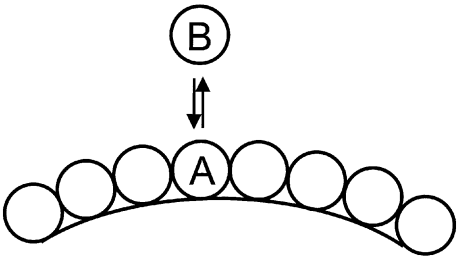

Fig. 26. Lipid binding sites on the transmembrane surface of a membrane protein. Two lipids, A and B, are shown exchanging at one 'site'.

Table 2
Relative association constants for lipid–protein interactions, determined from ESR experiments with spin-labelled lipids

Protein	Association constant (relative to phosphatidylcholine)				
	CL	PA	PS	PG	PE
Na^+,K^+-ATPase	3.8	1.5	1.7	0.9	0.9
Cytochrome *c* oxidase	5.4	1.9	1.0	1.0	1.0
ADP–ATP carrier	3.8	4.3	2.4	0.8	–
Acetylcholine receptor	–	2.7	0.7	–	1.1
Cytochrome *c* reductase	1.4	2.4	1.8	1.7	1.3
Rhodopsin	1.0	1.0	1.0	1.0	1.0

CL, cardiolipin; PA, phosphatidic acid; PS, phosphatidylserine; PG phosphatidylglycerol, PE, phosphatidylethanolamine.
Data from Ref. [1].

5.1. Effects of lipid headgroup structure

Relative association constants for phospholipids binding to a number of membrane proteins, determined from ESR experiments with spin labelled lipids, are given in Table 2. Values tend to be close to 1, showing that there is relatively little selectivity in the binding of annular phospholipids to intrinsic membrane proteins [1]. Rhodopsin shows no selectivity between phospholipid species, but most other proteins show a small selectivity for anionic phospholipids. For Na^+,K^+-ATPase, the selectivity for anionic phospholipids decreased with increasing ionic strength showing an important electrostatic component to the interaction [1]. However, not all the selectivity for anionic phospholipids was screened out at high ionic strength showing that non-electrostatic interactions are also important [1]. Of the anionic lipids listed in Table 2, cardiolipin shows the strongest binding to Na^+,K^+-ATPase, cytochrome *c* oxidase and to the mitochondrial ATP–ADP carrier, although it is necessary to remember that a cardiolipin molecule contains four chains, compared to the two chains in the other phospholipids (see Ref. [101]).

Interactions between lipids and Ca^{2+}-ATPase also show relatively little structural specificity, as shown in Table 3 [78,99,102]. Binding of phosphatidylethanolamine is a

Table 3
Relative binding constants of phospholipids and hydrophobic molecules to Ca^{2+}-ATPase

Molecule	Relative association constant[a]
Phosphatidylethanolamine	0.45
Phosphatidylserine	1
Phosphatidylserine + Ca^{2+}	0.45
Di(C14:0)PC in gel phase	0.04
Cholesterol	<0.2
Cholesterol hemisuccinate	0.5
Oleylamine	1.6
Oleic acid	0.5
Oleyl alcohol	<0.2
Methyl oleate	<0.1

Data from Refs. [78,102].
[a] Measured relative to di(C18:1)PC.

factor of 2 weaker than binding of phosphatidylcholine [103], but anionic lipids bind as strongly as phosphatidylcholines [104]. Comparison of the relative binding constants for uncharged and charged single chain molecules shows that charge interactions are important for binding at the lipid–protein interface (Table 3). Weak binding of cholesterol at the lipid–protein interface follows both from the lack of a charged headgroup and from the effect of the rigid ring system; cholesterol hemisuccinate with its negatively charged 'headgroup' binds more strongly than cholesterol, and, although a phosphatidylcholine in which one fatty acyl chain has been replaced by a cholesterol moiety, binds less well than a normal phosphatidylcholine, the difference is only a factor of about 2 [104]. Additional evidence for the importance of charge effects in lipid–protein interactions has come from studies of the interactions between anionic phospholipids and simple transmembrane α-helices [100,105].

Although binding at the annular sites on a membrane protein shows little headgroup selectivity, binding to the non-annular sites is likely to be more selective. A number of examples of such selectivity are described in Section 8.5. The binding of cardiolipin to specific sites on cytochrome oxidase provides a classic example. Despite the selectivity dependent on headgroup structure, hydrophobic interactions are also important; monolysocardiolipin, lacking one fatty acyl chain, bound to cytochrome oxidase about 3–10 fold less strongly than cardiolipin, and dilysocardiolipin, lacking two fatty acyl chains, bound about 30–100 fold less strongly than cardiolipin [106].

5.2. Effects of phospholipid phase

Many membrane proteins show a preference for lipid in the fluid, liquid crystalline phase over lipid in the rigid, gel phase, as expected from simple considerations of free volume and packing effects; lipid in the gel phase will make poorer van der Waals contact with the rough surface of a protein than lipid in the liquid crystalline phase. For example, binding of gel phase lipid to Ca^{2+}-ATPase is a factor of 25 weaker than binding of lipids in the liquid crystalline phase (Table 3) and the binding constant of the peptide L_{16} for di(C16:0)PC in the gel phase relative to di(C18:1)PC in the liquid crystalline phase is ca. 0.15 [105]. Preferential binding of membrane proteins to phospholipids in the liquid crystalline phase means that, in bilayers containing both gel and liquid crystalline domains, proteins will partition preferentially into domains in the liquid crystalline phase. This preferential partitioning has been demonstrated using freeze-fracture electron microscopy [107], fluorescence [78] and infrared techniques [108]. In bilayers containing predominantly gel phase lipid, simple transmembrane α-helices form ordered line-like aggregates surrounded by lipids in a liquid crystalline-like state [109].

Ca^{2+} binds to bilayers of phosphatidylserine (PS) forming gel-like domains of $(PS)_2Ca$ [110,111] and formation of these gel-like domains leads to exclusion of a wide variety of small molecules [112]. The affinity of Ca^{2+}-ATPase for phosphatidylserine is less in the presence of Ca^{2+} than in its absence (Table 3) consistent with weak van der Waals interactions between the Ca^{2+}-ATPase and gel-like $(PS)_2Ca$ domains. Similarly, in mixtures of di(C18:1)PC and di(C18:1)PS, the presence of Ca^{2+} leads to exclusion of gramicidin from the gel-like patches of $[di(C18:1)PS]_2Ca$ [113]. Addition of Ca^{2+} to the Ca^{2+}-ATPase reconstituted into mixtures of phosphatidylcholine and phosphatidic acid also leads to exclusion of the Ca^{2+}-ATPase from domains of phosphatidic acid–Ca^{2+} complex [99].

5.3. Effects of fatty acyl chain length and hydrophobic mismatch

A particularly important feature of a membrane protein is the thickness of its hydrophobic, membrane-spanning region. The cost of exposing hydrophobic fatty acyl chains or peptide residues to water is such that the thickness of the hydrophobic region of the peptide should match the hydrophobic thickness of the bilayer. Hydrophobic mismatch between a protein and a lipid bilayer could be compensated for in a number of ways. The lipid bilayer around a protein could either thicken or thin to match the hydrophobic thickness of the protein. There will, however, be an energetic cost associated with any such changes in the thickness of the bilayer. This could be minimised by aggregation of the protein, to reduce the exposure of the protein surface to the lipid bilayer. If the transmembrane helices of a membrane protein were too thick to match the surrounding lipid bilayer, tilting of the helices could reduce their effective length across the bilayer. In principle, a transmembrane α-helix could distort to provide better matching to the lipid bilayer. Experimental studies of transmembrane α-helices of the type $AW_2(LA)_nW_2A$ showed that, in fact, the structure remained α-helical, independent of the extent of hydrophobic mismatch [114]. However, one form of distortion away from an ideal α-helical structure that might be possible is rotation of a side chain about the Cα–Cβ bond linking

the side chain to the polypeptide backbone. For a residue at the end of a helix such a rotation would change the effective length of the helix. For example, rotation of a Tyr residue to lie roughly parallel to the long axis of a helix would extend the length of the helix by about 3 Å and rotation of the larger Trp residue would have an even larger effect [105]. Finally, if the cost of incorporating the protein into the bilayer was too high, the protein could be excluded from the bilayer [115] and, at relatively high contents of hydrophobic peptides, hydrophobic mismatch could lead to the formation of nonbilayer lipid phases [116].

Most models of hydrophobic mismatch assume that the lipid chains in the vicinity of a membrane protein adjust their length to the hydrophobic thickness of the protein, with the protein acting as a rigid body. When the thickness of the bilayer is less than the hydrophobic thickness of the protein, the lipid chains must be stretched around the protein (Fig. 27). Conversely, when the thickness of the bilayer is greater than the hydrophobic thickness of the protein, the lipid chains must be compressed around the protein. Stretching the fatty acyl chains will effectively decrease the surface area they occupy in the membrane surface, and, conversely, compressing the chains, will increase the effective area occupied in the surface. A number of terms have been suggested to contribute to the total free energy cost of deforming a lipid bilayer around a protein [117–119]. Fattal and Ben-Shaul [117] calculated the total lipid–protein interaction free energy as the sum of chain and headgroup terms. The resulting profile of energy of interaction as a function of hydrophobic mismatch was fairly symmetrical about the point of zero mismatch [120,121]. The calculated membrane perturbation energy ΔG_{def} (in units of kJ mol^{-1}) for a rigid single transmembrane α-helix of radius 5 Å and hydrophobic length 30 Å in a lipid bilayer fits closely to the quadratic equation

$$\Delta G_{\mathrm{def}} = 963.1 - 65.18 d_{\mathrm{L}} + 1.1 d_{\mathrm{L}}^2 \quad (2)$$

where d_{L} is the hydrophobic thickness of the lipid bilayer. For a protein of radius 17 Å, corresponding to a bundle of six transmembrane α-helices, again of length 30 Å, the perturbation energy fits the equation

$$\Delta G_{\mathrm{def}} = 119.7 - 8.1 d_{\mathrm{L}} + 0.137 d_{\mathrm{L}}^2 \quad (3)$$

Calculations were performed in the range of bilayer thicknesses from 20 to 40 Å [121]; it is not clear if Eqs. (2) and (3) can be used to calculate values for the deformation energy outside this range. If all the lipid perturbation energy were to be concentrated in the first shell of lipids around the protein, and assuming that a lipid occupies 9.4 Å of the protein circumference, the lipid–protein interaction energy would change by about 5 kJ mol^{-1} of lipid for a six-helix protein with hydrophobic mismatch of 10 Å. A change in interaction energy of this amount corresponds to a decrease in lipid binding constant by a factor of about 10. If the change in lipid–protein interaction energy were to propagate out from the protein surface to affect more than the first shell of lipids, effects of hydrophobic mismatch would be reduced. Other approaches such as that of Nielsen et al. [118] and the mattress model of Mouritsen and Bloom [122,123] come to rather similar conclusions.

Comparing experiment with theory requires a method for estimating the hydrophobic thickness of a lipid bilayer from the length of the fatty acyl chains. The hydrophobic thickness d of a lipid bilayer of a saturated phosphatidylcholine in the liquid crystalline phase is related to fatty acyl chain length by the equation

$$d = 1.75(n - 1) \quad (4)$$

where n is the number of carbon atoms in the fatty acyl chain [124,125]. The thickness of a bilayer of a phosphatidylcholine with two monounsaturated chains was estimated by Lewis and Engelman [124] to be about 2.5 Å less than that of the corresponding phosphatidylcholine with two saturated chains estimated from Eq. (4). The thickness of a bilayer of di(C18:0)PC calculated from Eq. (4) is 29.7 Å, giving a thickness for a bilayer of di(C18:1)PC of about 27.2 Å, in good agreement with the estimated thickness given by Nagle and Tristram-Nagle [126], which is 27.1 Å. This is significantly less than the hydrophobic thickness of a bilayer of di(C18:1)PC estimated from the data shown in Fig. 1, which is 32 Å [17]. However, the data in Fig. 1 were

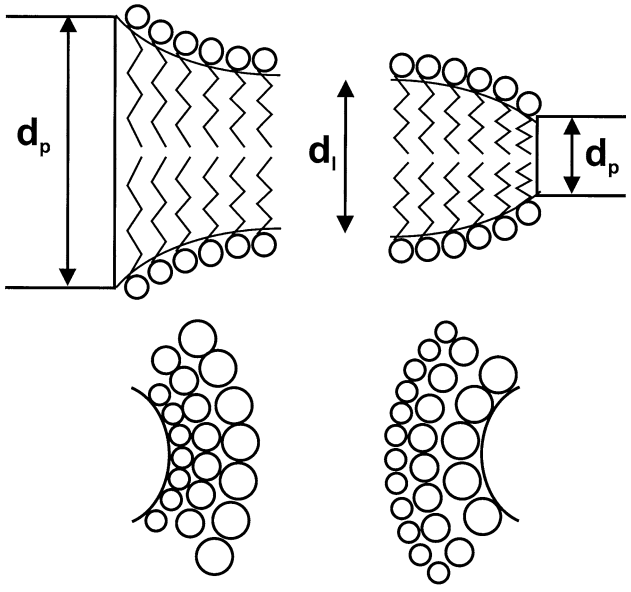

Fig. 27. Hydrophobic mismatch. The diagram shows how a lipid bilayer could distort around a membrane protein whose hydrophobic thickness was greater than that of the lipid bilayer (left; $d_{\mathrm{p}} > d_{\mathrm{l}}$) or less than that of the lipid bilayer (right; $d_{\mathrm{p}} < d_{\mathrm{l}}$). When the hydrophobic thickness of the protein is greater than the thickness of the bilayer, the lipid chains must be stretched so that the surface area occupied by a lipid molecule will be less in the vicinity of the protein than for bulk lipid. Conversely, to match a protein with a thin transmembrane region, the fatty acyl chains of neighbouring lipids will be compressed and they will occupy a greater surface area.

collected for a sample at low hydration (5.4 water molecules per molecule of lipid) and bilayer thickness decreases with increasing hydration [17,126]. Bilayer thickness is also temperature dependent, decreasing by about 2 Å for a 40 °C increase in temperature [127].

Binding constants have been measured as a function of fatty acyl chain length for a number of membrane proteins, as shown in Fig. 28 [78,99,128,129]. The theories of hydrophobic mismatch described above show that there is an energetic cost associated with any change in the thickness of the bilayer around a membrane protein. These costs would be reflected in values for the equilibrium constant describing the binding of lipids to the protein. A lipid that can bind to a protein without a change in bilayer thickness would bind more strongly to the protein than one for which binding requires a change in bilayer thickness. Models of hydrophobic mismatch that assume that a membrane protein is rigid might be expected to be particularly applicable to β-barrel proteins, which are likely to be more difficult to distort than membrane proteins whose transmembrane domains consist of a bundle of α-helices. Relative lipid binding constants for the β-barrel porin OmpF as a function of acyl chain length show a maximum for di(C14:1)PC, phosphatidylcholines with shorter or longer fatty acyl chains binding less strongly (Fig. 28) [128]. The hydrophobic thickness of OmpF, defined by the positions of the bands of aromatic residues at the two membrane–water interfaces, is about 24 Å (Table 1; Fig. 24), similar to the hydrophobic thickness of a bilayer of di(C14:1)PC (about 21 Å), consistent with the observation that this is the phosphatidylcholine showing strongest binding to OmpF.

Lipid binding constants for OmpF decrease by about a factor of 3 between di(C14:1)PC and di(C24:1)PC (Fig. 28). The changes in binding constant for OmpF from di(C14:1)PC to di(C20:1)PC are comparable to those calculated by the approaches of Fattal and Ben-Shaul [117] and Mouritsen and Bloom [122,123,130], which assume a rigid protein around which the lipid bilayer distorts to achieve hydrophobic matching. However, on increasing the fatty acyl chain length beyond C20, changes in binding constant are relatively small (Fig. 28), whereas theory predicts a continuing decrease in interaction energy. These results suggest therefore that on changing the fatty acyl chain length from C14 to about C20, the lipid bilayer thins around the β-barrel but that beyond a chain length of C20, the β-barrel also deforms to help maximise the interaction with the bilayer.

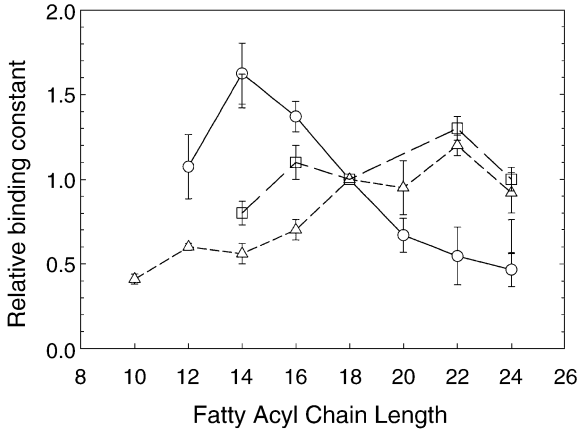

Fig. 28. Relative lipid binding constants for OmpF, KcsA and Ca^{2+}-ATPase. The binding constants of OmpF (○), KcsA (△) and Ca^{2+}-ATPase (□) for phosphatidylcholines relative to that for di(C18:1)PC are plotted as a function of fatty acyl chain length. Data from Refs. [78,128,129].

Effects of fatty acyl chain length on binding of lipids to the α-helical K^+ channel KcsA of *S. lividans* are very different to those for OmpF [129], as shown in Fig. 28. For KcsA, there is a gradual increase in relative binding constant with increasing chain length from C10 to C22, with a small decrease from C22 to C24. The hydrophobic thickness of a bilayer of di(C22:1)PC is about 34 Å. As shown in Fig. 7, a bilayer of this thickness would locate the Trp side chains totally within the hydrocarbon core of the bilayer, consistent with the location of the lipid molecule in the structure, modelled as a diacylglycerol. The fatty acyl chains of *Streptomyces* are unusual in being mostly branched-chain saturated C14, C15 and C16 iso-acids and C15 anteiso-acids [131]. The thicknesses of bilayers of branched-chain lipids appear not to have been determined and may be different to those of the normal unsaturated phospholipids. However, if the thickness of the lipid bilayer in *Streptomyces* is comparable to that in a bilayer of di(C16:1)PC, then the hydrophobic thickness of the bilayer would be significantly less than that giving optimal binding to KcsA.

Changes in lipid binding constants for KcsA with changes in chain length are small compared to those seen with OmpF (Fig. 28), suggesting that KcsA distorts to match the lipid bilayer rather than the lipid bilayer distorting to match the protein. The change in relative free energy of lipid binding per fatty acyl chain carbon atom is 0.1 kJ mol^{-1} [129]. This can be compared to a value of 0.4 kJ mol^{-1} per fatty acyl chain carbon atom estimated from ESR studies of phosphatidylcholine binding to rhodopsin [132]. The chain length dependence of relative free energy of binding for KcsA extrapolates to 4.1 kJ mol^{-1} at zero chain length [129]. If this is equated with the loss of interaction energy of the fatty acyl chains with KcsA, then the fatty acyl chain contribution to the di(C18:1)PC-KcsA interaction is more favourable than the fatty acyl chain contribution to the di(C18:1)PC-di(C18:1)PC interaction by about 4.1 kJ mol^{-1}. This figure can be compared to the free energy cost of creating a void equivalent to a methyl group in the hydrophobic core of a soluble protein, which is about 6.7 kJ mol^{-1} [133]. Thus, a slightly larger fatty acyl chain contribution to the lipid–KcsA interaction than to the lipid–lipid interaction, with a gradual decrease in the free energy of the lipid–KcsA interaction with decreasing chain length, would explain the results. The decreasing relative contribution of the chains to the lipid–KcsA interaction could

represent the cost of distorting KcsA to achieve hydrophobic matching.

The efficiency of hydrophobic matching of KcsA to its surrounding lipid bilayer has been demonstrated from observations of the fluorescence emission of the Trp residues located at the ends of the transmembrane α-helices in KcsA [129]. Fluorescence emission spectra of Trp residues are environmentally sensitive and any major change in the location of the Trp groups in KcsA relative to the lipid bilayer with changing bilayer thickness would be reflected in changes in the fluorescence emission spectra. In fact, observed changes in Trp emission spectra with changing bilayer thickness are very small, suggesting that the Trp residues maintain their positions close to the glycerol backbone region of the bilayer [129]. The most likely changes in KcsA to achieve hydrophobic matching with the surrounding lipid bilayer are a rotation of the Trp residues at the ends of the transmembrane α-helices about their $C_\alpha - C_\beta$ bonds and/or a tilt of the transmembrane α-helices. The transmembrane α-helices M1 and M2 in KcsA are organised as a pair of antiparallel helices in which each M1 only contacts M2 from its own subunit, with the M2 helices participating in subunit–subunit interactions (see Fig. 7) [46]. M2 helices cross at an angle of about $-40°$ and the relatively steep packing angle of the M2 helices means that the contact interface between the helices is localised to a fairly narrow region, making helix–helix rearrangements relatively easy. Indeed, it has been suggested that opening of the KcsA channel involves movement of the M2 helices relative to the plane of the bilayer [134].

Lipid binding constants for Ca^{2+}-ATPase depend less on fatty acyl chain length than those for KcsA, as shown in Fig. 28 [78,99]. Binding constants hardly change with changing chain length from C16 to C22, although there is a slight increase in binding constant from C14 to C16, with a small decrease from C22 to C24 (Fig. 28). This again suggests that the helix bundle that makes up the transmembrane region of the Ca^{2+}-ATPase can easily distort to match changes in lipid bilayer thickness. Tilting of the transmembrane α-helices in Ca^{2+}-ATPase would be expected to lead to changes in activity, and changes in activity with changing fatty acyl chain length are, indeed, observed experimentally (Section 8.4). Lipid binding constants for the Ca^{2+}-ATPase are unaffected by methyl branching of the fatty acyl chains [104].

Relative lipid binding constants have also been determined for simple transmembrane α-helices L_{16} and $KKGL_{10}WL_{12}KKA$ (L_{22}) in bilayers of phosphatidylcholines in the liquid crystalline phase [115]. Although strongest binding is seen when the hydrophobic length of the peptide matches the hydrophobic thickness of the bilayer, relative binding constants change much less with changing chain length than expected from theories of hydrophobic mismatch. The effects of aromatic residues at the ends of transmembrane α-helices have been studied using peptides $K_2GFL_6WL_8FK_2A$ (F_2L_{14}) and $K_2GYL_6WL_8YK_2A$ (Y_2L_{14}) in which one Leu residue at each end of the poly-Leu stretch is replaced by either a Phe or a Tyr [105]. The effect of the aromatic residues is to increase the effective hydrophobic length of the peptides so that optimal matching is now to a thicker bilayer, but with changes in binding constant with changing lipid bilayer thickness still being relatively small [105]. Helices are excluded from thick lipid bilayers when the hydrophobic mismatch exceeds about 10 Å [115].

The results described above suggest that long helices probably match thin bilayers by rotation of residues at the ends of the helices and/or by tilting, with little distortion of the lipid bilayer. Nevertheless, there is a variety of experimental evidence in favour of models for hydrophobic matching in which the major changes are in the thickness of the lipid bilayer. For example, attempts to measure helix tilt angles in lipid bilayers have found that changes in tilt angle with changes in bilayer thickness are very small and suggest that the tilt angle of a helix in a bilayer is an intrinsic property of the helix, depending little on the thickness of the bilayer [136–138]. These experimental results are in agreement with molecular dynamics simulations for peptides of the $W_2(LA)_nW_2$ type, which showed that there was no simple relationship between the tilt of the helix and the thickness of the lipid bilayer [139]. However, these same simulations showed that changes in bilayer thickness with changes in helix length were rather small (a 2–3 Å change in bilayer thickness for a 10 Å increase in peptide length) so that distortion of the lipid bilayer alone is not sufficient to achieve hydrophobic matching. It could be that the presence of a pair of Trp residues at each end of the helix allowed efficient matching by rotation of the Trp residues relative to the helix axis. Further, both the experimental data and the simulations were performed at relatively high concentrations of peptide (peptide/lipid molar ratio of about 1:20 to 1:40) and it is possible that steric interactions between the peptides prevent extensive tilting at high concentrations. Interactions between helices with the formation of dimers or higher aggregates are also possible at high peptide concentrations (see Section 6).

Further evidence favouring models of hydrophobic matching by distortion of the lipid bilayer comes from studies of the effects of peptides and proteins on bilayer phase transition temperatures. For example, although bacteriorhodopsin has relatively little effect on the phase transition temperatures of di(C14:0)PC or di(C16:0)PC [140], it increases the transition temperature of di(C12:0)PC and slightly decreases that of di(C18:0)PC [141]. This is largely consistent with hydrophobic matching models; since di(C12:0)PC gives a too thin bilayer in the liquid crystalline phase to match the bacteriorhodopsin molecule, the presence of bacteriorhodopsin will favour the thicker gel phase, whereas di(C18:0)PC gives a too thick bilayer in the gel phase so that the presence of bacteriorhodopsin will favour the thinner liquid crystalline phase. The small effect of bacteriorhodopsin on the phase transition temperature of

di(C16:0)PC suggests that the hydrophobic thickness of bacteriorhodopsin should be close to the average of the hydrophobic thickness of a bilayer of di(C16:0)PC in the liquid crystalline phase and gel phase, which is about 30 Å. In fact, the hydrophobic thickness of bacteriorhodopsin is closer to 35 Å, which would match the average hydrophobic thickness of a bilayer of di(C18:0)PC (34 Å). Similar effects on phase transition temperatures have been observed with melibiose permease (MelB) [142]. The presence of MelB leads to an increase in transition temperature for phosphatidylcholines with chain lengths less than C12 and a decrease in transition temperature for chain lengths greater than about C18, suggesting a hydrophobic thickness of the protein of about 31 Å to match the average hydrophobic thickness of a bilayer of di(C16:0)PC [142]. Effects of peptides of the type $KKGL_7WL_9KKA$ on the phase transition properties of bilayers of phosphatidylcholine are also consistent with the expectations of hydrophobic matching [143,144] although effects of the peptides on the phase transition properties of phosphatidylethanolamines are not [145] and effects of peptides of the $K_2(LA)_nK_2$ and $W_2(LA)_nW_2$ types on bilayers of phosphatidylcholines or phosphatidylethanolamines also do not fit the expectations of hydrophobic matching [144,146–148].

Of course, if the presence of peptides and proteins had major effects on the thickness of the surrounding lipid bilayer, these changes should be readily detectable. In fact, measurements of the effects of transmembrane α-helices on lipid bilayer thickness suggest that any changes in bilayer thickness are generally very small. Although long helices increase lipid order and so thicken a lipid bilayer, and short helices decrease order, and so thin a lipid bilayer, as expected for hydrophobic matching [144], estimates of the actual changes in bilayer thickness based on deuterium NMR measurements suggest that the changes in thickness are very small [149–152]. It appears that lipids will distort slightly to improve the match between the hydrophobic length of the peptide and the hydrophobic thickness of the bilayer, but that the extent of these changes is very limited and much less than required to produce full hydrophobic matching. Significant changes in transmembrane α-helices can therefore be expected where there is a large hydrophobic mismatch between the protein and the lipid bilayer.

Examples where some distortion of the lipid bilayer is likely are provided by bacteriorhodopsin, rhodopsin, and the potassium channel KcsA. The locations of the glycerol backbones of the lipids around bacteriorhodopsin (Fig. 4; Table 1) suggest a hydrophobic thickness for the lipid bilayer of about 35 Å, similar to the hydrophobic thickness of a bilayer of di(C22:1)PC. However, the chain lengths of the lipids in the purple membrane are normally only C16 (see Fig. 3). The hydrophobic thickness of a bilayer of lipids containing phytanyl chains appears not to have been determined, but, even if it is slightly thicker than a bilayer of a lipid

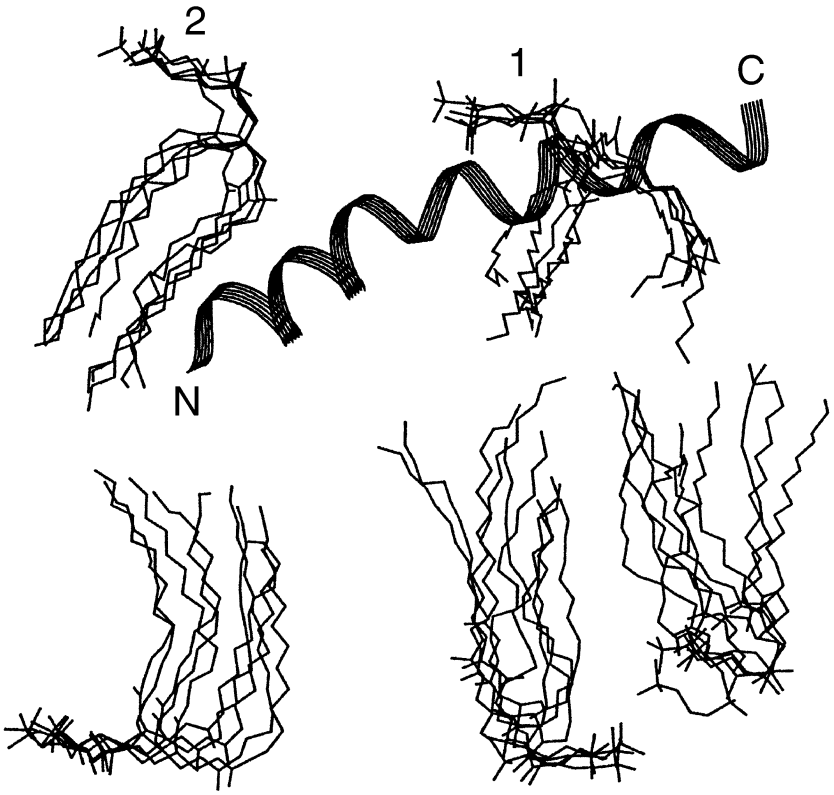

Fig. 29. Superposition of five configurations of lipid molecules around melittin bound to the surface of a bilayer of di(C14:0)PC in the liquid crystalline phase. The configurations are taken at times 100 ps apart. Modified from Ref. [135].

containing normal, unbranched fatty acyl chains, it is likely that the presence of bacteriorhodopsin results in an increase in thickness for the surrounding lipid bilayer. Thickening of a lipid bilayer requires the fatty acyl chains in the bilayer to be stretched, but the energy required to stretch the chains could be offset by increased van der Waals contacts with the protein surface, if straighter chains give better packing with the surface than disordered chains (Fig. 5). A similar effect is seen with rhodopsin. The retinal rod membrane contains lipids enriched in the polyunsaturated C22:6 chain (see Section 8.2). The effective chain length for a palmitoyl chain at the *sn*-1 position in a phosphatidylcholine with C22:6 at the *sn*-2 position is 13.8 Å at 37 °C [127]. Assuming that there is no extensive chain interdigitation in the liquid crystalline phase, this defines the hydrocarbon thickness of a bilayer of (C16:0, C22:6)PC as about 27.6 Å, significantly less than the estimated hydrophobic thickness for rhodopsin. Thus, as for bacteriorhodopsin, the presence of rhodopsin is likely to lead to an increase in thickness for the lipid bilayer around the protein molecule. Finally, the hydrophobic thickness of the potassium channel KcsA is about 37 Å (Fig. 7), again thicker than the expected hydrophobic thickness for the lipid bilayer surrounding it in the bacterial inner membrane. In agreement with the estimated hydrophobic thickness of the protein, the phosphatidylcholine that binds most strongly to KcsA is di(C22:1)PC, which gives a bilayer of thickness about 34 Å, as described above. Thus, either the structure of KcsA in the native membrane is slightly different to that shown in the crystal structure, or the protein will be in a state of stress in the membrane, being surrounded by phospholipids with stretched fatty acyl chains.

Finally, the ways in which a lipid bilayer might accommodate a tilted helix are shown in the molecular dynamics simulation of melittin modelled in a surface-bound form and illustrated in Fig. 29 [135]. The simulation shows that two different lipid molecules in the membrane (molecules 1 and 2 in Fig. 29) respond very differently to the presence of the melittin molecule. The simulation shows the melittin molecule inserted into only half of the bilayer, making a steep angle with the bilayer surface so that the effective transmembrane length of the melittin molecule is small. As a consequence, the outer leaflet of the bilayer has to thin to match the melittin molecule. Lipid 1 in Fig. 29 thins by splaying, occupying a greater area in the membrane surface. Lipid 2 in Fig. 29 thins by tilting its chain to match the tilt of the melittin molecule.

6. Effects of lipid structure on helix–helix interactions

An analysis of helix packing in membrane proteins shows that the most common packing angle between adjacent helices is close to 20°, giving a nearly parallel packing of the helices, thus maximising the area of the interface between the helices [153]. Packing is similar to that in coiled-coil proteins where helix–helix interactions are mediated by heptad repeats in which residues at the *a* and *d* positions of the repeat pack tightly as 'knobs into holes' at the helix–helix interface [81,154]. Oligomerisation of soluble coiled-coil proteins is driven by packing of hydrophobic residues at the interface, but hydrophobic interactions cannot be important in packing of transmembrane α-helices since hydrophobic interactions are already accounted for in insertion of the helices into the lipid bilayer. The free energy of association of two transmembrane α-helices in a lipid bilayer, ΔG_a, can be written as

$$\Delta G_a = \Delta G_{HH} + n/2\Delta G_{LL} - n\Delta G_{HL} \quad (5)$$

where ΔG_{HH}, ΔG_{LL} and ΔG_{HL} are the free energies of helix–helix, lipid–lipid and helix–lipid interactions, respectively, and it is assumed that formation of a helix–helix pair displaces *n* lipids from around the two helices [133,155]. Dimerisation of the helices could be driven by a favourable value for ΔG_{HH}, arising, for example, from salt bridge or hydrogen bonding interactions between the two helices. Good packing at the helix–helix interface with strong van der Waals interactions could also contribute to a favourable value for ΔG_{HH}. Weak interactions between the polar headgroups of the lipids and the helices and poor packing between the lipid fatty acyl chains and the rough surface of the transmembrane α-helices would also drive dimerisation since ΔG_{HL} would then be unfavourable compared to ΔG_{HH} and ΔG_{LL}. Any decrease in motional freedom for the lipid fatty acyl chains due to the presence of the relatively rigid transmembrane α-helices will lead to a decrease in chain entropy, also leading to an unfavourable ΔG_{HL}.

The free energy of dimer formation by a pair of transmembrane α-helices in a lipid bilayer has been determined by measuring the quenching of the fluorescence of a Trp-containing helix by a dibromotyrosine-containing helix [156]. The free energy of dimerisation of two transmembrane α-helices in bilayers of phosphatidylcholine was found to increase with increasing fatty acyl chain length, but to depend rather little on the length of the helix. In di(C18:1)PC, the free energy of dimerisation of a Trp-containing helix and a dibromotyrosine-containing helix was 8.4 kJ mol^{-1} [156]. As described by White and Wimley [157], this can be compared to the free energy cost of creating a void equivalent to a methyl group in the hydrophobic core of a soluble protein, which is about 6.7 kJ mol^{-1}. The free energy change favouring helix dimer formation in di(C18:1)PC is therefore that expected if helix–helix packing were more efficient than helix–lipid packing by an amount equivalent to the volume of about one methyl group. A comparison can also be made with the entropy change corresponding to disordering of the lipid fatty acyl chains at the gel to liquid crystalline phase transition [158], which corresponds to a free energy change of ca 2.9 kJ mol^{-1} per carbon atom. The increase in free energy for dimer formation with increasing fatty acyl chain length is about 0.5 kJ mol^{-1} per carbon atom [156]. Thus, a

relatively small increase in chain order caused by the presence of the peptide could make a significant contribution to the free energy for oligomerisation of transmembrane α-helices. A chain-length dependence of the energy of helix–helix packing could be part of the explanation for the chain-length dependence of the activities of some membrane proteins (Section 8.4); changes in the energies of helix–helix interactions as a result of changing phospholipid chain length could have significant effects on the packing of the transmembrane α-helices and so affect activity.

The physical phase of the phospholipids also has a marked effect on oligomerisation of transmembrane α-helices. In lipid bilayers containing domains of liquid crystalline and gel phase lipid, transmembrane α-helices partition preferentially into regions of liquid crystalline lipid [105]. The result will be an increase in the local concentration of transmembrane α-helices with a consequent increase in oligomer formation, an effect observed experimentally [156]. In the presence of cholesterol, domains of liquid-ordered lipid are formed with properties intermediate between those of the gel and liquid crystalline phases [159]. Transmembrane α-helices are not excluded from liquid-ordered lipid [105] and helix dimerisation is stronger in liquid-ordered lipid than in liquid crystalline lipid [156]. In part, this follows from an increase in the effective chain length of the phospholipid caused by cholesterol but this does not explain the full effect of cholesterol [156]. It is possible that the cost of formation of voids at the lipid–protein interface in the liquid-ordered state will be higher than in the liquid crystalline state and this could also contribute to favourable dimerisation.

It has been suggested that the presence in a bilayer of a phospholipid such as a phosphatidylethanolamine that prefers the hexagonal H_{II} phase will result in curvature frustration in the bilayer, because the phosphatidylethanolamine will make unequal contributions to the headgroup and chain areas [160]. Curvature frustration will result in increased surface free energy (increased surface tension) because of increased water contact with the hydrocarbon core of the bilayer. The increased surface tension will, in turn, result in an increased lateral compression in the acyl chain region, and it has been suggested that this could modulate the function of some membrane proteins [160]. However, dimer formation by transmembrane α-helices in di(C18:1)PC and in a 1:1 mixture of di(C18:1)PC and di(C18:1)PE were identical, suggesting that the presence of lipids favouring the hexagonal H_{II} phase had no significant effect on helix–helix interactions [156].

7. Effects of lipid structure on protein–protein interactions

One possible response of a membrane protein to unfavourable interaction with lipids is to aggregate and so reduce the surface area of the protein exposed to the lipid bilayer [161]. The extent to which transmembrane domains of membrane proteins can come into contact will depend, of course, on the shape of the protein. Bacteriorhodopsin has a rather cylindrical shape with small extramembranous domains and bacteriorhodopsin forms trimers in the native membrane. However, the extent to which the transmembrane domains of proteins with large extramembranous domains like the Ca^{2+}-ATPase (Fig. 22) can come into contact will be limited. Indeed, the fact that the minimum number of lipid molecules per protein molecule required to maintain activity for the Ca^{2+}-ATPase is 30:1 [162,163], equal to the number of annular lipids for the Ca^{2+}-ATPase [6], suggests that each ATPase molecule maintains its own, independent unshared lipid annulus with little protein–protein contact between transmembrane domains, even at very low molar ratios of lipid/ATPase.

Further information about sharing of annular shells of lipid comes from the structural studies of bacteriorhodopsin discussed in Section 2.1. Since many of the lipid molecules around the bacteriorhodopsin trimer are not resolved in the available high-resolution structures, it is not possible to give any definitive answer. However, in the structure determined by Belrhali et al. [35], only one lipid molecule in the space between trimers has one of its phytanyl chains interacting with one trimer and its other chain interacting with a second trimer. The situation for the other lipid molecules between the trimers is not always clear, but in many cases, the two trimers appear to be separated by two shells of lipid molecules, in a protein–lipid–lipid–protein arrangement, implying that the trimers do not share many of the lipid molecules in their annular shells, even in the purple membrane.

There have been several studies of the state of aggregation of bacteriorhodopsin in reconstituted membranes. The state of aggregation depends on the concentration of bacteriorhodopsin in the membrane, the nature and length of the fatty acyl chains and on temperature. Roughly, it can be said that at molar ratios of bacteriorhodopsin/lipid less than 1:100, at temperatures below the phase transition temperature, bacteriorhodopsin is aggregated, probably as trimers, whereas for more dilute bacteriorhodopsin at higher temperatures in the liquid crystalline phase, bacteriorhodopsin is monomeric for lipids with fatty acyl chain lengths around C18 [141,164–166,]. Studies using electron microscopy have shown that bacteriorhodopsin aggregates in bilayers when there is a large hydrophobic mismatch [164]. Thus, bacteriorhodopsin is monomeric when reconstituted into bilayers of phosphatidylcholines in the liquid crystalline phase over the chain length range C12–C22 but is aggregated in bilayers of di(C10:0)PC or di(C24:1)PC [164].

Most of the interface between bacteriorhodopsin monomers in the trimer in the purple membrane is located within the hydrocarbon core of the bilayer, involving contact between helix B in one monomer and helices D and E in the adjacent monomer (Fig. 30). Residues involved in these

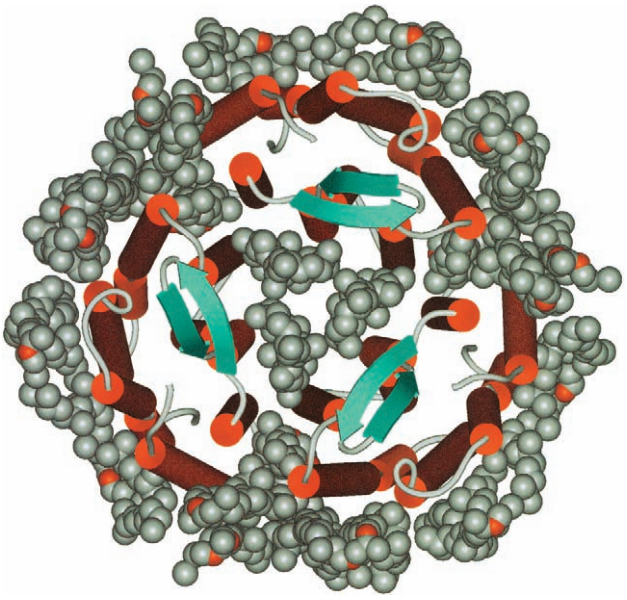

Fig. 30. The structure of a bacteriorhodopsin trimer with associated lipid molecules. The view is from the extracellular face of the membrane. (PDB file 1QHJ).

helical contacts are nonpolar and contact is driven by van der Waals interactions. Since STGA is bound tightly and specifically to bacteriorhodopsin in the centre of the trimer, interacting with two bacteriorhodopsin molecules (Fig. 6), it is likely that STGA is important for lattice assembly. Also important is a lipid molecule on the cytoplasmic face of the membrane, located between bacteriorhodopsin monomers in the trimer (Fig. 30). This molecule appears in all the high-resolution structures [35,41,42], suggesting both that the lipid is highly ordered and that it is essential for formation of the bacteriorhodopsin trimer. Bacteriorhodopsin reconstituted into di(C14:0)PC only forms 2D hexagonal arrays of trimers in the presence of the highly negatively charged lipids phosphatidylglycerophosphate or phosphatidylglycerosulfate, suggesting a special role for these phospholipids [167]. This could reflect a requirement for negative charge to reduce electrostatic repulsions between positively charged residues on the bacteriorhodopsin molecules. Unexpectedly, STGA is not required for lattice assembly, although the lattice formed by bacteriorhodopsin in reconstituted systems is different to the native lattice, possibly suggesting the formation of a different form of the trimer [167].

8. Effects of lipid structure on membrane protein function

8.1. The gel to liquid crystalline phase transition

The transition from the liquid crystalline to the gel phase results in a very marked change in the physical properties of a lipid bilayer. This transition might, therefore, be expected to have a significant effect on the activity of a membrane protein embedded in a lipid bilayer. An example is provided by the experiments with Ca^{2+}-ATPase reconstituted into bilayers of defined composition illustrated in Fig. 31. The phase transition temperature for di(C18:1)PC is −21 °C and the Ca^{2+}-ATPase in bilayers of di(C18:1)PC is active over the whole temperature range from 10 to 45 °C shown in Fig. 31 [163,168]. However, di(C14:0)PC transforms from the liquid crystalline to the gel phase at 24 °C and the Ca^{2+}-ATPase in di(C14:0)PC has no activity below 24 °C (Fig. 31). Although the phase transition temperature for di(C16:0)PC is 42 °C, the Ca^{2+}-ATPase in di(C16:0)PC has appreciable activity down to about 30 °C; no breaks in ATPase activity are seen at 42 °C (Fig. 31). Changes in ESR spectra of spin labelled lipids in the di(C16:0)PC/Ca^{2+}-ATPase system suggest an increase in motion for the annular lipids starting at about 30 °C [168] and the rate of rotation of the Ca^{2+}-ATPase in di(C16:0)PC also increases markedly at temperatures above 30 °C [169]. Thus, the activity of the Ca^{2+}-ATPase is controlled by the effects of the lipids in its immediate vicinity (the annular lipids) and, in di(C16:0)PC, these undergo a broad change from a rigid, gel-like to a fluid, liquid crystalline-like state at a temperature starting at about 30 °C [168]. A broad phase transition for the annular lipids is consistent with the observation that the enthalpy of the sharp phase transition characteristic of bulk phase lipid decreases in magnitude in bilayers of di(C14:0)PC or di(C16:0)PC with increasing content of Ca^{2+}-ATPase and disappears totally at about a molar ratio of ATPase/lipid of 1:40 [170] close to the number of lipids required to form a complete annular shell around the ATPase (30; Section 1).

The low activity observed for the Ca^{2+}-ATPase in gel phase lipid is not due to any aggregation of the Ca^{2+}-ATPase since low activities are also seen for the Ca^{2+}-

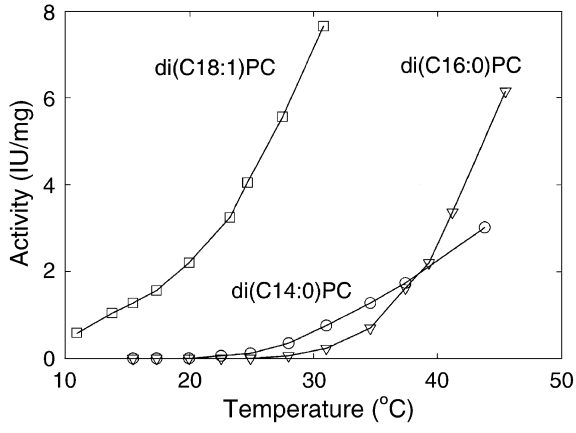

Fig. 31. Effects of temperature on the ATPase activity of the Ca^{2+}-ATPase of skeletal muscle sarcoplasmic reticulum. Activities are shown for the ATPase reconstituted into bilayers of; (□) di(C18:1)PC; (○) di(C14:0)PC; (▽) di(C16:0)PC. Data from Ref. [163].

ATPase reconstituted at high dilution into sealed vesicles where the number of ATPase molecules per vesicle is close to one, so that aggregation is not possible [171]. Thus, the effects of gel phase lipid follow directly from effects of the gel phase on the conformational state of the Ca^{2+}-ATPase. The reasons why the activity of the Ca^{2+}-ATPase is low in gel phase lipid have been studied in detail [172]. Surprisingly, the transition from liquid crystalline to gel phase had no effect on Ca^{2+} binding to the ATPase, even though the Ca^{2+} binding sites on the ATPase are located within the transmembrane region of the ATPase [172]. The slow rate of hydrolysis of ATP by the ATPase in gel phase lipid in fact follows from a very slow rate of formation of the phosphorylated intermediate [172].

Not all membrane proteins show low activities in gel phase lipid and it is necessary to consider the increase in bilayer thickness that occurs on transition into the gel phase; if the bilayer thickness in the liquid crystalline phase is less than optimum for the protein, the increase in bilayer thickness that occurs on transition into the gel phase will tend to lead to an increase in activity. For example, the activity of the integral membrane protein diacylglycerol kinase (DGK) of *E. coli* in di(C14:0)PC is comparable to that in di(C14:1)PC at all temperatures even though the activity in gel phase di(C16:0)PC is less than that in di(C16:1)PC at the same temperatures [173]. Similarly, the Na^+,K^+-ATPase has a very low activity in di(C18:0)PC in the gel phase but its activity in di(C14:0)PC is greater than that in di(C14:1)PC at all temperatures [97]. Surprisingly, however, the activity of the Na^+,K^+-ATPase in gel phase di(C14:0)PG is much less than that in liquid crystalline di(C14:0)PG [174]. Conversely, the glucose transporter of red blood cells has low activity in gel phase di(C14:0)PC but shows activity in gel phase di(C14:0)PG [175]. The reasons for the different activities in gel phase phosphatidylcholine and phosphatidylglycerol are not known.

As described above, the presence of Ca^{2+}-ATPase modifies the phase transition properties of the lipids surrounding it in the membrane, so that in di(C16:0)PC, the lipid molecules start to become fluid at about 30 °C, compared to 42 °C for unperturbed di(C16:0)PC [168]. Rather similar results have been obtained for the Na^+,K^+-ATPase reconstituted into bilayers of phosphatidylglycerols [174]. Breaks in activity/temperature plots were observed at 20, 31 and 44 °C for the ATPase reconstituted into di(C14:0)PG, di(C16:0)PG and di(C18:0)PG, respectively; these temperatures can be compared with phase transition temperatures of 22, 38 and 52 °C, respectively, for the three lipids [174]. Similarly, the presence of melibiose permease (MelB) leads to an increase in transition temperature for phosphatidylcholines with chain lengths less than C12 and a decrease in transition temperature for chain lengths greater than about C18 [142]. The effects of membrane proteins on lipid phase transition temperatures are probably related to the degree of hydrophobic mismatch between the protein and the lipid bilayer, as described in Section 5.3.

8.2. The liquid crystalline to hexagonal H_{II} phase transition and curvature frustration

Most, if not all, biological membranes contain lipids that, in isolation, prefer to adopt a hexagonal H_{II} phase rather than the normal bilayer phase. The presence of such lipids in a membrane results in curvature frustration and it has been suggested that this could be important for the proper function of the membrane [160]. Mixtures of two lipids, one preferring the bilayer phase and one the hexagonal H_{II} phase, adopt a bilayer phase if the mixture contains more than about 20 mol% of the bilayer-preferring lipid [176]. The presence of intrinsic membrane proteins also has a strong tendency to force a bilayer phase on phospholipids [177,178]. Thus, it is presumed that the lipid molecules surrounding an intrinsic membrane protein will be in a bilayer phase, even when the lipid molecules would, in isolation, adopt a hexagonal H_{II} phase.

The effects of lipid molecules favouring nonbilayer phases on the activities of membrane proteins have been tested in a few cases. For the Ca^{2+}-ATPase of sarcoplasmic reticulum and for *E. coli* diacyl glycerol kinase, the presence of phosphatidylethanolamine, a lipid favouring the hexagonal H_{II} phase, leads to decreased activity [103,173]. However, for rhodopsin, the presence of a lipid favouring the hexagonal H_{II} phase is required for proper function. The retinal rod membrane is unusual in containing a very high content of polyunsaturated fatty acids, a property shared with membranes of other neuronal cells [179]. The relative amounts of the two major intermediates of the rhodopsin photocycle, metarhodopsin I (MI) and metarhodopsin II (MII), depend on lipid structure [179]. Small amounts of MII are formed when rhodopsin is reconstituted with egg phosphatidylcholine, but the amounts are much less than those formed in the native membrane. Increasing the chain length and unsaturation of the phosphatidylcholine to di(C22:6)PC results in a very significant increase in the amount of MII formed [180]. However, the highest level of MII is seen when rhodopsin is reconstituted into mixtures of phosphatidylcholine and phosphatidylethanolamine containing C22:6n3 chains [181]. It does not matter which lipid carries the C22:6n3 chains. High levels of MII are seen in mixtures of di(C22:6)PE and egg phosphatidylcholine, or in mixtures of di(C22:6)PC, egg phosphatidylethanolamine and egg phosphatidylserine [181]. Further, MI/MII ratios equal to those in the native membrane are seen in mixtures of di(C18:1)PC and di(C18:1)PE when the di(C18:1)PE content is increased from the value of about 40% characteristic of the native membrane, to about 75% [179,181,182]. These results strongly suggest that the MI/MII ratio is sensitive to some physical property of the whole bilayer rather than to specific binding of a small number of phospholipid molecules to a few special sites on rhodopsin.

In the retinal rod membrane at near physiological temperatures, MI and MII are in a pH-dependent equilibrium

$$MI + nH^{+} \leftrightarrows MII$$

The low proportion of MII found in egg phosphatidylcholine at pH 7 is due to a shift in the pK describing the equilibrium, from a value of 7.8 in the native membrane to 6.3 for the reconstituted system [181]. The basis for this shift in p*K* is not known. Since the largest effects on the MI/MII equilibrium are seen for a combination of the small phosphatidylethanolamine headgroup with the bulky C22:6n3 chains, which are likely to favour hexagonal phase formation, it has been suggested that interfacial curvature free energy could be involved [181,182]. It has been suggested that MII has a greater hydrophobic thickness than MI and that the lipid bilayer has to thin to match the hydrophobic thickness of MI and to thicken to match MII [182]. The presence of a phospholipid such as phosphatidylethanolamine with a negative monolayer curvature (curvature towards the aqueous phase) will favour a thickening of the lipid around the protein since this corresponds to a negative curvature, and so will favour MII [182]. However, there are other possible explanations for the effects of phosphatidylethanolamines. It could be that changes in hydration at the lipid–water interface are important since the cross-sectional areas for lipids containing polyunsaturated chains are larger than those with saturated chains [183], resulting in changes in packing and hydration at the lipid–water interface. The MI–MII transition has been shown from studies of the effects of solvent to result in changes in hydration [184].

The level of cholesterol in the retinal rod membrane has also been shown to affect the MI/MII ratio for rhodopsin, low levels of cholesterol leading to high levels of MII [185]. It was suggested that the effect followed not from specific binding of cholesterol to rhodopsin but from an effect on the packing free volume in the bilayer, determined from measurements of the fluorescence polarisation of the probe diphenylhexatriene [185]. Voids or pockets of 'free volume' are present within a bilayer because of the low order of the fatty acyl chains and their low packing density and increased free volume in a bilayer was suggested to favour any conformational change in a protein leading to increased volume for the protein [185]. Packing free volume in the bilayer was also suggested to be important in determining the effects of phospholipid structure on the MI/MII ratio, an idea discussed in detail in Ref. [179]. The importance of curvature frustration for the function of rhodopsin is therefore still uncertain.

Phospholipid composition also has significant effects on the interaction between MII and the G-protein transducin [186,187]. The association constant between MII and transducin is higher in bilayers of di(C18:0,C22:6)PC than in bilayers of (C18:0,C18:1)PC, and is lower in the presence of cholesterol [187]. The changes in association constant with changing chain unsaturation presumably indicate a change in conformation for MII affecting the loops that interact with transducin. The rate of complex formation is also higher in the presence of polyunsaturated phosphatidylcholines [186]. It has been estimated that during normal physiological function, only about 1 rhodopsin out of every 100,000 is photoisomerised and active at any one time, so that the distance between MII molecules is about 1000 nm. The rate of complex formation between MII and transducin in the eye is therefore governed by the rate at which transducin can diffuse in the membrane surface and find a MII molecule [188]. Increased chain unsaturation leads to increased bilayer free volume because of more disordered chain packing [189], which could lead to increased rates of lateral diffusion.

8.3. Effects of lipid fluidity in the liquid crystalline phase

The early membrane literature contains many suggestions that the exact fluidity of the lipid bilayer component of a membrane is an important factor determining the activities of membrane proteins. This idea is now considerably less popular than it was and, in some cases, can be shown to be incorrect. Changes in fluidity cannot be the determining factor when a change is observed in an equilibrium property of a membrane protein such as a change in binding constant for a substrate or a change in the equilibrium constant describing some change on the protein; a change in lipid fluidity (a dynamic property of the system) cannot result in a change in an equilibrium property of a system [190].

8.4. Effects of bilayer thickness

Bilayer thickness has a large effect on the activities of many membrane proteins. Effects of bilayer thickness on the activity of the Ca^{2+}-ATPase are shown in Fig. 32. The activity of the Ca^{2+}-ATPase is highest when the ATPase is reconstituted into bilayers of di(C18:1)PC; activities are low in bilayers with shorter or longer fatty acyl chains so that fatty acyl chain length, and thus bilayer thickness, is important for function [78,88,90,163,191,192]. It is noticeable that activities vary little in the chain length range C16 to C20, which is the range of fatty acyl chain lengths, found in the native SR membrane [193]. The effects of bilayer thickness on the function of the Ca^{2+}-ATPase are complex, many of the steps in the reaction sequence being affected [104]. The changes in activity do not follow from any changes in aggregation state for the ATPase in the membrane since low ATPase activities are observed in short- or long-chain phospholipids when the ATPase is reconstituted into sealed vesicles containing isolated, single ATPase molecules, where aggregation is not possible [171].

Two other points can be made about the effects of fatty acyl chain length on the activity of the Ca^{2+}-ATPase. The first is that effects of chain length are highly cooperative, as shown by the data in Fig. 33A. This suggests that the

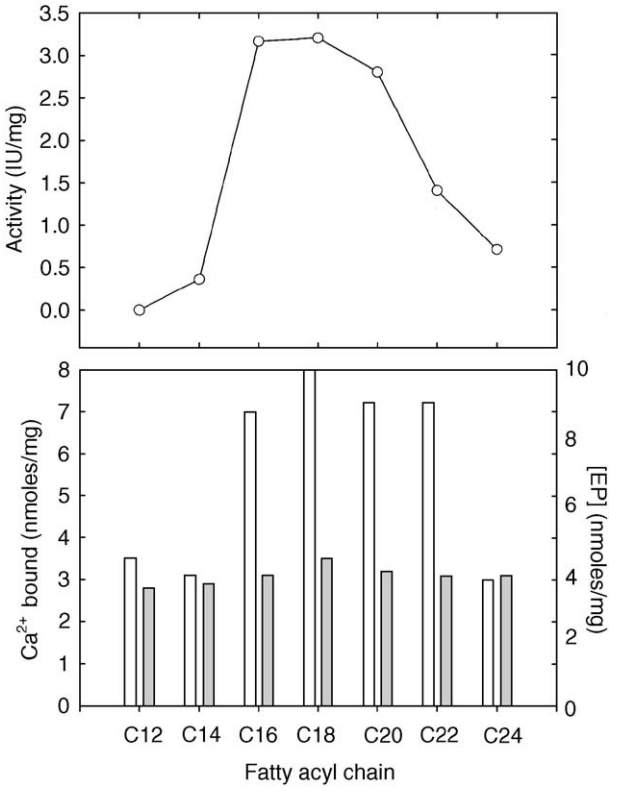

Fig. 32. Effects of phosphatidylcholine fatty acyl chain length on the Ca^{2+}-ATPase. The ATPase was reconstituted with phosphatidylcholines containing mono-unsaturated fatty acyl chains of the given length, all being in the liquid crystalline phase at 25 °C, the temperature of the experiment. The curve shows ATPase activity as a function of chain length. The hatched bars show the maximal level of phosphorylation of the ATPase (nmol [EP]/mg protein) by ATP in the presence of 1 mM Ca^{2+}, and the open bars show the level of Ca^{2+} bound (nmol/mg protein). Data from Ref. [104].

changes in conformation underlying the changes in stoichiometry of Ca^{2+} binding and ATPase activity follow from a cooperative effect of all the phospholipid molecules that surround the ATPase in the membrane (about 30); this point is discussed further below. The second point to be made is that although the effects of fatty acyl chain length presumably follow from changes in bilayer thickness, the bilayer thickness experienced by the Ca^{2+}-ATPase is not given simply by the average fatty acyl chain length in the membrane. For example, in a mixture of di(C14:1)PC and di(C24:1)PC of the appropriate composition the Ca^{2+}-ATPase binds two Ca^{2+} ions, compared to one in either di(C14:1)PC or di(C24:1)PC alone, and the ATPase activity is also higher, showing that a suitable combination of short- and long-chain phospholipids can produce a membrane equivalent in its properties to that produced by di(C18:1)PC, the phospholipid of optimal structure (Fig. 33B). However, studies with the Ca^{2+}-ATPase in single phospholipids (Fig. 32) show that chain lengths between C16 and C22 are compatible with a Ca^{2+} binding stoichiometry of 2:1, but average chain lengths in this range obtained with mixtures of di(C14:1)PC and di(C24:1)PC show a binding stoichiometry of 1:1 (Fig. 33B). Thus, the average chain length of the phospholipids in the bilayer does not give the bilayer thickness experienced by the ATPase.

The marked effects of bilayer thickness on ATPase activity indicate distinct changes in the conformation of the ATPase, which will have an associated energetic cost. These energetic costs would be expected to be reflected in different binding constants for phospholipids of different chain lengths. However, as described above, phospholipid binding constants for the Ca^{2+}-ATPase depend little on chain length (Fig. 28). The explanation is probably that a difference in the free energy of binding of a fraction of a kJ mol^{-1} for any one phospholipid molecule (which would not result in any detectable change in lipid binding constant) will become significant when summed over the 30 phospholipids that surround the ATPase in the membrane [6]. Thus, effects of chain length on the function of the Ca^{2+}-ATPase are highly cooperative, as described above.

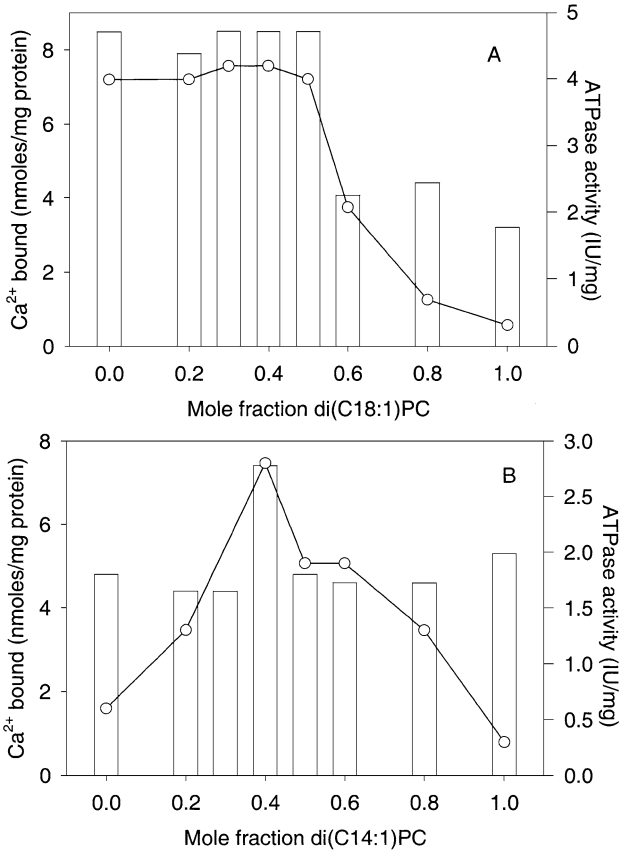

Fig. 33. Effects of mixtures of two phospholipids of different chain lengths on Ca^{2+} binding and activity of the Ca^{2+}-ATPase. In (A), the Ca^{2+}-ATPase was reconstituted with mixtures of di(C14:1)PC and di(C18:1)PC containing the given mole fraction of di(C18:1)PC. The bars show the level of Ca^{2+} binding (nmol Ca^{2+} bound/mg protein). Also shown are the ATPase activities (○) measured at 25 °C. In (B), the Ca^{2+}-ATPase was reconstituted with mixtures of di(C14:1)PC and di(C24:1)PC containing the given mole fraction of di(C14:1)PC. The bars show the level of Ca^{2+} binding (nmol Ca^{2+} bound/mg protein). Also shown are the ATPase activities (○) measured at 25 °C. Data from Ref. [104].

The chain length dependence of the activity of the plasma membrane Na^+,K^+-ATPase is slightly different to that of the Ca^{2+}-ATPase, with an optimum chain length of C22 in the absence of cholesterol but C18 in the presence of cholesterol [97]. The effect of cholesterol on the chain length optimum for ATPase activity is consistent with the bilayer-thickening effect of cholesterol [151]. However, the activity of the Na^+,K^+-ATPase in di(C18:1)PC in the presence of cholesterol is very considerably greater than that in di(C22:1)PC in the absence of cholesterol, suggesting that cholesterol has effects on the Na^+,K^+-ATPase additional to effects following from changing the thickness of the bilayer, possibly following from binding to non-annular sites (Section 4). The activity of DGK of *E. coli*, an intrinsic membrane protein with three transmembrane α-helices, is also dependent on bilayer thickness, with highest activity in di(C18:1)PC and lower activity in bilayers with shorter or longer fatty acyl chains [194]. Addition of 50 mol% cholesterol to DGK in di(C14:1)PC roughly doubled activity whereas addition of cholesterol to DGK in di(C18:1)PC or di(C24:1)PC caused a slight decrease in activity. It has been estimated from NMR order parameter data that, in the liquid crystalline phase, the effective length of the fatty acyl chains of di(C14:0)PC and di(C18:0)PC increase by 2.1–2.5 Å on incorporation of 50 mol% cholesterol [195]. The effect of 50 mol% cholesterol is therefore to increase the effective chain length by the equivalent of about 1 to 1.5 carbons. This is consistent with the observed increase in activity seen on addition of cholesterol to DGK in di(C14:1)PC and with the observed decreases in activity seen with longer-chain phospholipids [194].

Activities of a number of other membrane proteins have also been shown to be dependent on bilayer thickness, including rhodopsin [196–198], the glucose transporter from red blood cells [199,200], and cytochrome oxidase [201].

8.5. Effects of lipid headgroup structure

When considering the effects of lipid headgroup structure on the activity of a membrane protein, it is obviously necessary to distinguish between effects following from binding at the bulk annular sites and those that might arise from binding to a small number of 'special' (non-annular) sites, which may show specificity for a particular headgroup structure. A number of structures were discussed in Section 2 that show phospholipid molecules bound at specific sites on a membrane protein. In some cases, the lipid headgroup is well resolved, showing that the headgroup is immobilised on the surface of the protein, probably due to strong binding to the protein. However, this is not always the case. For example, in KcsA, there is strong biochemical evidence for a tightly bound phosphatidylglycerol molecule, but, although a lipid molecule is resolved in the crystal structure (Fig. 7), only the fatty acyl chains and glycerol backbone are well resolved, not the headgroup [48].

The bulk of the lipids in a biological membrane are generally zwitterionic, the anionic lipids making up just 10–20 mol% of the total lipid. A membrane protein is therefore likely to show high activity when reconstituted into bilayers of zwitterionic lipid. For example, the activities of Ca^{2+}-ATPase and DGK are high in bilayers of di(C18:1)PC but low in bilayers of dioleoylphosphatidylserine or dioleoylphosphatidic acid [104,173]. Amongst the zwitterionic lipids, the relative effects of phosphatidylcholine and phosphatidylethanolamine appear to be different for different membrane proteins, complicated by the preference of phosphatidylethanolamines for the hexagonal H_{II} phase, as described in Section 8.2. Thus, the activity of the Ca^{2+}-ATPase in bilayers of di(C18:1)PE at temperatures that favour the bilayer phase is the same as that in di(C18:1)PC, so that the structure of the zwitterionic headgroup is not important for function, but activities are lower in phosphatidylethanolamines than in phosphatidylcholines at temperatures that favour the hexagonal H_{II} structure for the phosphatidylethanolamine [104]. However, for rhodopsin, as described in Section 8.2, the presence of phosphatidylethanolamine is required to achieve a ratio of M1/MII comparable to that in the native membrane [182].

Although activities of membrane proteins reconstituted into bilayers of pure anionic phospholipids generally seem to be low, the presence of anionic phospholipids in mixtures with a zwitterionic phospholipid often leads to high activity. In some systems, there is strong evidence for a special role for particular lipid species, usually an anionic phospholipid, the best example probably being a requirement for cardiolipin in a variety of bioenergetic systems, including NADH dehydrogenase, cytochrome bc_1, ATP synthase, cytochrome oxidase, and the ADP/ATP carrier [202,203]. Bovine heart cytochrome oxidase copurifies with cardiolipin; in experiments in which preparations of cytochrome oxidase were treated with detergents, it was found that about 40 phospholipid molecules were 'loosely' associated with each cytochrome oxidase molecule (i.e., easily removed with detergent), between 6 and 8 were more tightly bound, and 2 to 3 molecules of lipid were tightly bound and very difficult to remove; these tightly bound molecules were found to be cardiolipin [204]. Robinson et al. [106] found that two molecules of cardiolipin bound with high affinity to cardiolipin-depleted samples of cytochrome oxidase, with weaker binding of a further two or three molecules. The strength of binding was found to depend on the number of fatty acyl chains; monolysocardiolipin, lacking one fatty acyl chain, bound about 3–10-fold less strongly than cardiolipin, and dilysocardiolipin, lacking two fatty acyl chains, bound about 30–100-fold less strongly than cardiolipin [106].

There is still some confusion about the functional importance of these tightly bound cardiolipin molecules. Initial studies suggested that removal of cardiolipin led to total loss of activity, but, given the rather harsh procedures necessary for this removal, loss of activity is probably not surprising.

A milder procedure to remove the cardiolipin is to exchange it out by detergent-mediated exchange with di(C14:0)PC; under these conditions, cytochrome oxidase remains active, although the level of activity is somewhat less than in the presence of cardiolipin [205–207]. This decrease in activity could, however, have been a result of the presence of the short-chain di(C14:0)PC [201]. Also arguing against an absolute requirement for cardiolipin is the observation that cytochrome oxidase prepared from dogfish contains no cardiolipin but shows normal activity [208] although the activity of cytochrome oxidase is reduced in mitochondria of yeast unable to synthesise cardiolipin [202]. In experiments in which cardiolipin was removed by treatment with phospholipase A_2, it was found that complete removal of cardiolipin lead to dissociation of subunits Via and Vib from the enzyme [209]. Thus cardiolipin probably enhances the activity of cytochrome oxidase whilst not being an absolute requirement for activity. In cytochrome bc_1 (Section 2.4), it has been suggested that cardiolipin could be part of a proton 'wire' conducting protons from the aqueous phase to the site of quinone reduction [60]. However, the mitochondrial ADP/ATP carrier shows an absolute dependence on the presence of cardiolipin for activity [210]. Cardiolipin is tightly bound to the carrier, as shown by detergent extraction studies, and is in slow exchange on the NMR time scale, in contrast to phosphatidylcholine and phosphatidylethanolamine, which are in rapid exchange [211].

The presence of phosphatidylserine in the bilayer increases the level of the MII intermediate for rhodopsin [212]; the presence of a negatively charged lipid will increase the concentration of H^+ close to the membrane surface and so could affect the level of MII through an effect on the pH-dependent equilibrium with MI. It has also been suggested that rhodopsin interacts specifically with a single phosphatidylserine molecule in the outer leaflet of the lipid bilayer and that this molecule is released when rhodopsin is activated [213].

The presence of anionic lipid is essential for the proper function of the AChR [91,92], for opening of the potassium channel KcsA [48,214] and for the function of a variety of other ion channels [215–218]. Although the presence of high concentrations of anionic phospholipids lead to low ATPase activities for the Ca^{2+}-ATPase, as described above, the presence of low concentrations of anionic phospholipids results in increased levels of accumulation of Ca^{2+}, an effect attributed to a reduction in the rate of slippage on the Ca^{2+}-ATPase [219]. It is not known whether this effect follows from binding of anionic phospholipid molecules to a small number of specific sites on the Ca^{2+}-ATPase or from a nonspecific effect following from occupancy of a proportion of the annular sites by anionic phospholipid. The phosphoinositides PtdIns(4)P and PtdIns(4,5)P_2 have been shown to bind tightly to band 3 [220] and glycophorin [221] in red blood cells, the interaction with glycophorin modulating the interaction with the protein 4.1 family of skeletal proteins [221].

9. Summary

Many of the questions posed at the start of this review can now be answered. Do lipid molecules form a distinct shell around a membrane protein? ESR studies show the presence of a shell or annulus of 'immobilised' lipids surrounding a protein in a membrane (Section 1). The concept of a lipid annulus is supported by a number of high-resolution structures that include lipid molecules, particularly that of bacteriorhodopsin (Figs. 4 and 5). The annular shell of lipid around a membrane protein is equivalent to the solvent layer around a water-soluble protein. The lipid bilayer appears to extend right up to the membrane protein, with a uniform thickness for the bilayer right around the protein (Section 2.1). There is very little sharing of annular shells between membrane proteins, even for bacteriorhodopsin in the purple membrane where the molar ratio of lipid to protein is relatively low (Section 2.1). For proteins with large extramembranous domains, sharing of annular shells will also be limited by steric clashes between the extramembranous domains.

Does the presence of an intrinsic membrane protein affect the properties of all the lipids in the membrane or just those in the immediate vicinity of the protein? ESR and simulation studies suggest that the effects of membrane proteins on the properties of the surrounding lipid bilayer are largely confined to the annular shell and do not extend further to affect more distant lipid molecules (Section 1).

If there is a distinct shell of lipid molecules around a membrane protein, what are the properties of the lipid molecules in the shell? The surface of the transmembrane domain of a membrane protein is molecularly rough, with many shallow grooves and protrusions to which the fatty acyl chains of the surrounding lipids must conform if packing of the protein into the lipid bilayer is to be tight, maintaining the membrane as a permeability barrier. This is clear in a number of high-resolution structures of membrane proteins that include lipid molecules, particularly that of bacteriorhodopsin (Figs. 4 and 5). Good van der Waals contact between a membrane protein and the surrounding lipids will lead to both a distortion of the lipid fatty acyl chains and to a decrease in the rate of *trans–gauche* isomerisation in the chains, consistent with ESR studies (Section 1). The effect of a membrane protein on the thickness of the surrounding lipid bilayer appears to be very limited (Section 5.3) although the thickness of the lipid annulus around bacteriorhodopsin is greater than expected from the chain length of the lipids (Section 2.1). Molecular dynamics simulations show that the energy of interaction of a particular lipid molecule with a membrane protein fluctuates over a wide range with time; the total interaction energy between a lipid and a protein molecule represents the sum of many weak van der Waals and electrostatic interactions and there is no single deep energy well into which the phospholipid falls to give a single favoured conformation (Section 1). Lipid molecules are not frozen in a single

long-lived conformation on the protein surface [8]. A particular lipid molecule remains in the annular shell around a protein for only a short period of time, typically about $1-2\times10^{7}\ s^{-1}$ at 30 °C [1]. However, this does not, of course, mean that the properties (chemical and physical) of the annular lipids are unimportant for the function of a membrane protein; rapid exchange of the lipids between the annulus and the bulk lipid bilayer can average the environment sensed by the lipid but will not average the environment sensed by the protein; the environment sensed by the protein (the annular lipid) is the same, however fast the lipids exchange.

If there is a distinct shell of lipid molecules around a membrane protein, how does the composition of the annular shell compare with the bulk composition of the membrane? Binding to the annulus shows relatively little structural specificity although the presence of a charged or polar headgroup is required, to provide good localisation of the molecule at the lipid–water interface and to interact with charged residues on the protein flanking the transmembrane region (Section 5.1). Partition between the bulk lipid phase and the annular shell shows only a small dependence on fatty acyl chain length (Section 5.3) despite the large effect of bilayer thickness on activity (Section 8.4). Thus, the composition of the annular shell of lipids will be similar to that of the bulk lipid bilayer.

Do all lipid molecules interact with a protein in the same way, or are some lipid molecules more tightly bound than others, acting more like cofactors for a protein than as a simple 'solvent'? There is strong evidence for the presence of tightly bound lipid molecules on membrane proteins, distinct from the 'solvent' or annular lipids. Studies with the Ca^{2+}-ATPase of sarcoplasmic reticulum suggested that cholesterol and other hydrophobic molecules could bind to sites on the transmembrane domain of the ATPase from which phospholipids were excluded. These sites were referred to as non-annular sites and were suggested to be located between transmembrane α-helices [10,12]. Since many of the lipid molecules observed in high-resolution structures of membrane proteins are bound in clefts between transmembrane α-helices (Section 2), it is useful to extend the term 'non-annular sites' to include all sites located in deep clefts between transmembrane α-helices, including sites showing specific binding of phospholipids and sites showing specific binding of other hydrophobic molecules. Using this definition, the majority of the lipid molecules observed in X-ray crystal structures will correspond to lipids at non-annular rather than at annular sites. Since the lipid molecules observed in high-resolution structures have been retained after detergent treatment of the proteins, the lipid molecules are likely to be tightly bound to the protein. In some cases, lipid headgroups are well resolved in the crystal structures, implying immobilisation of the headgroup on the protein surface; in other cases, the lipid headgroups are not resolved, suggesting a looser interaction between the headgroup and the protein surface. Tight binding of these lipids also involves a significant hydrophobic contribution from binding of the lipid fatty acyl chains to hydrophobic grooves on the surface of the protein. Although it has not yet been demonstrated experimentally, it is likely that exchange of lipid molecules between the non-annular sites and the bulk lipid bilayer will be relatively slow, and it is likely that binding at the non-annular sites will show much more specificity than binding to the annular sites. The simple fact of binding in a groove will, in itself, be likely to lead to a decrease in both the on and off rates of lipid binding, since steric factors will reduce the number of angles from which a lipid molecule can enter or leave the site. The non-annular sites appear generally to be an extension of the surrounding lipid bilayer. That is, lipid molecules will be able to enter the clefts between transmembrane α-helices by simple diffusion from the annular lipid shell. The backbones of the lipid molecules in the non-annular sites generally occupy the same plane as those in the annular shell. There are, however, two exceptions to this suggestion. In cytochrome bc_1, the phosphatidylinositol molecule located at the dimer interface is located deeper within the membrane than expected (Fig. 16) and the suggested locations for the phosphatidylcholine and glucosylgalactosyl diacylglycerol molecules in the photosynthetic reaction centre of *R. sphaeroides* (Fig. 11) are very unlike those of the bilayer lipids.

Are there particular features of the transmembrane α-helices that help ensure a tight packing into the lipid bilayer? Trp residues are often observed at the ends of transmembrane α-helices with the indole N atom in the backbone region of the bilayer (Sections 1.1, 2 and 3). Tyr residues are also often located at the ends of transmembrane α-helices. Lys and Arg residues can be located within the hydrophobic core of a transmembrane α-helices, snorkelling up to the membrane surface to locate the charged group at the interface (Fig. 2). Rotation of Trp and Tyr residues about the Cα–Cβ bonds linking them to the helix backbone could modulate the effective length of a transmembrane α-helix and so help it match the surrounding lipid bilayer.

How is the hydrophobic, transmembrane domain of a membrane protein matched to the hydrophobic core of the surrounding lipid bilayer? Since intrinsic membrane proteins must have co-evolved with the lipid component of the membrane to give optimal function for the membrane, it could be expected that the hydrophobic thickness of a membrane protein will match that of the surrounding lipid bilayer. The average hydrophobic thickness of an α-helical membrane protein is 29 Å (Table 1), very similar to the hydrophobic thickness of a bilayer of di(C18:1)PC, suggesting that lipids and proteins will generally be well matched in a membrane. Similarly, the average hydrophobic thickness of the β-barrel proteins in bacterial outer membrane (24 Å; Table 1) is likely to match the hydrophobic thickness of the bacterial outer membrane (Sections 2.6, 3 and 5.3). However, for some proteins, hydrophobic thicknesses do not seem to match so well. For example, the hydrophobic thicknesses of bacteriorhodopsin and rhodopsin are about

35 Å, and the thickness of the annular lipid shell around bacteriorhodopsin is greater than expected given the chain length of the surrounding lipids (Section 2.1). Similarly, the hydrophobic thickness of the potassium channel KcsA is about 37 Å (Fig. 7) comparable to the thickness of a bilayer of di(C22:1)PC, the phosphatidylcholine to which it binds most strongly (Fig. 28), but thicker than the expected hydrophobic thickness for the lipid bilayer surrounding it in the bacterial inner membrane. On the other hand, the hydrophobic thicknesses of the ClC chloride channel and of the Ca^{2+}-ATPase appear to be much less than the expected thickness of the surrounding lipid bilayer (Table 1; Section 3). The observation of a significant mismatch between the hydrophobic thicknesses of a membrane protein and the bulk lipid bilayer implies either that the structure of the protein when crystallised from detergent is slightly different to that in the native membrane, or that the lipid bilayer is distorted around the protein in the membrane, exerting stress on the membrane protein.

Does any hydrophobic mismatch between lipid and protein lead to distortion of the lipid bilayer, to distortion of the protein, or to distortion of both? Hydrophobic mismatch between a protein and a lipid bilayer could be compensated for by a thickening or thinning of the lipid bilayer to match the hydrophobic thickness of the protein. Although there is evidence in favour of this form of hydrophobic matching, measurements of changes in bilayer thickness on incorporation of membrane proteins suggests that effects are too small to account for all the mismatch (Section 5.3). Further, there will be an energetic cost associated with any such changes in the thickness of the bilayer, which should be reflected in a reduced binding constant for the lipid but, in fact, lipid binding constants depend only weakly on chain length (Section 5.3). Thus, distortion of the protein to match the lipid bilayer is also likely to occur. If the transmembrane α-helices of a membrane protein are too thick to match the surrounding lipid bilayer, tilting of the helices could reduce their effective length across the bilayer but direct evidence for tilting to provide hydrophobic matching has not yet been obtained (Section 5.3). Rotation of side chains about the Cα–Cβ bonds linking the side chains to the polypeptide backbone could also change the effective length of a helix, and this could be an important mechanism for hydrophobic matching, particularly when the residues at the ends of helices are Trp and Tyr (Section 5.3).

How important are the surrounding lipid molecules in determining the packing of transmembrane α-helices in a membrane protein? Packing of transmembrane α-helices is likely to be affected by the structure of the surrounding lipids. In particular, increasing chain length leads to increased helix–helix interactions (Section 6), which could have important consequences for function.

What range of lipid structures is compatible with proper function of a membrane protein? The chain length of the lipids in a bilayer is an important parameter determining the activities of membrane proteins (Section 8.4). Low activities are seen in too thin and too thick bilayers, consistent with changes in the conformation of the membrane protein, necessary to achieve hydrophobic matching with the bilayer. The bulk of the lipids in a membrane are zwitterionic but some membrane proteins require small amounts of anionic lipids or other hydrophobic molecules such as cholesterol for activity. Lipids bound to non-annular sites on membrane proteins are often anionic (Section 2), and it is possible therefore that the anionic lipids required for activity are bound to non-annular sites between transmembrane α-helices. A good example of how binding to non-annular sites can affect activity is shown by the effect of thapsigargin on the activity of the Ca^{2+}-ATPase, where binding of thapsigargin between transmembrane α-helices (Fig. 25) prevents the ATPase from adopting the conformation required to bind Ca^{2+} (Section 4).

Does the phase of the lipid (liquid crystalline or gel, or hexagonal H_{II}) affect the function of a membrane protein? Activity is generally, but not always, much lower in bilayers in the gel phase than in bilayers in the liquid crystalline phase. It is, however, necessary to take into account effects of hydrophobic matching; lipids that give too thin bilayers in the liquid crystalline phase can support higher than expected activities in the gel phase because of the thicker bilayer produced in the gel phase. Biological membranes generally contain lipids such as the phosphatidylethanolamines that prefer a curved hexagonal H_{II} phase rather than a planar bilayer phase (Section 8.2). Nonbilayer-preferring lipids are forced to adopt a bilayer structure by the presence of membrane proteins or bilayer-preferring lipids; the nonbilayer-preferring lipid will therefore be in a state of curvature frustration. It has been suggested that curvature frustration is necessary for the proper function of some membrane proteins such as rhodopsin [181,182]. However, this has still to be proved definitively. The phosphatidylethanolamine headgroup will interact differently with a membrane protein than, for example, a phosphatidylcholine headgroup (see Figs. 12 and 15) and hydration properties of phosphatidylethanolamines and phosphatidylcholines are different (Section 8.2), both of which could be important for the effect of phosphatidylethanolamines on membrane proteins.

References

[1] D. Marsh, L.I. Horvath, Biochim. Biophys. Acta 1376 (1998) 267–296.
[2] P.C. Jost, O.H. Griffith, Methods Enzymol. 49 (1978) 369–418.
[3] J.K. Brotherus, O.H. Griffith, M.O. Brotherus, P.C. Jost, J.R. Silvius, Biochemistry 20 (1981) 5261–5267.
[4] A.G. Lee, Trends Biochem. Sci. 2 (1977) 231–233.
[5] C. Toyoshima, M. Nakasako, H. Nomura, H. Ogawa, Nature 405 (2000) 647–655.
[6] J.M. East, D. Melville, A.G. Lee, Biochemistry 24 (1985) 2615–2623.
[7] J. Davoust, P.F. Devaux, J. Magn. Res. 48 (1982) 475–494.
[8] T.B. Woolf, B. Roux, Proteins Struct. Funct. Genet. 24 (1996) 92–114.

[9] S.W. Chiu, S. Subramaniam, E. Jakobsson, Biophys. J. 76 (1999) 1929–1938.
[10] A.C. Simmonds, J.M. East, O.T. Jones, E.K. Rooney, J. McWhirter, A.G. Lee, Biochim. Biophys. Acta 693 (1982) 398–406.
[11] A.C. Simmonds, E.K. Rooney, A.G. Lee, Biochemistry 23 (1984) 1432–1441.
[12] B. de Foresta, M. le Maire, S. Orlowski, P. Champeil, S. Lund, J.V. Moller, F. Michelangeli, A.G. Lee, Biochemistry 28 (1989) 2558–2567.
[13] J. Ding, A.P. Starling, J.M. East, A.G. Lee, Biochemistry 33 (1994) 4974–4979.
[14] R.J. Froud, J.M. East, E.K. Rooney, A.G. Lee, Biochemistry 25 (1986) 7535–7544.
[15] E.K. Rooney, M.G. Gore, A.G. Lee, Biochemistry 26 (1987) 3688–3697.
[16] O.T. Jones, M.G. McNamee, Biochemistry 27 (1988) 2364–2374.
[17] M.C. Wiener, S.H. White, Biophys. J. 61 (1992) 434–447.
[18] A.G. Lee, N.J.M. Birdsall, J.C. Metcalfe, G.B. Warren, G.C.K. Roberts, Proc. R. Soc. B 193 (1976) 253–274.
[19] C. Landolt-Marticorena, K.A. Williams, C.M. Deber, R.A.F. Reithmeier, J. Mol. Biol. 229 (1993) 602–608.
[20] M.D. Ulmschneider, M.S.P. Sansom, Biochim. Biophys. Acta 1512 (2001) 1–14.
[21] P. Braun, G. von Heijne, Biochemistry 38 (1999) 9778–9782.
[22] W.M. Yau, W.C. Wimley, K. Gawrisch, S.H. White, Biochemistry 37 (1998) 14713–14718.
[23] S. Persson, J.A. Killian, G. Lindblom, Biophys. J. 75 (1998) 1365–1371.
[24] R.E. Jacobs, S.H. White, Biochemistry 28 (1989) 3421–3437.
[25] J.W. Brown, W.H. Huestis, J. Phys. Chem. 97 (1993) 2967–2973.
[26] D.M. Engelman, T.A. Steitz, A. Goldman, Annu. Rev. Biophys. Biophys. Chem. 15 (1986) 321–353.
[27] J.P. Segrest, H. De Loof, J.G. Dohlman, C.G. Brouillette, G.M. Anantharamaiah, Proteins Struct. Funct. Genet. 8 (1990) 103–117.
[28] I.H. Shrivastava, C.E. Capener, L.R. Forrest, M.S.P. Sansom, Biophys. J. 78 (2000) 79–92.
[29] K. Belohorcova, J. Qian, J.H. Davis, Biophys. J. 79 (2000) 3201–3216.
[30] D.P. Tieleman, L.R. Forrest, M.S.P. Sansom, H.J.C. Berendsen, Biochemistry 37 (1998) 17554–17561.
[31] T.E. Creighton, Proteins, Freeman, New York, 1984.
[32] H.I. Petrache, S.E. Feller, J.F. Nagle, Biophys. J. 70 (1997) 2237–2242.
[33] M. Kates, S.C. Kushwaha, G.D. Sprott, Methods Enzymol. 88 (1982) 98–111.
[34] A. Corcelli, V.M.T. Lattanzio, G. Mascolo, P. Papadia, F. Fanizzi, J. Lipid Res. 43 (2002) 132–140.
[35] H. Belrhali, P. Nollert, A. Royant, C. Menzel, J.P. Rosenbusch, E.M. Landau, E. Pebay-Peyroula, Structure 7 (1999) 909–917.
[36] M. Kates, in: M. Kates, F.J. Kushner, A.T. Matheson (Eds.), The Biochemistry of Archae (Archaebacteria), Elsevier, Amsterdam, 1993, pp. 261–289.
[37] A. Corcelli, M. Colella, G. Mascolo, F.P. Fanizzi, M. Kates, Biochemistry 39 (2000) 3318–3326.
[38] R. Henderson, J.S. Jubb, S. Whytock, J. Mol. Biol. 123 (1978) 259–274.
[39] M. Weik, H. Patzelt, G. Zaccai, D. Oesterhelt, Mol. Cell 1 (1998) 411–419.
[40] N. Grigorieff, T.A. Cesta, K.H. Downing, J.M. Baldwin, R. Henderson, J. Mol. Biol. 259 (1996) 393–421.
[41] K. Mitsuoka, T. Hiral, K. Murata, A. Miyazawa, A. Kidera, Y. Kimura, Y. Fujiyoshi, J. Mol. Biol. 286 (1999) 861–882.
[42] H. Luecke, B. Schobert, H.T. Richter, J.P. Cartailler, J.K. Lanyi, J. Mol. Biol. 291 (1999) 899–911.
[43] O. Edholm, O. Berger, F. Jahnig, J. Mol. Biol. 250 (1995) 94–111.
[44] L.O. Essen, R. Siegert, W.D. Lehmannn, D. Oesterhelt, Proc. Natl. Acad. Sci. 95 (1998) 11673–11678.
[45] M.K. Joshi, S. Dracheva, A.K. Mukhopadhyay, S. Bose, R.W. Hendler, Biochemistry 37 (1998) 14463–14470.
[46] D.A. Doyle, J.M. Cabral, R.A. Pfuetzner, A. Kuo, J.M. Gulbis, S.L. Cohen, B.T. Chait, R. Mackinnon, Science 280 (1998) 69–77.
[47] Y. Zhou, J.H. Morals-Cabral, A. Kaufman, R. Mackinnon, Nature 414 (2001) 43–48.
[48] F.I. Valiyaveetil, Y. Zhou, R. Mackinnon, Biochemistry 41 (2002) 10771–10777.
[49] A. Gross, W.L. Hubbell, Biochemistry 41 (2002) 1123–1128.
[50] A. Gross, L. Columbus, K. Hideg, C. Altenbach, W.L. Hubbell, Biochemistry 38 (1999) 10324–10335.
[51] K.E. McAuley, P.K. Fyfe, J.P. Ridge, N.W. Isaacs, R.J. Cogdell, M.R. Jones, Proc. Natl. Acad. Sci. 96 (1999) 14706–14711.
[52] M.C. Wakeham, R.B. Sessions, M.R. Jones, P.K. Fyfe, Biophys. J. 80 (2001) 1395–1405.
[53] A. Camara-Artigas, D. Brune, J.P. Allen, Proc. Natl. Acad. Sci. 99 (2002) 11055–11060.
[54] T. Nogi, I. Fathir, M. Kobayashi, T. Nozawa, K. Miki, Proc. Natl. Acad. Sci. 97 (2000) 13561–13566.
[55] P. Jordan, P. Fromme, H.T. Witt, O. Klukas, W. Saenger, N. Krauss, Nature 411 (2001) 909–917.
[56] A. Harrenga, M. Michel, J. Biol. Chem. 274 (1999) 33296–33299.
[57] S. Iwata, C. Ostermeier, B. Ludwig, H. Michel, Nature 376 (1995) 660–669.
[58] T. Tsukihara, H. Aoyama, E. Yamashita, T. Tomizaki, H. Yamaguchi, K. Shinzawa-Itoh, R. Nakashima, R. Yaono, S. Yoshikawa, Science 272 (1996) 1136–1144.
[59] M. Schlame, D. Rua, M.L. Greenberg, Prog. Lipid Res. 39 (2000) 257–288.
[60] C. Lange, J.H. Nett, B.L. Trumpower, C. Hunte, EMBO J. 20 (2001) 6591–6600.
[61] E.T. Rietschel, T. Kirikae, F.U. Schade, U. Mamat, G. Schmidt, H. Loppnow, A.J. Ulmer, U. Zahringer, U. Seydel, F. Di Padova, M. Schreier, H. Brade, FASEB J. 8 (1994) 217–225.
[62] K. Brandenburg, Biophys. J. 64 (1993) 1215–1231.
[63] M. Kastowsky, T. Gutberlet, H. Bradaczek, Eur. J. Biochem. 217 (1993) 771–779.
[64] C.P. Nichol, J.H. Davis, G. Weeks, M. Bloom, Biochemistry 19 (1980) 451–457.
[65] A.D. Ferguson, E. Hofmann, J.W. Coulton, K. Diederichs, W. Welte, Science 282 (1998) 2215–2220.
[66] A.D. Ferguson, W. Welte, E. Hofmann, B. Lindner, O. Holst, J.W. Coulton, K. Diederichs, Struct. Fold. Des. 8 (2000) 585–592.
[67] J.L. Harwood, N.J. Russell, Lipids in Plants and Microbes, George Allen & Unwin, London, 1984.
[68] G. McDermott, S.M. Prince, A.A. Freer, A.M. Hawthornthwaite-Lawless, M.Z. Papiz, R.J. Cogdell, N.W. Isaacs, Nature 374 (1995) 517–521.
[69] K. Murata, K. Mitsuoka, T. Hirai, T. Walz, P. Agre, J.B. Heymann, A. Engel, Y. Fujiyoshi, Nature 407 (2000) 599–605.
[70] D. Fu, A. Libson, L.J.W. Miercke, C. Weitzman, P. Nollert, J. Krucinski, R.M. Stroud, Science 290 (2000) 481–486.
[71] F. Zhu, E. Tajkhorshid, K. Schulten, FEBS Lett. 504 (2001) 212–218.
[72] H. Luecke, B. Schobert, J.K. Lanyi, E.N. Spudich, J.L. Spudich, Science 293 (2001) 1499–1503.
[73] R. Dutzler, E.B. Campbell, M. Cadene, B.T. Chalt, R. Mackinnon, Nature 415 (2002) 287–294.
[74] G. Chang, R.H. Spencer, A.T. Lee, M.T. Barclay, D.C. Rees, Science 282 (1998) 2220–2226.
[75] E. Perozo, D.M. Cortes, P. Sompornpisut, B. Martinac, Nature 418 (2002) 942–948.
[76] M. Betanzos, C.S. Chiang, H.R. Guy, S. Sukharev, Nat. Struct. Biol. 9 (2002) 704–710.
[77] A.G. Lee, J.M. East, Biochem. J. 356 (2001) 665–683.
[78] J.M. East, A.G. Lee, Biochemistry 21 (1982) 4144–4151.
[79] C. Toyoshima, H. Nomura, Nature 418 (2002) 605–611.

[80] M. Wictome, Y.M. Khan, J.M. East, A.G. Lee, Biochem. J. 310 (1995) 859–868.
[81] A.G. Lee, Biochim. Biophys. Acta 1565 (2002) 246–266.
[82] A. Pautsch, G.E. Schulz, Nat. Struct. Biol. 5 (1998) 1013–1017.
[83] J. Vogt, G.E. Schulz, Structure 7 (1999) 1301–1309.
[84] S.W. Cowan, T. Schrimer, G. Rummel, M. Steiert, R. Ghosh, R.A. Pauptit, J.N. Jansonius, J.P. Rosenbusch, Nature 358 (1992) 727–733.
[85] E. Pebaypeyroula, R.M. Garavito, J.P. Rosenbusch, M. Zulauf, P.A. Timmins, Structure 3 (1995) 1051–1059.
[86] W. Im, B. Roux, J. Mol. Biol. 319 (2002) 1177–1197.
[87] M. Asahi, Y. Kimura, R. Kurzydlowski, M. Tada, D.H. MacLennan, J. Biol. Chem. 274 (1999) 32855–32862.
[88] A. Johannsson, C.A. Keightley, G.A. Smith, C.D. Richards, T.R. Hesketh, J.C. Metcalfe, J. Biol. Chem. 256 (1981) 1643–1650.
[89] A.G. Lee, J.M. East, P. Balgavy, Pestic. Sci. 32 (1991) 317–327.
[90] A.P. Starling, J.M. East, A.G. Lee, Biochemistry 32 (1993) 1593–1600.
[91] C. Sunshine, M.G. McNamee, Biochim. Biophys. Acta 1191 (1994) 59–64.
[92] S.E. Rankin, G.H. Addona, M.A. Kloczewiak, B. Bugge, K.W. Miller, Biophys. J. 73 (1997) 2446–2455.
[93] C.J.B. daCosta, A.A. Ogrel, E.A. McCardy, M.P. Blanton, J.E. Baenziger, J. Biol. Chem. 277 (2002) 201–208.
[94] G.H. Addona, H. Sandermann, M.A. Kloczewiak, S.S. Husain, K.W. Miller, Biochim. Biophys. Acta 1370 (1998) 299–309.
[95] A. Shouffani, B.I. Kanner, J. Biol. Chem. 265 (1990) 6002–6008.
[96] C.G. Tate, FEBS Lett. 504 (2001) 94–98.
[97] F. Cornelius, Biochemistry 40 (2001) 8842–8851.
[98] R. Aveyard, D.A. Haydon, An Introduction to the Principles of Surface Chemistry, Cambridge Univ. Press, London, 1973.
[99] E. London, G.W. Feigenson, Biochemistry 20 (1981) 1939–1948.
[100] S. Mall, R.P. Sharma, J.M. East, A.G. Lee, Faraday Discuss. 111 (1998) 127–136.
[101] A.G. Lee, FEBS Lett. 151 (1983) 297–302.
[102] A.G. Lee, J.M. East, in: A. Watts (Ed.), Protein–Lipid Interactions, Elsevier, Amsterdam, 1993, pp. 259–299.
[103] A.P. Starling, K.A. Dalton, J.M. East, S. Oliver, A.G. Lee, Biochem. J. 320 (1996) 309–314.
[104] A.G. Lee, Biochim. Biophys. Acta 1376 (1998) 381–390.
[105] S. Mall, R. Broadbridge, R.P. Sharma, A.G. Lee, J.M. East, Biochemistry 39 (2000) 2071–2078.
[106] N.C. Robinson, J. Zborowski, L.H. Talbert, Biochemistry 29 (1990) 8962–8969.
[107] W. Kleeman, H.M. McConnell, Biochim. Biophys. Acta 419 (1976) 206–222.
[108] M. Jaworsky, R. Mendelsohn, Biochemistry 24 (1985) 3422–3428.
[109] H.A. Rinia, R.A. Kik, R.A. Demel, M.M.E. Snel, J.A. Killian, J.P.J.M. van der Eerden, B. de Kruijff, Biochemistry 39 (2000) 5852–5858.
[110] H. Hauser, G.G. Shipley, Biochemistry 23 (1984) 34–41.
[111] R.A. Dluhy, D.G. Cameron, H.H. Mantsch, R. Mendelsohn, Biochemistry 22 (1983) 6318–6325.
[112] K.I. Florine, G.W. Feigenson, Biochemistry 26 (1987) 1757–1768.
[113] A.R.G. Dibble, M.D. Yeager, G.W. Feigenson, in: S. Ohki (Ed.), Cell and Model Membrane Interactions, Plenum, New York, 1991, pp. 15–24.
[114] M.R.R. de Planque, E. Goormaghtigh, D.V. Greathouse, R.E. Koeppe, J.A.W. Kruijtzer, R.M.J. Liskamp, B. de Kruijff, J.A. Killian, Biochemistry 40 (2001) 5000–5010.
[115] R.J. Webb, J.M. East, R.P. Sharma, A.G. Lee, Biochemistry 37 (1998) 673–679.
[116] J.A. Killian, Biochim. Biophys. Acta 1376 (1998) 401–416.
[117] D.R. Fattal, A. Ben-Shaul, Biophys. J. 65 (1993) 1795–1809.
[118] C. Nielsen, M. Goulian, O.S. Andersen, Biophys. J. 74 (1998) 1966–1983.
[119] A. Ben-Shaul, N. Ben-Tal, B. Honig, Biophys. J. 71 (1996) 130–137.
[120] A. Ben-Shaul, in: R. Lipowsky, E. Sackmann (Eds.), Handbook of Biological Physics, Structure and Dynamics of Membranes, vol. 1A, Elsevier, Amsterdam, 1995, pp. 359–401.
[121] A. Kessel, N. BenTal, Curr. Top. Membr. 52 (2002) 205–253.
[122] O.G. Mouritsen, M. Bloom, Biophys. J. 46 (1984) 141–153.
[123] O.G. Mouritsen, M. Bloom, Annu. Rev. Biophys. Bioeng. 22 (1993) 145–171.
[124] B.A. Lewis, D.M. Engelman, J. Mol. Biol. 166 (1983) 211–217.
[125] M.M. Sperotto, O.G. Mouritsen, Eur. Biophys. J. 16 (1988) 1–10.
[126] J.F. Nagle, S. Tristram-Nagle, Biochim. Biophys. Acta 1469 (2000) 159–195.
[127] L.L. Holte, S.A. Peter, T.M. Sinnwell, K. Gawrisch, Biophys. J. 68 (1995) 2396–2403.
[128] A.H. O'Keeffe, J.M. East, A.G. Lee, Biophys. J. 79 (2000) 2066–2074.
[129] I.M. Williamson, S.J. Alvis, J.M. East, A.G. Lee, Biophys. J. 83 (2002) 2026–2038.
[130] O.G. Mouritsen, M. Bloom, Annu. Rev. Biophys. Bioeng. 22 (1993) 145–171.
[131] J.N. Verma, G.K. Khuller, Adv. Lipid Res. 20 (1983) 257–316.
[132] N.J.P. Ryba, D. Marsh, Biochemistry 31 (1992) 7511–7518.
[133] S.H. White, W.C. Wimley, Annu. Rev. Biophys. Biomol. Struct. 28 (1999) 319–365.
[134] Y. Jiang, A. Lee, J. Chen, M. Cadene, B.T. Chalt, R. Mackinnon, Nature 417 (2002) 523–526.
[135] S. Berneche, M. Nina, B. Roux, Biophys. J. 75 (1998) 1603–1618.
[136] U. Harzer, B. Bechinger, Biochemistry 39 (2000) 13106–13114.
[137] P.C.A. van der Wel, E. Strandberg, J.A. Killian, R.E. Koeppe, Biophys. J. 83 (2002) 1479–1488.
[138] D.H. Jones, K.R. Barber, E.W. VanDerLoo, C.W.M. Grant, Biochemistry 37 (1998) 16780–16787.
[139] H.I. Petrache, D.M. Zuckerman, J.N. Sachs, J.A. Killian, R.E. Koeppe, T.B. Woolf, Langmuir 18 (2002) 1340–1351.
[140] A. Alonso, C.J. Restall, M. Turner, J.C. Gomez-Fernandez, F.M. Goni, D. Chapman, Biochim. Biophys. Acta 689 (1982) 283–289.
[141] B. Piknova, E. Perochon, J.F. Tocanne, Eur. J. Biochem. 218 (1993) 385–396.
[142] F. Dumas, J.F. Tocanne, G. Leblanc, M.C. Lebrun, Biochemistry 39 (2000) 4846–4854.
[143] M.R. Morrow, J.C. Huschilt, J.H. Davis, Biochemistry 24 (1985) 5396–5406.
[144] Y.P. Zhang, R.N.A.H. Lewis, R.S. Hodges, R.N. McElhaney, Biochemistry 31 (1992) 11579–11588.
[145] Y.P. Zhang, R.N.A.H. Lewis, R.S. Hodges, R.N. McElhaney, Biophys. J. 68 (1995) 847–857.
[146] Y.P. Zhang, R.N.A.H. Lewis, R.S. Hodges, R.N. McElhaney, Biochemistry 34 (1995) 2362–2371.
[147] Y.P. Zhang, R.N.A.H. Lewis, R.S. Hodges, R.N. McElhaney, Biochemistry 40 (2001) 474–482.
[148] S. Morein, J.A. Killian, M.M. Sperotto, Biophys. J. 82 (2002) 1405–1417.
[149] M.R.R. de Planque, D.V. Greathouse, R.E. Koeppe, H. Schafer, D. Marsh, J.A. Killian, Biochemistry 37 (1998) 9333–9345.
[150] M.R.R. de Planque, J.A.W. Kruijtzer, R.M.J. Liskamp, D. Marsh, D.V. Greathouse, R.E. Koeppe, B. de Kruijff, J.A. Killian, J. Biol. Chem. 274 (1999) 20839–20846.
[151] F.A. Nezil, M. Bloom, Biophys. J. 61 (1992) 1176–1183.
[152] W.K. Subczynski, R.N.A.H. Lewis, R.N. McElhaney, R.S. Hodges, J.S. Hyde, A. Kusumi, Biochemistry 37 (1998) 3156–3164.
[153] J.U. Bowie, J. Mol. Biol. 272 (1997) 780–789.
[154] P.B. Harbury, T. Zhang, P.S. Kim, T. Alber, Science 262 (1993) 1401–1407.
[155] M.A. Lemmon, D.M. Engelman, Q. Rev. Biophys. 27 (1994) 157–218.

[156] S. Mall, R. Broadbridge, R.P. Sharma, J.M. East, A.G. Lee, Biochemistry 40 (2001) 12379–12386.
[157] S.H. White, W.C. Wimley, Annu. Rev. Biophys. Biomol. Struct. 28 (1999) 319–365.
[158] D. Marsh, CRC Handbook of Lipid Bilayers, CRC Press, Boca Raton, 1990.
[159] J.H. Ipsen, G. Karlstrom, O.G. Mouritsen, H. Wennerstrom, M.J. Zuckermann, Biochim. Biophys. Acta 905 (1987) 162–172.
[160] S.M. Gruner, Proc. Natl. Acad. Sci. 82 (1985) 3665–3669.
[161] T. Gil, J.H. Ipsen, O.G. Mouritsen, M.C. Sabra, M.M. Sperotto, M.J. Zuckermann, Biochim. Biophys. Acta 1376 (1998) 245–266.
[162] G.B. Warren, P.A. Toon, N.JM. Birdsall, A.G. Lee, J.C. Metcalfe, Proc. Natl. Acad. Sci. 71 (1974) 622–626.
[163] G.B. Warren, P.A. Toon, N.JM. Birdsall, A.G. Lee, J.C. Metcalfe, Biochemistry 13 (1974) 5501–5507.
[164] B.A. Lewis, D.M. Engelman, J. Mol. Biol. 166 (1983) 203–210.
[165] R.J. Cherry, U. Muller, R. Henderson, M.P. Heyn, J. Mol. Biol. 121 (1978) 283–298.
[166] N.A. Dencher, K.D. Kohl, M. Heyn, Biochemistry 22 (1983) 1323–1334.
[167] B. Sternberg, C. L'Hostis, C.A. Whiteway, A. Watts, Biochim. Biophys. Acta 1108 (1992) 21–30.
[168] T.R. Hesketh, G.A. Smith, M.D. Houslay, K.A. McGill, N.J. Birdsall, J.C. Metcalfe, G.B. Warren, Biochemistry 15 (1976) 4145–4151.
[169] W. Hoffmann, M.G. Sarzala, J.C. Gomez-Fernandez, F.M. Goni, C.J. Restall, D. Chapman, G. Heppler, W. Kreutz, J. Mol. Biol. 141 (1980) 132–141.
[170] J.C. Gomez-Fernandez, F.M. Goni, D. Bach, C.J. Restall, D. Chapman, Biochim. Biophys. Acta 598 (1980) 502–516.
[171] A.P. Starling, J.M. East, A.G. Lee, Biochem. J. 308 (1995) 343–346.
[172] A.P. Starling, J.M. East, A.G. Lee, Biochemistry 34 (1995) 3084–3091.
[173] J.D. Pilot, J.M. East, A.G. Lee, Biochemistry 40 (2001) 14891–14897.
[174] H.K. Kimelberg, D. Papahadjopoulos, J. Biol. Chem. 249 (1974) 1071–1080.
[175] A. Carruthers, D.L. Melchior, Annu. Rev. Physiol. 50 (1988) 257–271.
[176] L.T. Boni, S.W. Hui, Biochim. Biophys. Acta 731 (1983) 177–185.
[177] B. de Kruijff, P.R. Cullis, A.J. Verkleij, M.J. Hope, C.J.A. Van Echteld, T.F. Taraschi, P. Van Hoogevest, J.A. Killian, A. Rietveld, A.T.M. Van der Steen, in: A. Watts, J.J.H.H.M. De Pont (Eds.), Progress in Protein–Lipid Interactions, Elsevier, Amsterdam, 1985, pp. 89–142.
[178] I. Simidjiev, S. Stoylova, H. Amenitsch, T. Javorfi, L. Mustardy, P. Laggner, A. Holzenburg, G. Garab, Proc. Natl. Acad. Sci. 97 (2000) 1473–1476.
[179] B.J. Litman, D.C. Mitchell, in: A.G. Lee (Ed.), Biomembranes, Rhodopsin and G-Protein Linked Receptors, vol. 2A, JAI Press, Greenwich, CT, 1996, pp. 1–32.
[180] D.C. Mitchell, M. Straume, B.J. Litman, Biochemistry 31 (1992) 662–670.
[181] M.F. Brown, Chem. Phys. Lipids 73 (1994) 159–180.
[182] A.V. Botelho, N.J. Gibson, R.L. Thurmond, Y. Wand, M.F. Brown, Biochemistry 41 (2002) 6354–6368.
[183] H.I. Petrache, A. Salmon, M.F. Brown, J. Am. Chem. Soc. 123 (2001) 12611–12622.
[184] D.C. Mitchell, B.J. Litman, Biochemistry 38 (1999) 7617–7623.
[185] S.L. Niu, D.C. Mitchell, B.J. Litman, J. Biol. Chem. 277 (2002) 20139–20145.
[186] D.C. Mitchell, S.L. Niu, B.J. Litman, J. Biol. Chem. 276 (2001) 42801–42806.
[187] S.L. Niu, D.C. Mitchell, B.J. Litman, J. Biol. Chem. 276 (2001) 42807–42811.
[188] P.D. Calvert, V.I. Govardovskii, N. Krasnoperova, R.E. Anserson, J. Lem, C.L. Makino, Nature 411 (2001) 90–94.
[189] D.C. Mitchell, B.J. Litman, Biophys. J. 74 (1998) 879–891.
[190] A.G. Lee, Prog. Lipid Res. 30 (1991) 323–348.
[191] M. Caffrey, G.W. Feigenson, Biochemistry 20 (1981) 1949–1961.
[192] A.P. Starling, Y.M. Khan, J.M. East, A.G. Lee, Biochem. J. 304 (1994) 569–575.
[193] G.W. Gould, J.M. McWhirter, J.M. East, A.G. Lee, Biochem. J. 245 (1987) 751–755.
[194] J.D. Pilot, J.M. East, A.G. Lee, Biochemistry 40 (2001) 8188–8195.
[195] M.B. Sankaram, T.E. Thompson, Biochemistry 29 (1990) 10676–10684.
[196] P.A. Baldwin, W.L. Hubbell, Biochemistry 24 (1985) 2624–2632.
[197] P.A. Baldwin, W.L. Hubbell, Biochemistry 24 (1985) 2633–2639.
[198] T.S. Wiedmann, R.D. Pates, J.M. Beach, A. Salmon, M.F. Brown, Biochemistry 27 (1988) 6469–6474.
[199] A. Carruthers, D.L. Melchior, Biochemistry 23 (1984) 6901–6911.
[200] R.E. Tefft, A. Carruthers, D.L. Melchior, Biochemistry 25 (1986) 3709–3718.
[201] C. Montecucco, G.A. Smith, F. Dabenni-sala, A. Johansson, Y.M. Galante, R. Bisson, FEBS Lett. 144 (1982) 145–148.
[202] F. Jiang, M.T. Ryan, M. Schlame, M. Zhao, Z.M. Gu, M. Klingenberg, N. Pfanner, M.L. Greenberg, J. Biol. Chem. 275 (2000) 22387–22394.
[203] S. Heimpel, G. Basset, S. Odoy, M. Klingenberg, J. Biol. Chem. 276 (1902) 11499–11506.
[204] N.C. Robinson, Biochemistry 21 (1982) 184–188.
[205] G.L. Powell, P.F. Knowles, D. Marsh, Biochim. Biophys. Acta 816 (1985) 191–194.
[206] N.C. Robinson, J. Bioenerg. Biomembranes 25 (1993) 153–163.
[207] D.A. Abramovitch, D. Marsh, G.L. Powell, Biochim. Biophys. Acta 1020 (1990) 34–42.
[208] W.F. Al-Tai, M.G. Jones, K. Rashid, M.T. Wilson, Biochem. J. 209 (1983) 901–903.
[209] E. Sedlak, N.C. Robinson, Biochemistry 38 (1999) 14966–14972.
[210] B. Hoffmann, A. Stockl, M. Schlama, K. Beyer, M. Klingenberg, J. Biol. Chem. 269 (1994) 1940–1944.
[211] K. Beyer, M. Klingenberg, Biochemistry 24 (1985) 3821–3826.
[212] N.J. Gibson, M.F. Brown, Biochem. Biophys. Res. Commun. 176 (1991) 915–921.
[213] E. Hassel, P. Muller, A. Herrmann, K.P. Hofmann, J. Biol. Chem. 276 (2001) 2538–2543.
[214] L. Heginbotham, L. Kolmakova-Partensky, C. Miller, J. Gen. Physiol. 111 (1998) 741–749.
[215] Z. Fan, J.C. Makielski, J. Biol. Chem. 272 (1997) 5388–5395.
[216] C.L. Huang, S. Feng, D.W. Hilgemann, Nature 391 (1998) 803–806.
[217] H.P. Ma, S. Saxena, D.G. Warnock, J. Biol. Chem. 277 (2002) 7641–7644.
[218] G.G. MacGregor, K. Dong, C.G. Vanoye, L. Tanf, G. Giebisch, S.C. Herbert, Proc. Natl. Acad. Sci. 99 (2002) 2726–2731.
[219] K.A. Dalton, J.D. Pilot, S. Mall, J.M. East, A.G. Lee, Biochem. J. 342 (1999) 431–438.
[220] A. Hanicak, D. Maretzki, B. Reimann, E. Pap, A.J.W.G. Visser, K.W.A. Wirtz, D. Schubert, FEBS Lett. 348 (1994) 169–172.
[221] R.A. Anderson, V.T. Marchesi, Nature 318 (1985) 295–298.
[222] S.H. White, A.S. Ladokhin, S. Jayasinghe, K. Hristova, J. Biol. Chem. 276 (2001) 32395–32398.
[223] M. Jormakka, S. Tornroth, B. Byrne, S. Iwata, Science 295 (2002) 1863–1868.
[224] P.L. Yeagle, D. Rice, J. Young, Biochemistry 27 (1988) 6449–6452.
[225] P.L. Yeagle, Biochimie 73 (1991) 1303–1310.
[226] P.L. Yeagle, J. Membr. Biol. 78 (1984) 201–210.
[227] D. Schubert, K. Boss, FEBS Lett. 150 (1982) 4–8.
[228] R.M. Esnouf, Acta Crystallogr., D 55 (1999) 938–940.